BULLETIN
OF THE AMERICAN PHYSICAL SOCIETY

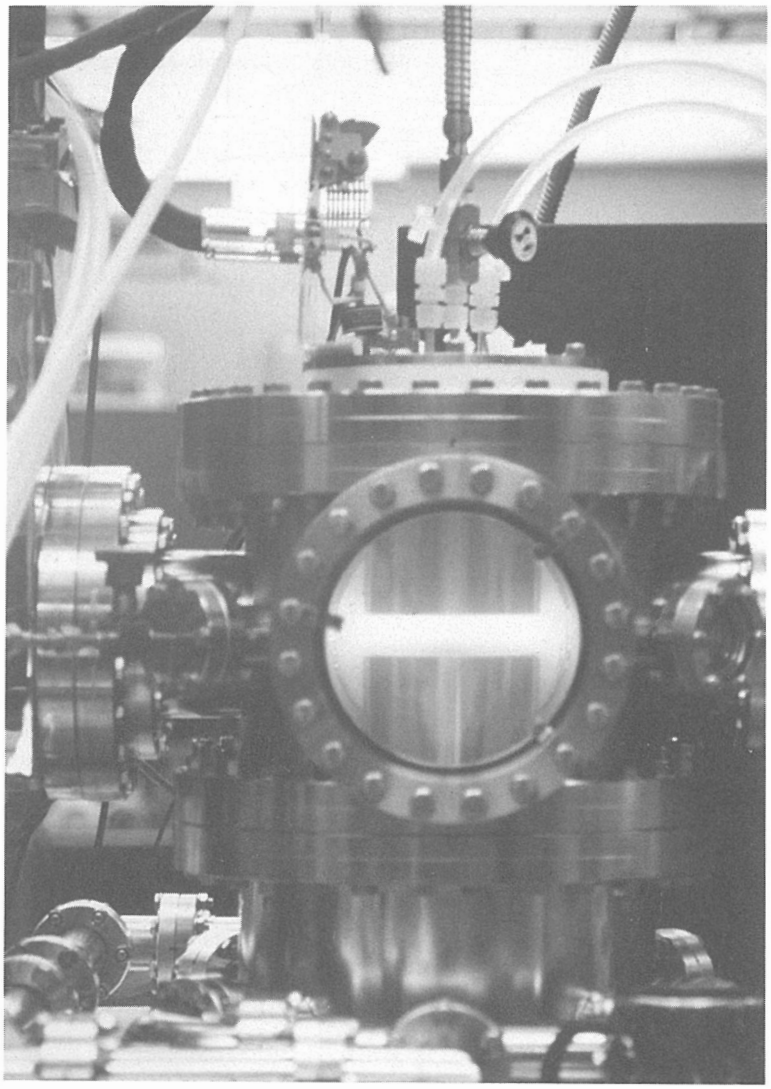

Program of the 47th Annual Gaseous Electronics Conference (GEC)

October 1994
Volume 39, No. 6

BULLETIN
OF THE AMERICAN PHYSICAL SOCIETY

Coden BAPSA6
Series II, Vol. 39, No. 6

ISSN: 0003-0503
October 1994

APS COUNCIL 1994

Editor: Neil Baggett
Coordinator: TammanyYoung

APS MEETINGS DEPARTMENT
One Physics Ellipse
College Park, MD 20740-3844
Telephone: (301) 209-3200
FAX: (301) 209-0866
Michael Scanlan, *Meetings Manager*
Tammany Young, *Assistant Meetings Manager*
Lauri A. Nichols, *Meetings Coordinator*
Desiree Atherly, *Secretary*

The *Bulletin of The American Physical Society* is published 10X in 1994: March, April, July, October (3X), November (3X), and December, by The American Physical Society, through the American Institute of Physics. It contains advance information about meetings of the Society, including abstracts of papers to be presented, as well as transactions of past meetings. Reprints of papers can only be obtained by writing directly to the authors.

The *Bulletin* is delivered, on subscription, by 2nd Class Mail. Complete volumes are also available on microfilm. **APS Members** may subscribe to individual issues, or for the entire year. **Nonmembers** may subscribe to the Bulletin at the following rates: Domestic $330; Foreign Surface $340; Air Freight $350. Information on prices, as well as subscription orders, renewals, and address changes, should be addressed as follows: **For APS Members**—Membership Department, The American Physical Society, One Physics Ellipse, College Park, MD 20740-3844. **For Nonmembers**—Circulation and Fulfillment Division, The American Institute of Physics, 500 Sunnyside Blvd., Woodbury, NY 11797. Allow at least 6 weeks advance notice. For address changes, please send both the old and new addresses, and, if possible, include a mailing label from a recent issue. Requests from subscribers for missing issues will be honored without charge only if received within 6 months of the issue's actual date of publication.

Second-class postage paid at Woodbury, NY and additional mailing offices. Postmaster: Send address changes to *Bulletin of The American Physical Society*, Membership Department, The American Physical Society, One Physics Ellipse, College Park, MD 20740-3844.

ON THE COVER: GEC RF Discharge Reference Cell. *Photo courtesy of J.R. Roberts, NIST.*

BULLETIN
OF THE AMERICAN PHYSICAL SOCIETY

Series II, Vol. 39, No. 6, October 1994

PROGRAM OF THE 47th ANNUAL GASEOUS ELECTRONICS CONFERENCE (GEC)

PROGRAM OF THE 47th ANNUAL GASEOUS ELECTRONICS CONFERENCE (GEC) 18–21 October 1994; Gaithersburg, Maryland

GENERAL INFORMATION

The Gaseous Electronics Conference (GEC) is an annual topical conference of The American Physical Society sponsored by the Division of Atomic, Molecular, and Optical Physics. The focus of this conference is on basic phenomena and plasma processes in ionized gases, and on the relevent theory and measurement of basis atomic and molecular collision processes. The 47th Annual GEC was hosted by the National Institute of Standards and Technology (NIST) and held at NIST in Gaithersburg, Maryland, USA on 18–21 October 1994. Support for this conference was provided by NIST and the U. S. Army Research Office. Partial support for social functions held in conjunction with the conference was provided by General Electric, OSRAM, EXTREL, and Norcal. An updated list of the sponsors will be distributed to the participants. Special topics highlighted at the 1994 GEC included: electron-metal atom collisions, recent developments in electron-molecule scattering, negative ions in plasmas, plasma displays, diamond-film deposition, plasma treatment of waste gases, and innovative plasma applications. The Will Allis Prize Lecture was delivered by Eldon E. Ferguson. The conference also included a GEC Reference Cell Users Group Meeting and tours of the NIST Research Facilities.

The members of the Executive Committee for the 47th GEC are:

James T. Dakin, Chairman
GE Lighting

Richard J. Van Brunt, Secretary
NIST

James E. Lawler, Treasurer
University of Wisconsin

J. Norman Bardsley, Chairman-Elect
Lawrence Livermore National Laboratory

David B. Graves, Secretary Elect
University of California-Berkeley

Michel Moisan, Past-Secretary
University of Montreal

Paul D. Burrow
University of Nebraska

Michael A. Dillon
Argonne National Laboratory

Jean W. Gallagher
NIST

John H. Keller
IBM

Toshiaki Makabe
Keio University

The Local Committee included: R.J. Van Brunt, J.W. Gallagher, J.K. Olthoff, K. Kilmer, and L. Phillips.

MAP TO NIST

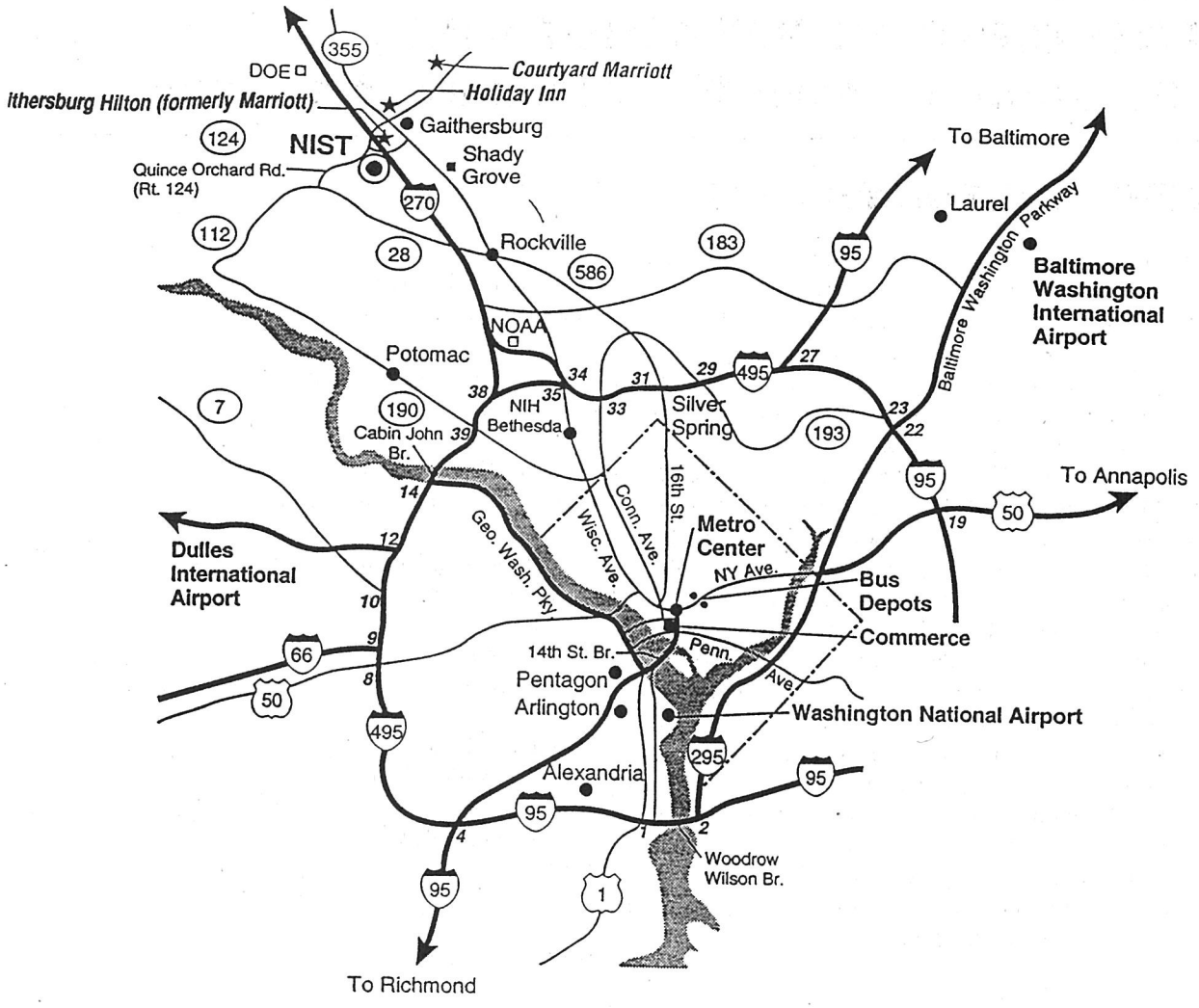

Driving Instructions

NIST is located in Gaithersburg, Maryland, just off Interstate Route 270, about 25 miles (40 kilometers) from Washington, DC. From Washington (northbound on Route 270) visitors to NIST should enter the Collector/Distributor lanes at Exit 9. Stay in the Collector/Distributor lanes until you reach Exit 10, Route 117 West, Clopper Road. Once on Clopper Road, turn left at the first traffic light onto the NIST grounds. Proceed through the main gate. If coming southbound on Route 270, take Exit 11B, Route 124 West, Quince Orchard Rd.

To reach the **Gaithersburg Hilton, formerly the Gaithersburg Marriott, (301/977-8900)**, take Exit 11, Route 124 East, Montgomery Village Avenue. At the second light, turn right on to Route 355 (Frederick Avenue). Follow Route 355 to the first light, which is Perry Parkway. Turn right on to Perry Parkway. The hotel will be on the right.

To reach the **Gaithersburg Holiday Inn (301/948-8900)**, take Exit 11, Route 124 East, Montgomery Village Avenue. At the intersection of Montgomery Village Avenue and Route 355 (Frederick Avenue) turn left; the hotel will be the first right.

To reach the **Gaithersburg Courtyard by Marriott (301/670-0008)**, take Exit 11, Route 124 East, Montgomery Village Avenue. Proceed straight through the first two lights, at the third light, turn left on to Russell Avenue; the hotel will be on the right.

NIST SITE MAP

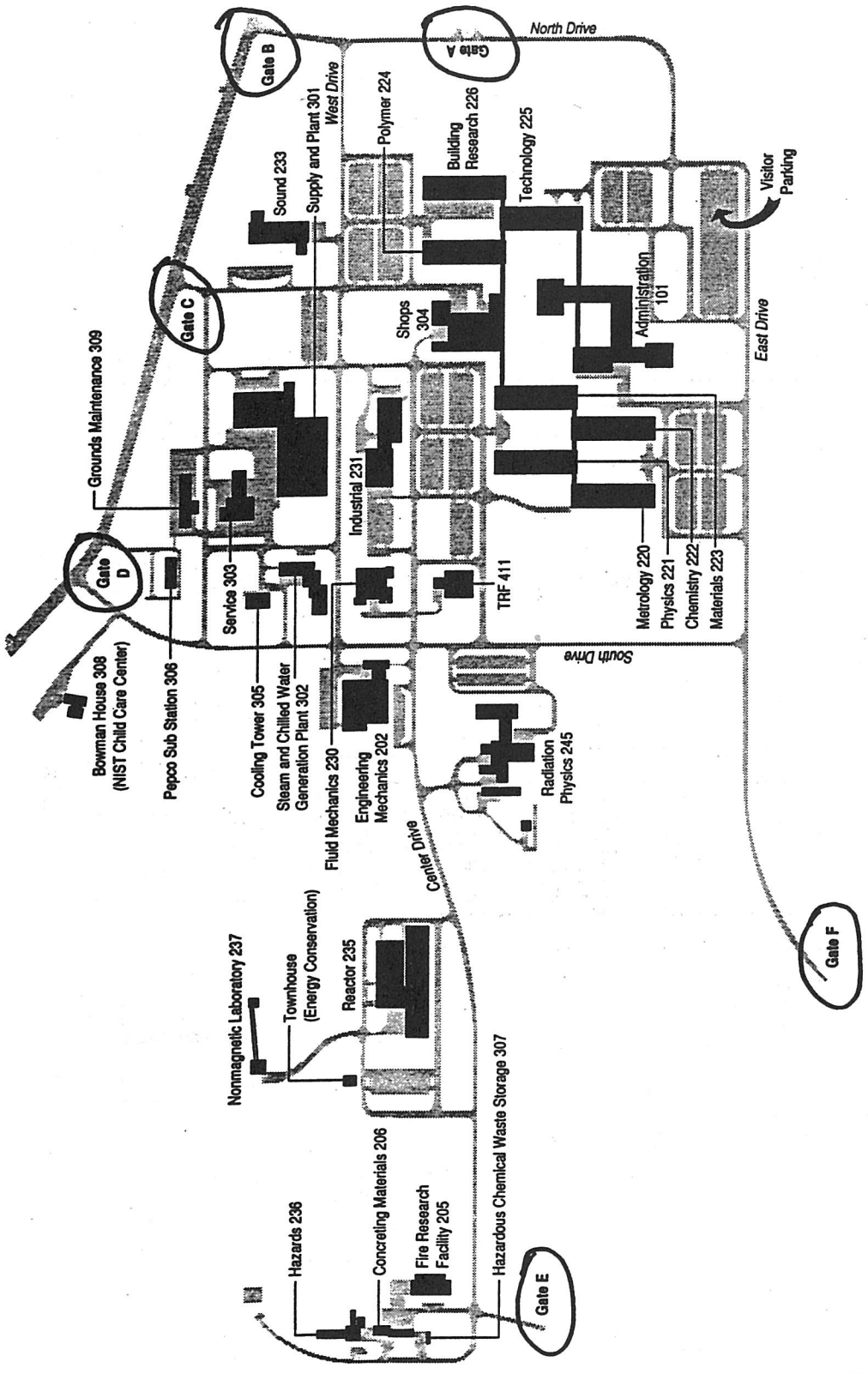

NIST—FIRST FLOOR PLAN

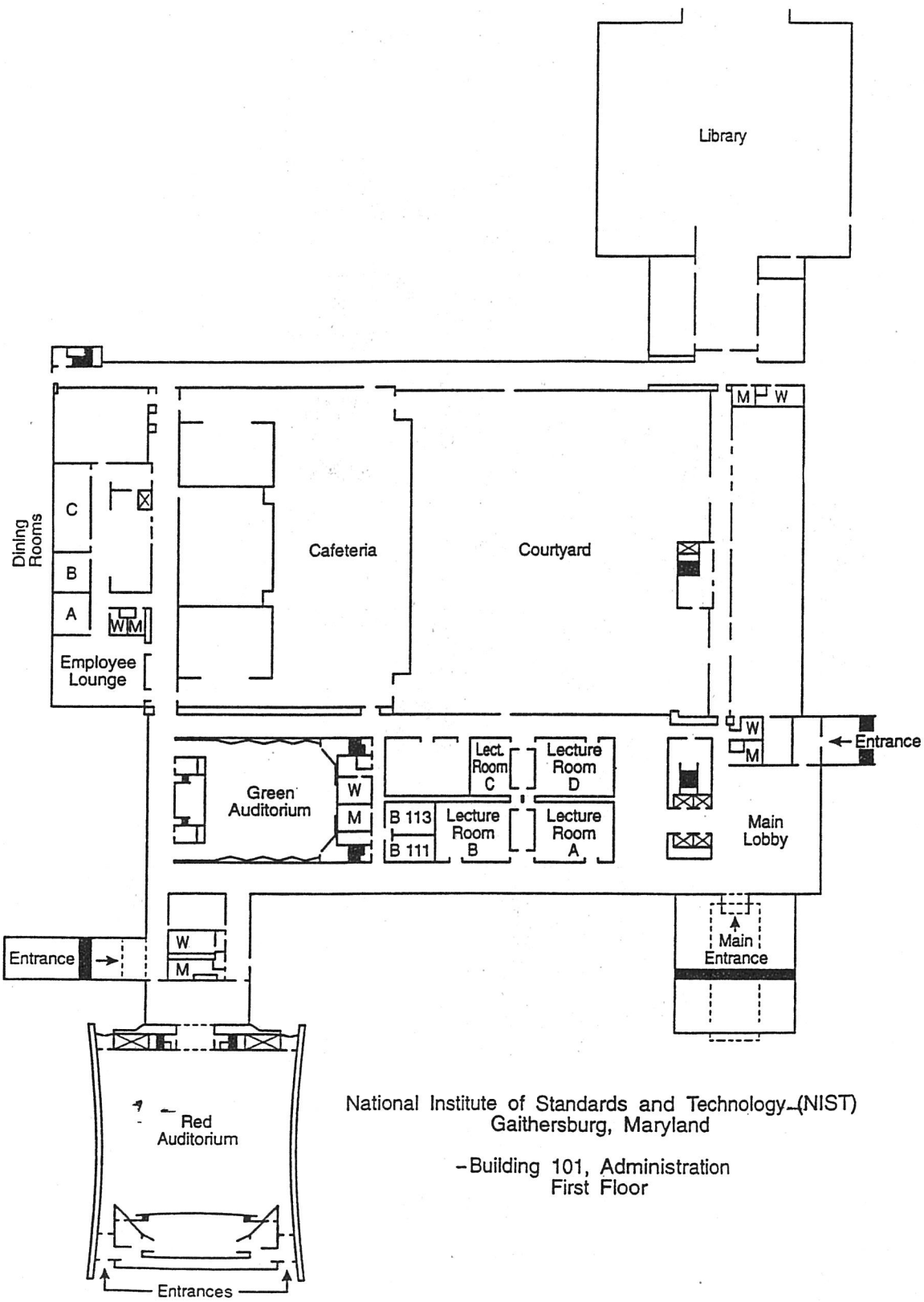

National Institute of Standards and Technology (NIST)
Gaithersburg, Maryland

–Building 101, Administration
First Floor

EPITOME OF THE 47th ANNUAL GASEOUS ELECTRONICS CONFERENCE

MONDAY, 17 OCTOBER 1994, HILTON HOTEL

14:00-22:00 Registration
19:00 Welcome reception

TUESDAY, 18 OCTOBER 1994, NIST

8:00 AA High Density Plasma Processing. Chair: *J. H. Keller*
8:00 AB Electron Metal-Atom Collisions. Chair: *Y.-K. Kim*
10:15 BA Negative Ions in Plasmas. Chair: *L. Christophorou*
10:15 BB Diagnostics I. Chair: *H. Sugai*
13:30 CA Plasma Surface Interactions. Chair: *W. L. Hsu*
13:30 CB Diagnostics and Control. Chair: *M. D. Bowden*
15:45 **Posters** Chair: *J. R. Roberts*
DA Electrical-Optical Diagnostics
DB Electron Collisions
DC Electron-Ion Recombination and Photon Processes
DD Charged Particle Transport—Energy Distributions

WEDNESDAY, 19 OCTOBER 1994, NIST

8:00 EA Magnetically Enhanced Plasmas I. Chair: *M. Lampe*
8:00 EB Transport and Energy Distributions. Chair: *J. Wu*
10:30 F William P. Allis Prize Lecture. Chair: *M. R. Flannery*
11:30 G Business Meeting. Chair: *J. T. Dakin*
13:30 HA Inductively Coupled Plasmas I. Chair: *T. J. Sommerer*
13:30 HB Electron-Molecule Scattering Chair: *I. I. Fabrikant*
15:45 **Posters** Chair: *J. K. Olthoff*
JA Microwave Discharges
JB Magnetically Enhanced Plasmas II
JC Positive Columns
JD Plasma Processing—Etching and Deposition
JE Plasma Chemistry
JF Heavy Particle Interactions

THURSDAY, 20 OCTOBER 1994, NIST

8:00 KA Flat Planel Displays. Chair: *W. Hofer*
8:00 KB Electron Collisions. Chair: *S. K. Srivastava*
10:15 **Posters** Chair: *E. Benck*
LA Plasma Techniques for Waste Treatment I
LB Coronas, Arcs and Breakdown
LC Plasma Displays
LD Electron Collisions
13:30 MA Diamond Films. Chair: *B. Lane*
13:30 MB Glows. Chair: *D. A. Doughty*
15:45 **Posters** Chair: *M. A. Sobolewski*
NA RF Capacitively Coupled Glows
NB Inductively Coupled Plasmas II
NC Cathodes and Sheaths
ND Dusty Glows

FRIDAY, 21 OCTOBER 1994, NIST

8:00 PA Inductively Coupled Plasmas III. Chair: *M. Barnes*
8:00 PB Plasma Techniques for Waste Treatment II. Chair: *J. Herron*
10:15 QA Innovative Plasma Applications. Chair: *R. B. Piejak*
10:15 QB Dusty Plasmas. Chair: *C. Cui*

TUESDAY MORNING

MAIN TEXT

REGISTRATION
Monday afternoon/evening, 17 October 1994
Gaithersburg Hilton Hotel, 14:00–22:00

WELCOME RECEPTION
Monday evening, 17 October 1994
Gaithersburg Hilton Hotel, 19:00–22:00

SESSION AA: HIGH DENSITY PLASMA PROCESSING

Tuesday morning, 18 October 1994
NIST Building 101
Red Auditorium, 8:00–10:00
J. Keller, presiding

Invited Paper

AA-1 Transformer Coupled Plasma: An Inductive Source for Advanced Semiconductor Manufacturing, RALPH KERNS, *LAM Research* — Transformer Coupled Plasma (TCP) technology has progressed from the R&D phase to large scale production in semiconductor manufacturing worldwide. The most successful and widespread application is for etching of aluminun alloy and barrier metal interconnects implemented on the LAM Research TCP 9600 etch tool. This tool includes another application of TCP technology in a separate chamber for stripping of photoresist and corrosion prevention. This high density inductive source offers several advantages in process performance and reactor characteristics for advanced semiconductor manufacturing applications.

Contributed Papers

AA-2 Control of Radicals in a Fluorocarbon Plasma by Heating Walls and/or Pulsing RF Powers, H. SUGAI, K. NAKAMURA, Nagoya University, Nagoya, Japan, Y. HIKOSAKA, M. NAKAMURA, Fujitsu Ltd., Kawasaki, Japan - The entire vessel of a RF diode etching reactor was heated to control the radical composition of a CF_4/H_2 plasma. Appearance mass spectrometry revealed that the CF_3 and CF_2 densities are 2 to 3 orders of magnitude higher in the heated reactor at 230℃, compared with the conventional reactor at 30℃. Some mechanisms for the dramatic change are suggested in view of reactions on surface and in gas phase. Similar phenomena were observed also in a high density ICP (inductively coupled plasma) and they enabled to attain a high etch selectivity of SiO_2 to Si. In addition, the high selectivity was also obtained in a pulsed mode operation of ICP where 13.56 MHz power is repeatedly applied for 5-50 μsec and switched off for 2-50 μsec. The radical density ratio, CF_2/F, turned out to decrease with increasing the discharge-on time. The experimental results are discussed based on the time-resolved measurements of electron temperature and density.

AA-3 Instability Mechanisms in Inductive Glow Discharges, JOHN HOLLAND and MICHAEL BARNES, *Lam Research Corporation, Fremont, CA* — Under certain conditions, instability phenomena have been observed in rf inductive glow discharge systems typically used in plasma processing at low pressures (e.g., 1–100 mT). These instabilities appear in the form of amplitude modulation to the rf system and exhibit behavior very similar to discharge instabilities typically observed in CO_2 lasers. Experimental rf and plasma probe data will be presented for some of the instabilities that have been observed. Hypotheses will be presented for the actual discharge kinetics which support these instabilities.

AA-4 Modification of Inductive Plasma Sources by RF B-Fields* T.D. ROGNLIEN, R.H. COHEN, G.J. DIPESO, V. VAHEDI, AND D.W. HEWETT, *Lawrence Livermore National Laboratory*—**The RF electric field $\mathbf{E}_{rf}$ in an inductive source decays going into the plasma owing to the skin effect and finite geometry. This short scale length gives rise to a strong RF magnetic field $\mathbf{B}_{rf} \propto 1/f$, where f is the RF frequency. The resulting $q\mathbf{v} \times \mathbf{B}_{rf}$ force for electrons typically exceeds the $q\mathbf{E}_{rf}$ force for $f \leq 14$ MHz. In the linear regime ($v_{rf} \ll v_{thermal}$), the magnitude of the collisionless (or stochastic) heating is not changed by $\mathbf{B}_{rf}$, but it does cause the energy to be deposited primarily in the velocity component along $\mathbf{E}_{rf} \times \mathbf{B}_{rf}$ rather than along $\mathbf{E}_{rf}$. In the low frequency, nonlinear regime, $\mathbf{B}_{rf}$ can stop most of the electrons before they reach the wall, with an effect that is qualitatively like a ponderomotive potential, but the electron velocity is strongly nonlinear. Here the collisionless heating level is reduced below that predicted from linear theory. Analytical results are given for the linear regime and for the nonlinear regime when the transit time is negligible compared to the wave period. Numerical results complete the picture to show the effect of $\mathbf{B}_{rf}$ on the collisionless heating rate and the improved plasma uniformity through the ponderomotive-like potential for etching applications.**

*Work performed under USDoE contract W-7405-ENG-48 at LLNL

AA-5 Silicon Dioxide Etch Characterization in a Planar Inductively-Coupled Plasma (TCP) as a Function of RF and Geometric Coil Parameters A.J. LAMM, Lam Research Corp., Fremont, California 94538 - The silicon dioxide etch performance in an inductively-coupled discharge is dependent on the RF voltage and current parameters of the coil used. In this experiment, etch results are studied in terms of these RF coil parameters as well as coil geometries. Besides showing etch dependencies on coil voltage and current, comparisons are made among sets of concentric loops that occupy the same annular area: 1) dual flat loops, 2) dual vertical loops, and 3) 4 vertical loops. The flat and vertical loop conductors have the same cross sectional area. These experiments allow for the observation of capacitive versus inductive effects and turns ratio effects (coil turns to the effective plasma single turn). The coil is operated at 13.56 MHz. A 4 MHz bias is applied at the wafer chuck at a fixed power level.

AA-6 Symmetric Rate Model for Fluorocarbon Plasma Etching of SiO_2.* NOAH HERSHKOWITZ and JI DING, University of Wisconsin-Madison — Plasma etching of SiO_2 by CF_4 plasma is often viewed as a complicated process involving many chemical reactions in the gas, at chamber surfaces and at the wafer surface. This is certainly true when viewed in terms of external parameters such as neutral pressure, discharge power, flow rates, self-bias voltage, etc. Here, a rate model for plasma etching and plasma deposition in fluorocarbon plasmas is presented which includes both etching and deposition symmetrically. This model argues etching and deposition depend only on the ion energy flux J_iE_i, the flux of the chemical etching species J_e and the flux of the deposition species J_d. Experimental SiO_2 etch rates in ECR and RIE etch tools using CF_4 at pressures ranging from 0.5-50 mtorr are found to agree with an approximate version of the symmetric rate model

$$R_t = \frac{K_{es}\, J_i\, E_i\, [1 - C_{sp}\, (\frac{J_d}{J_e})^2]}{1 + A_s\, \frac{J_i\, E_i}{J_e}}$$

where K_{es}, A_s and C_{sp} are universal constants, independent of the specific etching tool.

*Work supported by NSF Grant No. ECD-8721545 for the Engineering Research Center for Plasma-Aided Manufacturing.

AA-7 The Characteristics of the Transformer-Coupled Plasma (TCP) Photoresist Stripper, Y. Ra, J. Yang, W.-B. Chow, and C.-H. Chen, Lam Research Corporation, Fremont, California. The transformer-coupled plasma technology has been successfully applied to photoresist stripping by using an oxygen plasma. The plasma is inductively generated at the frequency of 13.56MHz by a planar pancake-type coil separated from the vacuum chamber by a dielectric window. The typical operation condition consists of a gas pressure of 1Torr, 1KW of rf power, and 1000sccm of O_2 gas flow. Ion current is strongly reduced due to collisions while diffusing to the wafer and stripping is mainly achieved by radicals at the rate of more than 1μm/min. The oxygen plasma parameters have been measured by a Langmuir probe and compared to the results of 0-D surface PSR code[1]. The characteristics of stripping process is discussed in terms of plasma parameters.

[1] E. Meeks, J.W. Shon, R.J. Kee and H.K. Moffat, International Conference on Plasma Science, Santa Fe, New Mexico, 1994

SESSION AB: ELECTRON-METAL ATOM COLLISIONS
Tuesday morning, 18 October 1994
NIST Building 101
Green Auditorium, 8:00–10:00
Y.-K. Kim, presiding

Invited Papers

AB-1 Recent Advances in Atomic and Molecular Collisions: Experimental Electron-Metal Atom Scattering.* BERNHARD STUMPF, Dept. of Physics, University of Idaho. --- Past work on electron-metal atom scattering has mostly concentrated on sodium, the "poor man's hydrogen". In recent years, interest has shifted to more complex metal atoms like heavy alkali and transition metal atoms. We review the present status of research on these atoms. Emphasis is on measurements of electron cross sections and polarizations for rubidium, cesium, copper, and silver in the energy range from threshold to 1000 eV.

*Supported by NSF/Idaho-EPCoR under grants RII-8902065 and OSR-9350539, by seedgrants from the University of Idaho Research Council, by a grant from the State Board of Education of the State of Idaho, and by contracts with Westinghouse-INEL (C85-110544-046) and Lawrence Livermore National Laboratory (B160497).

AB-2 Recent Progress in Electron — Metal Atom Scattering Theory.* K. BARTSCHAT, Drake University — A review of recent theoretical results for electron scattering from various metal atoms, ranging from rather simple alkali targets to complex systems such as Fe, Hg or Pb, will be presented. Comparison with experimental data in the "intermediate energy range" (about one to five times the ionization threshold) shows that special emphasis must be given to the inclusion of the target continuum states (ionization channels) in "Convergent Close Coupling" or "Second-Order Distorted Wave" methods. Furthermore, the differences of treating relativistic effects through algebraic recoupling of non-relativistic results, in first-order perturbation theory by using the Breit-Pauli hamiltonian, or fully *ab initio* in the Dirac formalism will be discussed.

* Work supported by the National Science Foundation under grant # PHY-9318377.

Contributed Papers

AB-3 Orbital Effects in Elastic Electron Scattering by a Polarize Excited Target,* Z. SHI, C. H. YING, New York U. and I VUŠKOVIĆ, Old Dominion U.-The role of the valence electron i elastic scattering is being studied by measuring an azimutha asymmetry as an orbital effect in the collision of unpolarized electron by laser excited polarized (3P)Na atoms. While spin asymmetr effects in superelastic and ground state elastic scattering with polarize electron beams has been recently observed by the NIST[1] group, a asymmetry caused by the Coulomb interaction alone has never beer observed before. Asymmetry effects due to M_L state perpendicular tc the scattering plane (orbital effects) are being studied in the inciden electron energy range comparable with the kinetic energy of the atomic valence electron. Experiments are being performed with 0.5 eV to 10 eV electrons. A classical interpretation of such effects as wel as comparison of preliminary results with close coupling[2] calculatior will be presented at the conference.

* Research supported by U.S. National Science Foundation.
[1] J. J. McClelland, M. H. Kelley, and R. J. Celotta, Phys. Rev. A **40**, 2321 (1989); S. R. Lorentz et all., Phys. Rev. Lett. **67**, 3761 (1991).
[2] H. L. Zhou, D. W. Norcross, and B. L. Whitten, IOP Conf. Proc. No. 122, pp.39-48 (1992).

AB-4 Full Atom Beam Cooling and Electron Collision,* C. H. YING Z. SHI, New York U. and L. VUŠKOVIĆ, Old Dominion U.-A number of experiments have been demonstrated to provide longitudinal cooling of an atomic beam by employing differen methods to compensate for the Doppler shift of the decelerating atoms. The resulting beams were of low density due to the transverse heating or to partial capture of the initial beam by longitudina cooling. The strength of our approach to generate sodium beam having a cross sectional area of 1 mm^2, a flux of 10^{12} atoms/s

monochromaticity of 400±2 m/s, and a 1 mrad divergence, is th construction of a Zeeman slower with a decreasing parabolic magneti field. The water-cooled tapered solenoid generates the field on th axis from 1800 G to 480 G with 1.5 G standard deviation from th expected parabolic field, which allows full capture of the initial beam The final beam preparation includes compression and deflection a well. The application of this bright monoenergetic atomic beam[1] to b used in electron scattering experiment with recoil atom arrangemen is not limited to scattering experiments only. Benefits for the othe experiments will be presented.

* Research supported by U.S. National Science Foundation.

[1]C. H. Ying, , Z. Shi, W. Tan, and L. Vušković, QELS '93, Technical Digest **12**, 101 (1993).

AB-5 Electron Collisions with Cold Trapped Atoms: A New Method for Measuring Cross Sections.* R. SCOTT SCHAPPE, PAUL FENG, THAD G. WALKER, L. W. ANDERSON, and CHUN C. LIN, U. of Wisconsin–**Electron collisions with trapped ^{85}Rb atoms have been studied. Very cold Rb atoms are held in a magneto-optical trap through which an electron beam is passed. An electron-Rb collision imparts a recoil velocity to the Rb atom large enough that the atom is lost from the trap except for collisions with very low momentum transfer. The magnetic field is turned off for 4 msec and the electron beam is pulsed on for 1.6 msec during this time. The ejection rate of the trapped atoms due to the electron beam is measured. The off-time for the magnetic field is increased in order to reduce the minimum recoil velocity for escaping the trap, and the effect on the atom loss is studied. Preliminary analysis shows that the observed fractional ejection rate corresponds to an electron-impact cross section of about $5x10^{-15}$ cm^2 at 50 eV.**

*Supported by the Air Force Office of Scientific Research, the National Science Foundation, and the Packard Foundation.

AB-6 Temporary Negative Ion States of Na, K, Rb and Cs P.D. BURROW and A.R. JOHNSTON*, U. of Nebraska, Lincoln– Electron transmission spectroscopy[1] is used to observe resonances in the scattering cross sections due to temporary negative ion formation. A strong "family" resemblance is apparent among the alkalis. From published calculations and angular scattering studies, the lower lying features are known with some confidence. Plausible assignments for some of the higher lying features are put forth. We propose that the absence of resonances at the Na 4^2P, 5^2P and Cs 5^2D thresholds is associated with the negative polarizabilities of these excited states.

*Present address: AT&T Bell Laboratories, 200 Laurel Avenue South, Middletown, NJ 07748-4801.

[1]L. Sanche and G.J. Schulz, Phys. Rev. A 5, 1672 (1972).

SESSION BA: NEGATIVE IONS IN PLASMAS
Tuesday morning, 18 October 1994
NIST Building 101
Red Auditorium, 10:15–12:00
L. G. Christophorou, presiding

Invited Paper

BA-1 Measurement of Negative Ions In Plasmas, F.J. de HOOG, Eindhoven U of Technology, The Netherlands

Negative ion production in plasma used to be the concern of the fusion and gaseous breakdown communities. Through recent development in plasma etching and plasma deposition applications of electronegative gases, the rôle of negative ions in plasma gained renewed interest. The study of the behaviour of negative ions in discharges is hampered by the fact that in an active plasma these ions will not be transported out of the plasma. Various model studies show the influence of the negative ions on the overall transport properties of the plasma, e.g. the Bohm velocity. Although through mass spectrometric detection and Langmuir probe measurements new results have been obtained, absolute detection of negative ion species and their densities remains difficult. Some promising laser techniques make use of photodetachment and subsequent galvanic or nongalvanic detection of the photoelectrons. Results of these technique for halogen or oxygen containing RF plasmas will be presented. Interest in negative ions as precursors of nanoparticle formation in silane containing plasmas underline the importance of developing advanced methods for their detection.

Contributed Papers

BA-2 Modeling of O_2 RF Glow Discharges by RCT Model, M.SHIBATA,* N.NAKANO and T.MAKABE, Keio Univ.

O_2 rf glow discharges have been applied to various plasma processings of semiconductors such as etching of polymers, oxidation and resist removal . We investigated the spatiotemporal structure of O_2 rf glow discharges in 2cm gap parallel-plates for 13.56MHz by using the Relaxation Continuum (RCT) model.[1] We considered four ions (O_2^+, O^+, O_2^-, O^-) and electrons as the charged particles, and the ground-states O_2 and O as the neutral particles. The electron swarm parameter is prepared in advance from the Boltzmann equation over a very wide range of dc-E/N. The results for pressure of 0.1-1.0Torr and the sustaining voltage of 120-200sin(ωt)Volt are studied. In oxygen plasma, the presence of high density atomic oxygen strongly controls the spatiotemporal plasma structure. Electronegativity of the plasma depends on the density of atomic oxygen which varies as a function of discharge conditions.

[1] N.Nakano, N.Shimura, Z.Lj.Petrovic and T.Makabe, Phys.Rev.E 49,4455(1994)

*Permanent address: Process Development Division, FUJITSU LIMITED

BA-3 **Efficient Negative Ion Formation in UV-Laser Irradiated Silane: Implications for Plasma Deposition of Amorphous Silicon,*** L. A. PINNADUWAGE, M. Z. MARTIN, and L. G. CHRISTOPHOROU, Oak Ridge National Laboratory and Univ. Tenn., Knoxville - Observation of enhanced electron attachment to ArF-excimer-laser-irradiated silane is reported. Evidence is presented that highly-excited electronic states of silane or its photofragments, produced directly or indirectly via laser irradiation, may be responsible for the observed electron attachment. Since such excited states may be populated in silane plasmas, this may explain the recently reported large negative ion densities in silane plasmas.

*Work supported by the National Science Foundation under contract CHE-9022903, U. S. Air Force Wright Laboratory under contract F33615-92-C-221 with the University of Tennessee, Knoxville, and by the Office of Environmental Research, U.S. Department of Energy, under contract DE-AC05-84OR21400 with Martin Marietta Energy Systems, Inc.

BA-4 Photodetachment in a Dusty RF Discharge*, G.M.W. KROESEN, W.W. STOFFELS, E. STOFFELS, F.J. DE HOOG, TUE, Eindhoven, The Netherlands
In low pressure RF discharges, already after100 ms of discharge nanometer scale clusters are formed prior to larger particles.We have studied the charging kinetics of these fine clusters by means of laser-induced photodetachement of electrons from particles and negative ions in the plasma. The density decay of detached electrons after the laser shot is monitored by means of a microwave method. The decay frequency illustrates the charging kinetics of clusters. In the first 10 ms of the discharge (120 mTorr, 10 W, 5% in Ar) only a weak signal has been found, most likely from negative ions. Its decay frequency agrees with the attachment rate to SiH_4 (< 100 kHz). After about 50 ms of plasma operation the decay frequency of extra electrons becomes higher (200 kHz) and it increases further up to 1 MHz at 1 s of plasma operation. At the same time the free electron density in the discharge decreases, while the height of the photodetachment signal increases. This shows that after 50 ms of plasma operation clusters start to acquire negative charge and their charging frequency rapidly increases as they become larger.

*Work supported by the European Commission contract, BE II 7328

BA-5 **Negative Ion Kinetic Energy Distributions in Etching Plasmas***, B. SMITH and L. OVERZET., U. of Texas at Dallas - Cl^-, F^-, and other negative ions created in the body of the plasma may play an important role in many etching processes. We have used a quadrupole mass spectrometer equipped with a Bessel Box energy analyzer to find the species of positive and negative ions present in Ar, CF_4, and N_2 plasmas and their kinetic energy distributions. Modulated rf power at 13.56 MHz drives the plasmas for negative ion measurements. The ions are collected at the grounded electrode of a capacitively coupled reactor through a 100 micron pinhole. The energy resolution is approximately 1 eV. We report the time-resolved positive and negative ion energy characteristics of modulated plasmas to provide information about the plasma and sheath potential in modulated systems. Comparisons of positive ion energy distributions in continuous and modulated plasmas are also made.

* This work is supported in part by the National Science Foundation and by The State of Texas Advanced Research Program.

BA-6 Photodetachment of SF_6^- and $C_6F_6^-$ Negative Ions in the Gaseous Phase#, P. G. DATSKOS, L. G. CHRISTOPHOROU, and J. G. CARTER, Oak Ridge National Laboratory and University of Tennessee. - A method to measure the photodetachment cross section, $\sigma_{pd}(E)$, as a function of photon energy, E, is described. An electron swarm generated by a laser pulse at the cathode drifts (under an applied electric field) towards the anode and is depleted by attachment forming SF_6^- or $C_6F_6^-$. A second tunable dye laser pulse photodetaches these anions directly or via superexcited anionic states. The measurement of the ratio of the number of initial anions to the number of photodetached electrons allows $\sigma_{pd}(E)$ to be determined. For $C_6F_6^-$, the measured $\sigma_{pd}(E)$ exhibits (at least) two peaks for E $\leq$ 3.5 eV. In the case of SF_6^-, $\sigma_{pd}(E)$ increases monotonically with increasing E below 3.5 eV and has a threshold at ~3.2 eV. These findings will be reported and discussed.

#Research sponsored by the Wright Laboratory, U.S. Department of the Air Force, under contract No. AF 33615-92-C-2221 with the University of Tennessee and the Office of Health and Environmental Research, U.S. Department of Energy under contract No. DE-AC05-84OR21400 with Martin Marietta Energy Systems, Inc.

SESSION BB: DIAGNOSTICS
Tuesday morning, 18 October 1994
NIST Building 101
Green Auditorium, 10:15–12:00
H. Sugai, presiding

Invited Paper

BB-1 **Probe Measurements of RF Source and RF Bias Fields in Plasma Reactors***, J. E. STEVENS#, PPPL, Princeton NJ; M. J. SOWA and J.L. CECCHI, Univ. of New Mexico, Albuquerque NM - Magnetic induction probes are a well known technique for measuring rf (1-50 MHz) magnetic fields in helicon, ECR, and inductively coupled plasma (ICP/RFI/etc.) reactors. We have investigated several new issues with this technique. First, how does current flow to ground from the rf biased substrate of an ECR reactor? It was generally assumed that the rf power went into increasing ion energy at the sheath. We found that rf biasing of the substrate in an ECR launches a helicon mode which can carry away a significant fraction of rf power and produce additional, nonuniform ionization in front of the chuck. A related question is how rf currents flow to ground from the substrate in a high density, non-magnetized plasma source such as an ICP. These plasmas are opaque to rf fields and differ from the situation in parallel plate reactors where the ground surfaces are much closer than an rf skin depth. We have also investigated the operation of a novel m=0 helicon plasma source produced by a flat spiral coil. This source has no defined parallel wavelength and no separate source region, giving it the compactness of an RFI with the arbitrary reactor length of a helicon. RF power is absorbed in this plasma source through both collisional and collisionless processes depending on the neutral pressure.
*Work supported by SRC/SEMATECH; #now at Sandia Nat. Labs.

Contributed Papers

BB-2 **Theory of Electron Retardation for Langmuir Probes in Anisotropic Plasmas,*** R. CLAUDE WOODS, U. of Wisconsin, and ISAAC D. SUDIT, UCLA. - We have extended the theory used for obtaining electron velocity distribution functions (EVDFs) and electron densities from Langmuir probe characteristics and their derivatives in several ways. The cylindrical probe theory for an axisymmetric plasma is derived in a modified form and shown to be valid for arbitrary ratio of probe radius to sheath thickness. A new formulation that applies to plasmas with no velocity space symmetry at all is given; in it the EVDF is expanded into a series of spherical harmonic functions and the Volterra integral equations that need to be solved are shown to be no more complicated than those occurring in the axisymmetric case. The geometrical relationships between the various coordinate systems are handled using the theory to the irreducible representations of the 3-d rotation group. The complete EVDF can be extracted from probe characteristics of a one-sided planar probe at a sufficient number of orientations. It is proven that for a cylindrical probe or a two-sided planar probe at an arbitrary orientation in a plasma with no assumed symmetry in velocity space the usual Druyvesteyn method of obtaining the plasma density by integrating the second derivative of the probe characteristic, applied exactly as if the plasma were isotropic, yields the true result, subject only to the same assumptions that apply to the isotropic case.

* Work supported by the Experimental Physical Chemistry Program of the National Science Foundation.

BB-3 Degenerate Four-Wave Mixing Diagnostics of Atmospheric Pressure Plasmas,* T.G. OWANO, E.H. WAHL, C.H. KRUGER, R.N. ZARE, Stanford University - The applicability of degenerate four-wave mixing (DFWM) as a spectroscopic probe of atmospheric

pressure reacting plasmas has been investigated. This powerful, nonlinear technique has been applied to the measurement of temperature and radical species concentrations in the boundary layer of a diamond growth substrate immersed in a flowing atmospheric pressure plasma. In-situ measurements of CH and C_2 radicals have been performed to determine spatially resolved profiles of vibrational temperature, rotational temperature, and species concentration. Results of these measurements are compared with those obtained by optical emission spectroscopy (OES), and with the predictions of a detailed numerical simulation.

Research supported by the Department of Energy, Basic Energy Sciences, and the Engineering Research Center for Plasma Aided Manufacturing.

BB-4 A Microwave Spectroscopy System for Plasma Diagnostics in an Electron Cyclotron Resonance (ECR) Deposition Reactor,* JIAN CHEN, KOK HENG CHEW, and R. CLAUDE WOODS, Engineering Research Center for Plasma-Aided Manufacturing, U. of Wisconsin at Madison - A workstation-based microwave spectroscopy system in the frequency range of 75 - 110 GHz has been developed. The Gaussian beam optics based on Teflon lenses was used for radiation propagation in free space. Using carbonyl sulfide (OCS), the absolute sensitivity of this spectrometer has been determined; it corresponds to an absorption coefficient of $\sim 10^{-8}$ cm^{-1} for a path length of 48 cm. This spectrometer is used to monitor gas phase silicon-containing molecular species in ECR plasma deposition of silicon based films. The $J = 1 \rightarrow 2$ rotational transition of silicon monoxide (SiO) was detected in ECR plasmas of $O_2 + SiH_4$ (silane) and of O_2 + TEOS (tetraethoxysilane). The absolute line-integrated densities of SiO in both of these plasma chemistries can be obtained from the integrated spectral intensity of this microwave transition, while the translational temperature can be extracted from the spectral linewidth.

*Work supported by the National Science Foundation under Grant No. ECD-8721545, and by Hewlett-Packard Co. and Schumacher Co. in the form of equipment donation.

BB-5 Optical Emission and Electrical Discharge Properties of High Pressure Pulsed RF Gas Discharges,* S.R.HUNTER, Consultec Scientific, Inc., and W.A.GIBSON, Pellissippi International Inc. - Time dependent pulsed RF excitation and fluorescence studies have been performed on ionizing radiation particle tracks in N_2/Ar and TMAE/Ar gas mixtures over the concentration range 1-10% (total gas pressure = 100-700 torr), using pulsed high voltage (up to ≈ 30-40 kV) RF field excitation (f = 27.125 MHz, duration ≈ 1-5 μs, $E/N_{av} = 10^{-16}$ - 10^{-15} V cm^2). The pulsed RF field excites the subexcitation electrons in the particle track, leading to additional ionization and electronic excitiation of the surrounding gas, and to the emission of light. The UV to visible radiation (220 - 600 nm) was imaged by a fast intensified CCD digital camera (shutter speed ≈ 0.1-20 μs) with single photon sensitivity. The spatial resolution of the observed particle track (primarily limited by the drift and diffusion of the subexcitation electrons in the particle track before and during excitation by the RF field) and sensitivity (governed by the wavelength and production efficiency of the radiation produced by the excited gas) with which the ionizing particle track is imaged are critically determined by the chamber gas composition and pressure, and RF pulse duration, frequency and amplitude. Electrical breakdown, relative optical emission efficiencies, and spatial resolution measurements of tracks produced by α and β particles will be reported as a function of the RF pulse duration and magnitude, and camera exposure time.

*Work supported in part by NCI, NIH, under grant No. CA45869-03

BB-6 Optical Emission Tomography of RF Plasma Processing Tools with Small Windows,* James Paul Holloway & Samuella Pollack, *University of Michigan.*

There is much interest[1] in using the Able integral equation as the basis for spatially resolved optical emissivitiy measurements in processing plasmas. The application of this method relies on the collection of light along parallel chords across the cylindrically symmetric plasma, necessitating the use of a large window and carefully aligned optics. We have worked out the analytic mathematics necessary to perform optical emissivity measurements using light collected from wedge shaped regions of the plasma (as would be seen by fiber optics looking through a narrow horizontal slit) centered around converging chords. This allows more light to be collected (potentially improving signal to noise ratios for faint fluorine lines) and allows the light to be collected through a much smaller window.

*Supported by NSF grant ECS-9358344.

[1] J. Pender *et al.*, J. Appl. Phys. **74**(5), 3590 (1993).

BB-7 Collisional Ionizations in Neon DC Discharge*. X.L.Han†, N.J.Perry, Dept. of Phys. and Astron.; V.Wisehart, and M.C.Su†, Dept. of Chemistry, Butler University. —— When a pulsed laser is tuned between two Ne excited levels in a DC discharge environment, the DC discharge current will experience a perturbation. This is known as the optogalvanic effect, and it is often considered too complicated, because so many processes contribute to its outcome. In this work, we present an experiment and a simple theoretical model that will greatly improve our understanding of Neon optogalvanic effects. We will present our extensive studies on Ne optogalvanic effect involving two energy levels which shows excellent agreement between theory and experiment. We will also present our preliminary results involving four energy levels. Our results indicate that we have identified the most important processes in optogalvanic effects. Our work also makes the connection between the fundamental collision cross sections and its effects in DC discharges.

* Supported by the Holcomb Research Institute, Butler University.

† Also with the Holcomb Research Institute, Laboratory for Quantum Physics, Butler University.

SESSION CA: PLASMA-SURFACE INTERACTIONS
Tuesday afternoon, 18 October 1994
NIST Building 101
Red Auditorium, 13:30-15:30
W. L. Hsu, presiding

Invited Paper

CA-1 Dynamics of Hyperthermal Atom-Surface Interactions during Steady-State Etching, K. P. GIAPIS and T. MINTON, CALTECH and JPL- A new technique to generate high fluxes of hyperthermal (≥ 2 eV) neutral beams of halogen atoms has facilitated the study of their inelastic and reactive scattering on semiconductor surfaces during steady-state etching. The fluorine plus silicon system was chosen for its fundamental and technological importance. By using a rotatable quadrupole mass spectrometer in a Time-Of-Flight mode of operation, we have *angularly resolved* the flux and energy distribution of fluorine atoms after the collision with the etched surface. A low (3.2 eV± 0.4 eV) and a high (6.4 eV± 1 eV) incident

translational energy have been employed. It is found that, for both energies, the flux-weighted angular distribution of inelastically scattered fluorine atoms peaks near the specular direction rather than following the widely assumed cosine law. More remarkably, for wide incident angles, the unreacted fluorine atoms scattering in the specular direction were measured to retain up to 60% of the incident energy. This wide-angle scattering mechanism dramatically affects profile evolution and explains phenomena such as microtrenching and reverse microloading. The reactive scattering was also angularly resolved. Bimodal product distributions were recorded with a dominant fast component for all SiF_x products monitored. SiF_2 was found to be the fastest moiety scattered from the surface, an indication that it is a direct reaction product. An analysis of our findings and a critical comparison with the literature will be presented.

Contributed Papers

CA-2 Energy distributions of ions and atoms sputtered by inert and reactive incident species S.P. MOUNCEY, R. Md NOR and W.G. GRAHAM. The Queen's University of Belfast, N. Ireland. An understanding of ion-surface interactions is not only of fundamental importance but is of great significance in understanding how a plasma interacts with it's surroundings. Here the interactions of 0.4 to 3.6 keV ions, both inert eg. Ar^+ and reactive eg. CF_x^+ with copper, silicon and aluminium surfaces has been investigated by measuring the energy distributions of the sputtered materials. The neutral particles are post ionised by a nonresonant multi-photon ionisation technique. The energy distributions are obtained by a combination of quadrupole and time-of-flight analysis. The linear collision cascade model is found to be generally valid for ions produced by atomic ion impact but for sputtered atoms and also for incident reactive species a more complex energy distribution is observed. This work was supported by UK SERC.

CA-3 Secondary Electron and Anion Emission from Surfaces at Low Impact Energies* J. C. TUCEK, D. H. BAKER, S. G. WALTON and R. L. CHAMPION, College of William and Mary -- Absolute yields for the sputtering of secondary electrons and negative ions due to collisions of alkali positive ions with heterogeneous metallic surfaces have been measured for impact energies E < 500 eV. The electron and anion yields, $Y_e(E)$ and $Y_i(E)$, behave in a remarkably similar manner as both the impact energy and the surface work function are varied, with both $Y_e(E)$ and $Y_i(E)$ exhibiting energetic thresholds for impact energies in the vicinity of E ≈ 50 eV. This, and the mass spectra of the sputtered anions, leads one to the conclusion that the high secondary electron yields observed in these experiments are caused by surface adsorbates (e.g., an oxide layer on Mo) or by an interstitial species (e.g., hydrogen in Nb). Specifically, it is suggested that sputtered negative ions, some of which detach when exiting the surface, serve as precursors for secondary electron emission.

*Supported in part by the U.S. DOE, Division of Chemical Sciences, Office of Basic Energy Sciences.

CA-4 **Dependence of Surface Dissociation of CH_x^+ Ion on Bombarding Energy**, Y. MITSUOKA,* H. TOYODA, H. SUGAI, Nagoya University, Nagoya, Japan, S. MUKAINAKANO, T. HATTORI, Research Labs, Nippondenso Co., Ltd., Aichi, Japan - There has been a great need to understand ion-surface interactions in plasma-assisted deposition and etching. In this paper, we describe observation of dissociation of $CH_x^+(x=2\text{-}4)$ ions incident on such materials as Al, Pt and InGaAs/InAlAs. An ionic species $CH_x^+(x=2\text{-}4)$ is extracted through a mass filter from a methane plasma and irradiated on a target material. In the case of CH_4^+ incidence, two types of dissociation processes are clearly found, depending on the incident energy E. One is the dissociation into CH_3^+ and CH_2^+ for $E < 30$ eV, and the other is the fragmentation into CH^+ and C^+ for $E > 100$ eV. Tentatively, the former is explained by dissociation of the molecule excited electronically with charge neutralization on the metal surface, and the latter by dissociation of the molecule excited vibrationally due to high translational energies.

*Permanent address: Research Laboratories, Nippondenso Co., Ltd., Nissin-cho, Aichi 470-01, Japan

CA-5

Energy Transfer Dynamics of Low Energy Ions Incident on Gold,M.E. BARONE, and D. B. GRAVES, U.C. Berkeley – Molecular dynamics simulations of energy transfer from low energy (<300 eV) rare gas ions (Xe, Ar and He) to gold surfaces have been performed. The simulations reproduce the recent experimental measurements of Winters and co-workers on the same system[1]. The Au-Au interactions were modelled using a Morse potential and the ion-Au interactions were described by a Moliere potential. These approximate potentials appear to capture the essential details of ion to substrate energy deposition. At very low incident ion energies (<20 eV) the fraction of kinetic energy deposited drops dramatically as a function of energy. Molecular dynamics simulations are ideal for exploring the details of ion-surface interactions at low energies because the technique captures the collective and many-body effects that can usually be neglected at higher energy (>1000 eV). We examine sputter yield, trapping and desorption probability of the ion, and penetration depth of the ion as a function of ion energy, mass and angle of incidence. Video illustrations of energy transfer are provided.

[1] H. Winters, H. Coufal, C. Rettner and D. Bethune, Physical Review **B41**, 6240-6256 (1990).

CA-6 **An In situ Investigation of Plasma-Surface Interactions During PECVD**, E. S. AYDIL and S. C. DESHMUKH, *UC-Santa Barbara* — Amongst all the phenomena that affect the properties of films deposited using plasma enhanced chemical vapor deposition (PECVD), surface reactions and plasma-surface interactions remain the least understood. In this talk, we address the question of what happens on the wafer surface during PECVD of SiO_2 from a tetraethylorthosilicate (TEOS) and O_2 plasma sustained by a helical resonator. Towards this end, we have used attenuated total reflection Fourier transform infrared (ATR-FTIR) spectroscopy to study surface reactions during SiO_2 PECVD. The goals are to identify and elucidate processes that govern the properties of the PECVD films and to improve our understanding of the fundamental phenomena occurring in PECVD processes, particularly on surfaces. ATR-FTIR studies were conducted on thin (~ 50 Å) silicon dioxide films deposited on GaAs. This approach allowed us to obtain the infrared spectrum of TEOS adsorbed on SiO_2 in the spectral region 4000 cm^{-1}–770 cm^{-1} for the first time. Studies were conducted where SiO_2 surface was exposed to TEOS and O_2-plasma sequentially and/or simultaneously. Surface processes were studied as a function of exposure to TEOS and substrate temperature. The insight gained from the ATR-FTIR studies allowed us to deposit SiO_2 films from an $TEOS/O_2$ plasma, with properties approaching to those of thermal oxide, even at room temperature.

SESSION CB: DIAGNOSTICS AND CONTROL
Tuesday afternoon, 18 October 1994
NIST Building 101
Green Auditorium, 13:30-15:30
M. D. Bowden, presiding

Invited Paper

CB-1 Absorption Spectroscopy of Diamond CVD Reactors, L.W. ANDERSON, K.L. MENNINGEN, M.A. CHILDS, and J.E. LAWLER Univ. of Wisconsin-Madison–Absorption spectroscopy has been carried out on both hot filament and hollow cathode dc discharge diamond CVD reactors. We have observed absorption spectra of C, CH, CH_3 CH_4, C_2H_2, H, and H_2. A synchrotron experiment between 115 and 185 nm yields spectra of C, H, vibrationally excited H_2, C_2H_2, and CH_4 with a fractional sensitivity for absorption of 10^{-3}. Multichannel absorption spectroscopy between 190-420 nm yields spectra of CH_3, CH, and C_2H_2 with a sensitivity of 10^{-5}. We find CH_3, CH_2, CH and C to be in partial equilibrium with each other via reactions with H and H_2. The observed CH_3, CH, and C densities yields the dissociation ratio $[H]/[H_2]$ as a function of position in the reactor. We find $[H]/[H_2]$ ratios larger than those reported by other techniques. We have also studied the poisoning of the hot filament by hydrocarbons and have observed impurities such as Ta and Zn under certain conditions.
*Work support by a grant from the Army Research Office and a grant from the NSF to the Synchrotron Radiation Center.

Contributed Papers

CB-2 **Nonlinear Spectroscopy for Diagnostics of Plasma Chemistry**, D.S.GREEN and J.W.HUDGENS, National Institute of Standards and Technology - Nonlinear laser spectroscopy based on degenerate four-wave mixing (DFWM) has been used to study the plasma-assisted generation of radicals. Transient radicals generated in a microwave discharge and from the reaction of fluorine atoms with various reagents, including ammonia and selected hydrocarbons, have been probed in a flow reactor. DFWM spectra were used to identify product species' and map the downstream concentration and temperature distributions. Measurements were made as a function of discharge operation and reaction conditions including gas mixing ratio, flow rate and pressure.

CB-3 **H_α (Balmer) Spectral Profiles Obtained from H_2 RF Plasma Discharges Studied by Intracavity Laser Spectroscopy**, M.J. LIPP and J.J. O'BRIEN, U. of Missouri-St.Louis - H_α (Balmer) spectral absorption profiles are obtained for 13.56 MHz RF discharges of hydrogen at pressures from 25 mTorr to 3.0 Torr. The H_α transitions are monitored by intracavity laser spectroscopy using high spectral resolution (> 500,000). Spatially resolved number densities of excited atomic hydrogen (n=2) (H^*) are measured across the region between the electrodes. The spatial H^* density distribution correlates with the region of the glow space. Electron densities are measured using microwave interferometry and are 1-3 x 10^{10} cm^{-3}. Analyses of the H^* profiles indicate that at low pressures (i.e., < 50 mTorr) nearly all the H^* are in the $2S_{1/2}$ and $2P_{1/2}$ states, whereas at higher pressures the $2P_{3/2}$ state also becomes populated. The profiles indicate that this occurs due to collisions of $2S_{1/2}$ and $2P_{1/2}$ atoms with other species in the discharge. The profiles show that the system is not in thermodynamic equilibrium but approaches it at pressures greater than 500 mTorr. The intracavity laser beam is normal to the direction of the electric field in the discharge. No evidence for fast H^* atoms (> 1eV) is observed which implies the motion of the majority of the fast species is normal to the laser beam.

CB-4 **2-D Argon Metastable Density Measurements in RF Plasmas by Laser-Induced Fluorescence Imaging**, B.K. McMILLIN and M.R. ZACHARIAH, National Institute of Standards and Technology, Gaithersburg, MD - Two-dimensional measurements of the time-averaged argon $1s_5$ metastable density distribution were obtained in a low pressure, 13.56 MHz parallel-plate discharge using planar laser-induced fluorescence imaging. The measurements were performed in an asymmetrically-driven Gaseous Electronics Conference reference cell and cover a wide range of conditions (13.3-133.3 Pa and 75-300 V). Generally, the measured density fields show significant radial and axial variations that depend more strongly on pressure than applied voltage. For example, the metastable density typically increases radially from the center of the discharge to the near the edge of the plasma by ~10-30 %. As the pressure is increased, the peak metastable density increases by ~3 times and the axial distribution changes from a center-peaked parabolic-like profile to an asymmetric profile peaked near the powered electrode. While our measurements to date have centered on pure argon discharges, we are currently investigating argon discharges diluted with either Cl_2, O_2, or CF_4, and will present additional results from these experiments.

CB-5 **Thomson scattering experiments on a 100 MHz argon Inductively Coupled Plasma**, J.M. DE REGT, R.A.H. ENGELN, J.A.M. VAN DER MULLEN and D.C. SCHRAM - To improve the applications of an inductively coupled plasma in spectrochemical analysis and in the use for light sources, Thomson scattering experiments are carried out using a photodiode array. This allows us to obtain the Thomson scattered profile with high spectral resolution. The profile gives the electron temperature and after calibration also the electron density. For the calibration the less conventional method of Raman scattering on nitrogen is chosen. The advantage is that stray light will no longer disturb the calibration. The inaccuracy in the electron temperature is about 500 K and in the electron density about 15%. The measurements show a large skin effect compared to the 27 MHz ICP as known from Huang[1] *et al.* This is due to the relatively high frequency (100 Mhz) of our generator. Typical max. values at 7 mm ALC and with 1.2 kW input power are T_e = 9000 K and $n_e = 4.5\ 10^{21}\ m^{-3}$.

[1] M. Huang, D.S. Hanselman, P.Yang and G.M. Hieftje, Spectr. Ch. Acta 47B, 765 (1992).

CB-6 **Population and Temperature Measurements in a Nonequilibrium Microwave Plasma**, M.H. GORDON and U. KELKAR, High Density Electronics Center, University of Arkansas at Fayetteville - Emission measurements have been acquired in a nonequilibrium microwave plasma used for diamond deposition (300

sccm H_2, 3 sccm CH_4, 40 Torr pressure, 1.6 kW input power). Measurements of atomic hydrogen excited state populations are compared with a zero-dimensional collisional-radiative model which accounts for deviations from a Maxwellian electron velocity distribution. The model uses as input an electron energy distribution function (average energy around 1 eV) and the total electron density (around 10^{19} m^{-3}) to calculate atomic hydrogen excited state populations. Relevant cross-sections for electron-atom and radiative processes are taken from the literature. Results show qualitatively good agreement between the experimental and the numerical data and clearly demonstrate the presence of nonequilibrium. These results also suggest possible methods for interpreting in-situ optical emission measurements which are relatively easy to acquire.

CB-7 Multi-Variable Feedback Regulation of Plasma Processing Reactors, M. A. FIRESTONE, JAYCOR - This paper will illustrate how model based, multi-variable feedback control can be used in plasma processing reactors. As an example, I will show how such a feedback scheme can be developed for a microwave plasma reactor. However, the methodology is generic and can be used for any plasma processing device. Modern multi-variable control techniques make use of the inherent system dynamics to derive stable robust feedback gains that are optimized for the desired objectives and reactor conditions. To show the feasibility of this approach for complex nonlinear systems, simulated results from plasma control in a tokamak reactor will be presented. Here, plasma position, shape, and current were simultaneously controlled with current density, temperature, and particle density profiles in a 160 state variable system.

SESSION D: POSTER SESSION
Tuesday afternoon, 18 October 1994
NIST Building 101
Lecture Rooms A and B
and Employee Lounge, 15:45-17:30
J. R. Roberts, presiding

DA: ELECTRICAL-OPTICAL DIAGNOSTICS

DA-1 Time Transients of the Vibrational Excitation in the Pulsed Nitrogen Discharge * ALEXANDER ERSHOV, EDWARD AUGUSTYNIAK and JACEK BORYSOW, Physics Department, Michigan Tech. University - The vibrational excitation to $v = 1$ level of the ground electronic state of nitrogen was measured in a positive column during the 40 μs pulsed electric discharge, and in the afterglow. The discharge was operating at 6 Torr pressure and at current densities in the range 0.7-6.4 A/cm^2. Temporal evolution of $N_2(X)$ vibrational excitation was measured using Coherent Anti-Stokes Raman Scattering (CARS). Vibrational temperatures were found to be ranging from 700 to 4000 K. The results are in fair agreement with model calculations based on energy transfer to vibrational excitation. Vibrational temperatures of $N_2(X)$ state, obtained from direct CARS measurements, were up to a factor of three below those deduced from the second positive system emission.

* Supported by The State of Michigan Research Excellence Fund

DA-2 Rotational/Vibrational Excitation within $X^1\Sigma_g^+$ State of N_2 in a Pulsed Electrical Discharge * JACEK BORYSOW and SERGUEI FILIMONOV, Physics Department, Michigan Tech. University - Time transients of vibrational/rotational excitation up to $v = 7$ level of the ground electronic state of nitrogen were measured in a positive column during the 1-3 μs long pulsed electric discharges, and in the afterglows. Current densities were up to 25 A/cm^2, and pressures up to 6 Torr. It is shown that initially energy is primarily being transfered, into vibrational levels above $v = 1$, resulting in a highly non Boltzmann distribution. The redistribution between vibrational levels takes place within 100 μs after the discharge pulse. Beyond 100 μs the vibrational population becomes of Boltzmann type. Significant rotational heating was observed in the afterglow and is attributed to collisions with electrons. The rotational temperature was as high as 3500 K and reached maximum values between 80 and 100 μs after the discharge pulse. Standard, Coherent Anti-Stokes Raman Scattering (CARS) spectroscopy was employed in all measurements.

* Supported by the 3M Foundation

DA-3 Atomic Density measurement of Cu in a Cylindrical magnetron Discharge, H-J. KIM, B.W. JAMES and I. S. FALCONER, School of Physics, U. of Sydney, Australia - Absorption spectroscopy and Hook Interferometry is being used to investigate the transport of sputtered copper atoms in a cylindrical magnetron discharge. The absorption has been made with a hollow cathode lamp and with a continuous spectral light source for both the 325 nm and 327nm resonance lines. The hook interferometry used a Mach-Zendher interferometer with photographic detection. The assumptions involved in these measurements are examined carefully and the results compared.

DA-4 Theoretical Study of the B^2A_1'–X^2A_2'' Band Transition of CH_3 *. ATUL D. PRADHAN, —

Multireference configuration interaction wavefunctions (MRCI) and quartic potential energy surfaces have been calculated for the X^2A_2'' and B^2A_1' states of CH_3. Fundamental frequencies and spectroscopic constants are determined and comparison is made to available experimental data. Dipole moment functions of the X and B states are presented as well as the B-X transition dipole. The B^2A_1'–X^2A_2'' transition dipole is utilized in computing the oscillator strengths, radiative lifetimes, and ro-vibrational intensities of the B-X system.

***This work is supported by the Office of Aeronautics (NASA) through its funding of an NRC Research Associateship.**

DA-5 Carbon Content Analysis of Mineral Coal Using Hollow Cathode Plume Spectroscopy, R. D. SEXTON, S. M. MAHAJAN, C. A. VENTRICE and S. S. MUNUKUTLA, Tenn. Tech. Univ. – The emission spectrum from a hollow cathode argon gas discharge was used to measure the carbon content of mineral coal. The base of the hollow cathode consisted of a copper matrix which was embedded with pulverized coal. The

emission spectrum was analyzed using a Spex 0.5 meter spectrometer interfaced with a computer. Four prominent emission lines of both carbon (247.8, 283.7, 392.0 and 426.7 nm) and copper (282.4, 324.7, 327.4 and 427.5 nm) were used in the analysis. Three samples of coal from different geographical locations were used in the study. Relative intensities of the carbon lines are consistent with the carbon content of the coal which was determined from the chemical analysis.

DA-6 Electron Energy Distribution Function in an RF Inductive Discharge over a Wide Range of Argon Pressure, V.A. Godyak, R.B. Piejak and B.M. Alexandrovich, OSRAM SYLVANIA INC., Danvers, MA - The electron energy distribution function (EEDF) has been measured in an inductively coupled plasma driven at 13.56 MHz using a Langmuir probe. EEDF's in the RF current zone were measured together with electrical discharge characteristics over a wide range of argon gas pressure between 1 mTorr and 1 Torr. The discharge was maintained by an internal induction coil which was electrostatically shielded to provide a purely inductive discharge. All measurements were related to RF power dissipated in the plasma. Non-Maxwellian EEDF's were found that differ significantly from those found at the same discharge power and argon pressures in capacitive RF discharges and in inductive discharges without electrostatic shielding .

DA-7 Magnetic Field Distribution Measurements in a Low Pressure Inductive Discharge, R.B. Piejak, V.A. Godyak and B. M. Alexandrovich, OSRAM SYLVANIA INC., Danvers, MA - A b-dot (dB/dt) probe has been built to measure the magnetic field in an inductively coupled (13.56 MHz) low pressure argon discharge. The discharge is maintained by an electrostatic shielded solenoidal coil that is coaxially surrounded by plasma. Magnitude and phase of an axially induced magnetic field have been measured as a function of discharge radius. Assuming a one dimensional radial symmetry about the axis, the radial dependence of current density and induced electric field have been determined as a function of discharge radius. Measurements were made between 3 and 300 mTorr (at constant discharge power) and between 25 W and 100 W (at constant gas pressure) and suggest that b-dot probe data can be useful in determining the spatial variation of plasma current and induced electric field in inductive discharges.

DA-8 Measurement of Electron Densities in non-resonant Microwave-powered Gas Discharges
H.F.MERKEL, H.-P.POPP, Graduiertenkolleg Numerische Feldberechnung, Universität Karlsruhe
The resonance shift of microwave modes is frequently used to obtain electron densities in microwave-powered discharges. A considerable simplification is achieved avoiding the measurement of the reflection coefficient of the power mode and using an orthogonal mode instead. In non-resonant microwave-powered plasmas evanescent modes leading to far-off resonance frequencies and cutoff-shifts due to the plasma are used to obtain electron densities in rotational symmetric high-pressure plasmas. The measured resonance data has to be filtered and the resonance shift is extrapolated using arctan functions in phase space. The resonance frequencies are calculated in zero order approximation assuming an effective evanescent length and a variation of the dielectric function in the plasma. The evanescent length is determined by calculation of the damping properties and the obtained electron densities are compared to spectroscopic results.

DA-9 Electrical Impedance of Plasma Sheaths and Plasma Glow Regions of Asymmetric RF Discharges in Argon, M. A. SOBOLEWSKI, NIST.

Measurements of the current and voltage at both electrodes of the GEC Reference Cell have been combined with capacitive probe measurements of the rf potential inside the cell, within the plasma glow. Together, these measurements completely determine the rf voltage, current, and impedance across each sheath and across the glowing regions of the plasma. Argon discharges were studied in detail, for pressures of 1.3-133 Pa (10-1000 mTorr) and peak-to-peak applied voltages ≤ 400 V. Simple power laws were found to describe the changes in the sheath and glow impedances observed as voltage and pressure were varied. Using these power laws, an equivalent circuit model for the electrical behavior of the discharge was obtained. The model contains a minimal number of parameters, yet it is valid over the entire range of experimental conditions. The equivalent circuit model can be used to relate electrical measurements at the electrodes to plasma properties such as electron densities, ion currents, sheath widths, and sheath potentials. Additional results for other gases and applications of the electrical measurements as real-time sensors of plasma properties will also be discussed.

DA-10 X-Ray Imaging During Plasma-Source Ion Implantation.* J.L. SHOHET, M. PIPER, J.H. BOOSKE, K.H. CHEW, J. JACOBS, L. ZHANG Engineering Research Center for Plasma Aided Manufacturing, U of Wisconsin-Madison - Plasma-source ion implantation (PSII) is a technique which has been optimized for surface modification of materials. Targets to be implanted are placed directly into a plasma source and then pulse biased with a high negative potential.[1] X-rays are generated during each pulse. This work describes techniques for imaging and spectral analysis of the x-rays. The goal is to relate the x-ray intensity and spectrum to the implantation dose so that it may be used as a process monitor and a control sensor. A pinhole camera was mounted on top of the PSII chamber to image the x-rays being emitted as electrons collided with surfaces of the chamber. Using 40 μs, 100 hertz implantation pulses at 10-15 kV and exposure times from 5 to 15 minutes, clear images were observed. These show that x-rays are generated at the chamber walls and near the target. Spectral analysis and time dependence of the X-ray emission will also be presented.

*Work supported by NSF grant #ECD-8721545
[1] J.R. Conrad, J.L. Radtke, R.A. Dodd, F.J. Worzala, and N.C. Tran, J. Appl. Phys. 62, 11 (1989)

DA-11 Comparison of Microwave Interferometer and Langmuir Probe results in the GEC reference reactor.* J. XIE, L. J. OVERZET, R. DOYLE† and M. B. HOPKINS†, University of Texas at Dallas, Richardson, TX 75083. — A Langmuir probe and microwave interferometer have been combined to measure the electron density in the GEC reference reactor. The two techniques track one another in predicting the electron density in helium,

nitrogen and argon. The electron temperature for argon discharges was approximately constant for an rf excitation between 250 and 450 Volts at 200 mTorr while it decreased slightly in nitrogen and increased somewhat in helium. The energy distribution functions of helium discharges indicated the presence of large energy electrons, while those of nitrogen exhibited a "hole" near the energy of the resonant peak in the vibrational excitation cross section which has been noted previously.[1]

* Work supported in part by the National Science Foundation and The State of Texas Advanced Research Program.

[1] M. B. Hopkins, C. A. Anderson and W. G. Graham, Europhys. Lett. 8, 141 (1989).

† Dublin City University, Dublin, Ireland

DA-12 Mass Spectrometric Diagnostic of a D.C. Electrical Discharge During a Plasma Nitriding Process*, C.V. SPELLER, P. Egert. A.R. DE SOUZA AND J.L. MUZART, Physics/LABMAT-U. F. Sta. Catarina, Brazil The main purpose of this work is to investigate the influence of oxygen on plasma nitriding of steel samples. Oxygen is very reactive and can be a contaminant from air and thus cannot be neglected in studies of the plasma nitriding process. The investigation was carried out in a d.c. low pressure discharge (3 Torr) in $N_2 - H_2 - O_2$ mixtures. Measurements were also made in $N_2 - O_2$. A quadrupole mass spectrometer (VG-SXP 600 Elite) coupled to a plasma-ion nitriding reactor through a small orifice was used to investigate the chemical composition in the discharge reactor during the nitriding process. Several products, such as N, NH_n, NO, as well as CO_2 were identified and their fragment intensities were studied as a function of oxygen concentration. Microstructural analysis of the treated steel samples shows no significant modification of the nitride white layer up to 3% of O_2 in the mixture. The results are interpreted in terms of probable reactions involving O_2 and H_2. These diagnostics are important for modeling the plasma-nitriding process.

* Supported by PADCT/FINEP, FUNCITEC and CNPq (Brazil).

DA-13 The UK GEC Reference Reactor*: comparison with previous benchmarks and time - resolved data, C.M.O. MAHONY, K.F. AL-ASSADI, W.G. GRAHAM, Queen's University Belfast, N. Ireland & N. StJ. BRAITHWAITE, Open University Oxford Research Unit, Oxford, England. - The UK GEC Reference Reactor has been commissioned and the experimental programme is under way. It has been set up to operate in the asymmetric capacitative mode initially using argon as the working gas. The first objective is to calibrate the plasma reactor using a single loop current and cylindrical voltage probe for comparison with benchmark I-V data published by others in the community. Plasma parameters will be measured using a compensated Langmuir probe technique. Work will then move on to correlate time resolved I-V measurements with optical emission signals. Results of these experiments will be presented.

*Work supported by the Engineering and Physical Sciences Research Council for Great Britain and Northern Ireland.

DA-14 Time resolved impedance measurements of pulsed rf discharges,* L. J. OVERZET, University of Texas at Dallas, Richardson, TX 75083. — The impedances of pulsed rf discharges in the Gaseous Electronics Conference Reference Reactor have been measured with sub-microsecond time resolution. The real part of the impedance of a 500 mTorr argon discharge determined by i-v measurements, decreases from approximately 200 Ω to 75 Ω, while the magnitude of the discharge reactance decreases from –450 Ω to –400 Ω. The measurements indicate that the rf electric field can initially penetrate the glow region of the discharge and cause the electron collision frequency (and average energy) to be larger than that in the continuous glow. The power to a 500 mTorr argon glow also requires approximately 500 microseconds to reach a steady state. At first, the delivered power is larger than that at steady state and it decreases with time toward the steady state value. Similar results in other discharge gases will also be presented.

* Work supported in part by the National Science Foundation, The State of Texas Advanced Research Program, and Texas Instruments Incorporated.

DA-15 Fractional dissociation of hydrogen in an rf discharge determined by probe and emission measurements. K. AL-ASSADI[1], K. DONNELLY[2], V. KORNAS[3], T. O'BRIEN[3], H.F.DöBELE[3], D. DOWLING[2] and W.G. GRAHAM[1]. The Queen's University of Belfast, N. Ireland. 2. Forbairt, Dublin, Ireland and 3. Universität GH Essen, Germany. The fractional dissociation of hydrogen in a rf discharge has been determined from combined Langmuir probe and emission spectroscopy measurements. A passively-compensated Langmuir probe was used to measure the electron energy distribution function while the relative intensity of the Balmer lines of atomic hydrogen and Fulcher bands of molecular hydrogen were determined from emission spectroscopy. Using the appropriate electron impact excitation cross sections it was possible to determine the fractional dissociation. These values are compared with a two photon LIF measurement of the atomic fraction, details of which are described in an accompanying paper. The preliminary results indicate that the probe and spectroscopy measurements tend to produce higher dissociation values than the lif-based measurements. A critical assessment of the potential errors will be presented. This work is supported by the EU BRITE EURAM program.

DA-16 Thomson Scattering Diagnostics of an Excimer Laser Plasma Using a Picosecond Laser, K. UCHINO, Y. KAWANABE, H. YAMAKOSHI, K. MURAOKA, M. MAEDA, A. TAKAHASHI and M. KATO, Kyushu U., Mitsubishi Heavy Industries, Ltd. and Fukuoka U. - Thomson scattering from plasmas in high-pressure discharges for rare-gas halide excimer laser pumping[1] was observed using a frequency-doubled 300 ps Nd:YAG laser. A temporal resolution of 1 ns was realized for the Thomson scattering measurement, and detailed temporal changes of the electron density and temperature were measured in Kr/Ne, Kr/He and Kr/F_2/Ne plasmas. Calculations using a computer simulation[2] showed good agreement with the experimental results, implying that the plasma dynamics is properly treated in the simulation.

[1] K. Uchino et al., J. Appl. Phys. 70, 41 (1991)
[2] M. Maeda et al., Jpn. J. Appl. Phys. 21, 1161 (1982).

DA-17 Gas Temperature Dependent Efficiency of Atomic Argon and Xenon Lasers, * GREGORY A. HEBNER, Sandia National Laboratories, Albuquerque NM, - Peak laser power and total laser energy have been measured for both the 1.73 and 2.03 μm atomic xenon, and the 1.27 and 1.79 μm atomic argon laser transitions. Nuclear pumping using ^{235}U fission-fragments provided pump powers between 2-10 W/cm^3. Time dependent laser output showed that the laser threshold increased as the gas temperature increased; consistent

with previous measurements of the atomic xenon small signal gain. The 2.03 μm xenon output power and energy were relatively insensitive to gas temperature for temperatures below 450 K. This was in contrast to the rest of the laser systems investigated in that they show minimal thresholds before the peak laser power and energy decreased with increasing gas temperature. The similarity between the temperature dependence of the atomic xenon and argon systems supports the conclusion that the temperature dependent kinetic processes are similar for the two laser systems.

*This work was performed at Sandia National Laboratories and supported by the United States Department of Energy under contract number DE-AC04-94AL85000.

DA-18 Ion Energy Distributions for Ar^+ Ions in Argon-Nitrogen Mixtures, R. SUROWIEC, *Univ. of Liverpool*, J. A. REES, *Univ. of Liverpool and Hiden Analytical*, J. K. OLTHOFF, S. B. RADOVANOV, R. J. VAN BRUNT, *NIST*, — Measurements of the energy distributions (ED) of Ar^+ ions arriving at the grounded electrode of a GEC rf Reference Cell have been carried out using mixtures of argon and nitrogen for total gas pressures in the range of 1.3 to 33.3 Pa. As expected, the flux of Ar^+ ions decreases as the proportion of nitrogen in the mixture increases and, particularly at low pressures, the EDs show an increase in the proportion of low energy ions. The EDs have been modeled using a Monte Carlo code which includes estimates of the effects of charge exchange from Ar^+ to N_2. For a 3:1 ($Ar:N_2$) mixture, excellent agreement with the experimental data is obtained for a wide range of pressures. For a 1:1 mixture, broad agreement is again obtained. However, for a 1:3 mixture too few Ar^+ ions survive the passage across the plasma sheath to be accurately simulated.

DA-19 Kinetic Energy Distributions of Ions Sampled from RF Glow Discharges in Hydrogen, S. B. RADOVANOV, J. K. OLTHOFF, R. J. VAN BRUNT, and M. A. SOBOLEWSKI, *NIST* — Mass-analyzed kinetic-energy distributions of positive ions sampled through an aperture in the grounded electrode of a GEC rf Reference Cell have been measured for radio-frequency discharges generated in hydrogen. Applied peak-to-peak rf voltages were varied from 120 to 380 V, and pressures ranged from 4 to 33 Pa. The ion flux at the grounded electrode consists primarily of H^+, H_2^+, and H_3^+. At low pressures the ion flux consists primarily of H_2^+, while H_3^+ dominates at higher pressures. Interpretation of the shapes and amplitudes of the ion energy distributions in light of known collisional cross sections provides information about the predominant ion-molecule reactions that influence the flux of ions toward the electrodes. Voltage and current waveforms were measured at both electrodes for all experimental conditions. Trends in electron densities, ion currents, sheath widths, and sheath potentials are derived from the electrical data. Measured kinetic energies for H_3^+ agree with the magnitude of the ground sheath potential calculated from the voltage waveforms.

DA-20 Temporally and Spatially Resolved Measurements of Optical Emission from RF Glow Discharges in Hydrogen, S. B. RADOVANOV, K. DZIERZEGA, J. R. ROBERTS and J. K. OLTHOFF, *NIST* — Measurements have been made of the spatial and temporal dependence of the H_α emission from radio-frequency glow discharges in hydrogen in a GEC rf Reference Cell. The emission was measured for plasma conditions with pressures ranging from 13.3 Pa to 133 Pa and applied rf voltages of 200 and 350 V. The H_α emission exhibits a double sheath structure near the powered electrode. Each bright band in the sheath is due to H_α excitation that occurs at different times in the rf cycle, thus indicating different excitation mechanisms. Emission corresponding to two different times in the rf cycle are also observed in the bulk of the plasma. Emission from fast hydrogen atoms with energies exceeding 150 eV is observed throughout the volume of the plasma. These fast atoms are detected by observing emission from the Doppler broadened wings of the H_α line. The energy of these neutral particles is determined by correlating the point of emission in the plasma with the phase of the rf cycle.

DA-21 Measurement of Hydrogen Dissociation in a Helical Resonator Discharge P.BLETZINGER and B.N.GANGULY, Aero Propulsion and Power Directorate, WPAFB, Ohio-- A 4.5 inch diam. helical resonator was used with a 2 inch diam. discharge tube at rf powers from 40 to over 100 W to dissociate H_2 and mixtures of H_2 with N_2 and other gases. The resonator was operated at 73 (capacitive mode) and 83 (inductive mode) MHz. Dissociation was measured using two-photon allowed LIF with 205nm excitation. Dissociation was maximum between 1 and 2 Torr for the inductive mode discharge. In the capacitive mode the measured H atom density decreased rapidly below 1 Torr relative to the inductive mode at the same power. Despite the lower H_2 concentration, at 0.5 Torr a 2:1 N_2:H_2 mixture showed more H atom signal than the pure H_2 discharge, at higher pressures the same signal was observed. The TALIF signal decay in pure H_2 decreased from a value close to the radiative lifetime at 0.5 Torr to less than 8 nsec (1/e value) at 10 Torr. The decay values for the H_2/N_2 mixture were identical, indicating that the quenching coefficients for the 3d and 3s states of H are the same for both H_2 and N_2. Absolute values for the dissociation using calibration with NO_2 will be reported.

DA-22 Uniformity Measurements - Comparing Two Diagnostics,* A. RICCI, M. J. BUIE, J. T. PENDER, W. B. McCOLL[1] and M.L. BRAKE, Department of Nuclear Engineering, University of Michigan - **Density and temperature uniformity measurements have been made using a single Langmuir probe and spatially resolved emission spectroscopy on the University of Michigan Gaseous Electronics Conference Reference Cell. The probe was configured to compensate for any distortions due to the fundamental or second harmonic.[2] The probe position was varied in the radial direction halfway between the two electrodes to determine the spatial uniformity of the glow discharge. Power levels was varied from 5 to 30 Watts with a flow rate 20 sccm for argon pressures ranging from 50 mTorr to 1 Torr. These results will be compared to spatially resolved optical emission spectroscopy measurements.[3]**

*supported by SRC 93-MC-085

1) Dublin College, Ireland
2) Overzet, L. J. and Hopkins, M. B., J. Appl. Phys. **74**(7), 1993.
3) Pender, J. et. al. J. Appl. Phys. **74** (5) 1993.

DB: ELECTRON COLLISIONS

DB-1 Absolute Experimental Electron Impact Cross Sections for the Silver $5^2S_{1/2} \rightarrow 5^2P_{1/2}$ and $5^2S_{1/2} \rightarrow 5^2P_{3/2}$ Resonance Lines,* CONNOR FLYNN AND BERNHARD STUMPF, Dept. of Physics, University of Idaho. --- We have measured the linear polarization and the

apparent excitation function of the silver $5^2S_{1/2} \rightarrow 5^2P_{1/2}$ (338.4 nm) and $5^2S_{1/2} \rightarrow 5^2P_{3/2}$ (328.2 nm) resonance transitions from threshold (3.664, 3.778 eV) to 1000 eV. Relative experimental cross section data, corrected for polarization, are normalized at an energy of 1000 eV with respect to first Born theory that includes the $5^2S_{1/2} \rightarrow 5^2P_{1/2,\,3/2}$ transitions with oscillator strengths of 0.214 and 0.445 [2] and cascading from the $(4d^{10}nd)^2D$ states with $n = 5, \ldots 12$. The Ag $5^2S_{1/2} \rightarrow 5^2P_{1/2}$ cross section has a steep onset at threshold, rapidly rising to 1.65 πa_0^2 at 3.8 eV, remains constant until 4.4 eV, then increases linearly to 3 πa_0^2 at 7.5 eV, and has a broad maximum of 3.3 πa_0^2 at 13 eV. The Ag $5^2S_{1/2} \rightarrow 5^2P_{3/2}$ transition has a cross section of similar shape and a linear polarization with a broad local minimum at 3.9 eV.

*Supported in part by NSF/Idaho-EPCoR under grant OSR-9350539 and by a grant from the State Board of Education of the State of Idaho.

[1] C. Flynn, Z. Wei, and B. Stumpf, Phys. Rev. A 48, 1239 (1993)
[2] J. Migdalek and W. E. Baylis, Can. J. Phys. 57, 1708 (1979)

DB-2 SMALL-ANGLE DIFFERENTIAL AND INTEGRAL CROSS SECTIONS FOR K 4s-4p*, P. Ozimba, Z. Chen and A.Z. Msezane, Clark Atlanta University--Small-angle experimental and theoretical electron differential cross sections (DCS) for the resonance transition in K are contrasted through the generalized oscillator strength (GOS) and compared with the results of the recent universal formula [1] for electron impact energies varying from 16eV to 200 eV. Integral cross sections (ICS) are also calculated, paying particular attention to small-angle contributions [2] through dividing the angular range into two regions; $\theta<\theta_s(\sigma_1)$ and $\theta>\theta_s(\sigma_2)$where θ_s is a small angle. We find that many of the measured small-angle DCS require renormalization and/or correction near $\theta=0^0$ and that the contribution to the ICS from $\theta\leq\theta_s(\theta_s=4^0)$ amounts to three times that from $\theta>\theta_s$ for E≥54.4eV and that at the smallest energy, σ_1 is over twenty times larger than σ_2 for which $\theta_s=10^0$. The investigation demonstrates the importance of the accuracy of small-angle DCS and strengthens the utility of the universal formula.

*Research was supported by NSF, the US DOE Office of Basic Energy Sciences, Division of Chemical Sciences and AFOSR.

[1] A.Z. Msezane and I.A. Sakmar, Phys. Rev. A49, 2405 (1994)
[2] Z. Chen and A.Z. Msezane, J Chem. Phys., Submitted (1994)

DB-3 Measurements of Absolute Total Electron Scattering Cross Sections using Laser-cooled Atoms.* PAUL FENG, R. SCOTT SCHAPPE, THAD G. WALKER, L. W. ANDERSON, and CHUN C. LIN, U. of Wisconsin– We have built an apparatus that uses Rb atoms in a magneto-optical trap (MOT) as a target for electron scattering measurements. External coils provide the switchable quadrupole magnetic fields for the MOT. In addition to the six windows for the MOT laser beams, the chamber has an electron gun, a Faraday cup, a movable thin wire for measurement of the spatial profile of the electron beam, and an additional port for observation of the fluorescence from the trapped atoms. A frequency-modulated, external cavity diode laser produces the two light frequencies required to trap the atoms. Electron-atom collisions result in ejection of the atoms from the trap, provided the recoil velocity of the atoms is greater than the capture velocity of the trap. The MOT and electron beam are alternated so that the MOT magnetic field does not affect the electron beam, and the capture velocity of the trap can be varied. The fractional atom loss rate in the trap is used to determine the total cross section making the absolute calibration particularly simple.

*Supported by the Air Force Office of Scientific Research, National Science Foundation, and the Packard Foundation.

DB-4 **Electron Excitation Cross Sections for 2p levels of Argon,** Z.M. JELENAK, J.V. BOŽIN, Z.Lj. PETROVIĆ and B.M. JELENKOVIĆ, Institute of Physics, Belgrade, Yugoslavia - Electron excitation cross sections for 2p levels (1, 5, 7, and 9, Pashen notation) of Ar were determined from the measured excitation coefficients of the above levels. The parallel plate, low current self-sustained discharge of Ar was used to obtain data in the range of E/N from 50 Td to 5 kTd (E -electric field, N - gas density, 1 Td = 10^{-21} Vm^2). Our analysis of the excitation processes in Ar discharge revealed the strong effect of cascading and quenching on $2p_9$, less for $2p_7$ and $2p_5$ and negligible on $2p_1$. level. The cross section set for the 2p levels was then determined from fitting the corrected experimental excitation coefficients to those obtained from Boltzmann calculations. The sross section for $2p_1$ has a peak value of $4*10^{-22}$ m^2 at around 30 eV, in the relative agreement with previous beam data[1].

[1]A. Chutijan and D.C. Cartwright, Phys.Rev. A 23, 2178 (1981).

DB-5 **Electron Density Measurement in GEC rf Plasma by Laser Induced Fluorescence,** K. DZIERŻĘGA, K. MUSIOŁ and J. R. ROBERTS, NIST - The LIF method was used to measure the radial electron distribution of a helium glow discharge in the GEC reference reactor. The electron density, n_e, and temperature, T_e, were determined by measuring the emission from the He(4^3P^o-2^3S) LIF and the He(4^3D-2^3P^o) and He(5^3D-2^3P^o) resulting from the population of the He 4^3D, and 5^3D levels due to free electrons collisions with the He 4^3P^o level. The ratio of the collision-induced and LIF emissions is written as the product of n_e and rate the coefficient which depends on T_e using a set rate equations involving only the above collisionally populated levels. From the intersection of the plots of these ratios for two different pairs of levels (4^3D, 4^3P^o and 5^3D, 4^3P^o) as a function of n_e, vs T_e, we determined $n_e = (1.05 - 11.5)x10^{10}$ cm^{-3} and estimated T_e = 1.8 eV- 3.8 eV for discharge pressures between 0.1 - 1 Torr and applied peak-to-peak voltages between 75 - 200 V. The radial profile of n_e changes drastically at the edge of the electrode to about 30% of its peak value at discharge pressure of 1 Torr while is flat at 100 mTorr. Comparisons with other measurements will be presented.

DC: ELECTRON-ION RECOMBINATION AND PHOTON PROCESSES

DC-1 OBSERVATION OF DISSOCIATIVE RECOMBINATION (DR) OF AR_2^+ DIRECTLY TO THE AR GROUND STATE G.B. Ramos, M. Schlamkowitz, J.W. Sheldon*, K.A. Hardy*, Florida International University and J.R. Peterson **, SRI International

A glow discharge in an effusive source produces a beam of metastable argon atoms with a characteristic Maxwellian velocity distribution. Using time-of-flight (TOF) spectroscopy, we have previously observed fast peaks[1] (velocity distributions at 2675m/s and 2596m/s) corresponding to the DR products of Ar_2^+ to metastable states. Now we report our observations, also by TOF, of another peak at 5906m/s. The velocity of this "super fast" peak corresponds to the DR of Ar_2^+ directly to the Ar ground state. We have also studied the DR of Ne_2^+ and have observed a "super fast" peak with a velocity of 9823m/s which corresponds to DR directly to the ground state of neon. TOF is the only method which can detect DR to the ground state.

[1]A. Barrios, J.W. Sheldon, K.A. Hardy and J.R. Peterson, Phys. Rev. Lett. 69, 1348 (1992).

*Supported by AFOSR Grant F49620-93-1-0159DEF
**Supported by NSF Grant PHY 911872

DC-2 NEW RESULTS FOR THE DISSOCIATIVE RECOMBINATION OF H_3^+. J.B.A. MITCHELL: Univ. of Western Ontario, CANADA. A recent study has been performed in which the analyzer field that follows the interaction region in our merged beams apparatus has been systematically reduced while the recombination of H_3^+ has been examined. Reduction of the field strength from 3 kV/cm down to 200 V/cm results in a factor of five increase in the measured recombination cross section. This is interpreted in terms of the survival of long-lived high Rydberg states that are formed as intermediates during the recombination process. The new measured cross section agrees with other experiments performed using afterglow plasmas and storage ring electron coolers. A discussion of this phenomenon and its implications to other experiments will be presented.

Supported by Canadian NSERC

DC-3 Comparison of Vibrational Populations Generated in E-I Recombination of HCO^+ and N_2H^+ with Bates' Theory[1]*, N. G. ADAMS and L. M. BABCOCK, U of Georgia - Vibrational state distributions have been determined for the electronically excited states, CO a and N_2 B, generated in dissociative electron recombination. The relative distributions are different in the two cases being 100, 58, 83, 46, 56, 31, 25 for v'=0 to 6 in the CO a state and 100, 28, 24, 14 for v'=2 to 5 in the N_2 B state. The populations decrease with v' but less rapidly than predicted by Bates' impulse and "relic" mechanisms.[1] An additional mechanism for excitation is proposed. For CO, oscillation in the odd and even populations is observed as predicted by Bates. Experiments are continuing with the deuterated analogs, DCO^+ and N_2D^+ for which the contribution of the impulse mechanism is expected to be greater.

* Work supported by NSF Grant No. AST-9023640.

[1] D. R. Bates, Mon. Not. R. Astr.Soc. 263 369 (1993).

DC-4 Vibrational States Populated in E-I Recombination of O- and S-containing Ions*, B. L. FOLEY, M. DRUCKER and N. G. ADAMS, U. of Georgia - Emissions in the wavelength range, 120-800 nm, from electronically excited states populated in the dissociative electron recombination of CO_2^+, HCO_2^+ and their S-containing analogs, CS_2^+ and HCS_2^+ have been identified. The ions HCO_2^+ and HCS_2^+ are implicated in interstellar molecular synthesis and CO_2^+ in the Mars and Venus ionospheres and in shuttle glow. Major observed emissions are CO(A→X) and spin-forbidden CO(a→X) from CO_2^+, CO(a→X) and OH(A→X) from HCO_2^+ and CS(A→X) from CS_2^+. CO_2^+ emissions are compared with those obtained previously[1,2]. Effects due to vibrational excitation in the ions were detected and quenched before recombination. Vibrational state distributions have been determined for the emitting states and contrasted with those previously obtained for the CO a state from HCO^+ recombination. Studies of the mixed O- and S-containing ions, OCS^+ and $OCSH^+$, are proceeding.

* Work supported by NSF Grant No. AST-9023640.

[1]R.A.Gutcheck and E.C.Zipf, J.Geophys.Res. 78, 5429 (1973).
[2]F.Vallee et al. Chem. Phys.Lett. 124, 317 (1986).

DC-5 Electron-Ion Recombination Measurements in Flowing Afterglow Plasmas*. T. GOUGOUSI, M.F. GOLDE, and R. JOHNSEN, U. of Pittsburgh -We have used the flowing-afterglow Langmuir-probe technique to determine recombination coefficients for the disscociative recombination of several ion species with electrons. At 300 K, the measured coefficients are:

O_2^+: $\alpha = (2.2 \pm 0.2)10^{-7}$ cm^3/s CH_5^+: $\alpha = (11 \pm 1)10^{-7}$ cm^3/s
H_3^+: $\alpha = (1.8 \pm 0.2)10^{-7}$ cm^3/s $C_2H_5^+$: $\alpha = (10 \pm 1)10^{-7}$ cm^3/s
D_3^+: $\alpha = (1.1 \pm 0.1)10^{-7}$ cm^3/s H_3O^+: $\alpha = (7.5 \pm 1)10^{-7}$ cm^3/s

In general, the agreement with earlier determinations is quite good, but we have not obtained any evidence that supports Smith and Spaniel's[1] recent finding of far smaller recombination rates for H_3^+ and D_3^+ in their vibrational ground states. We will also discuss some subtleties in the analysis of recombining afterglow plasmas, such as effects of radial and axial diffusion in a parabolic flow, more precise definitions of effective plasma velocities, and some problems that we encountered in using Langmuir probes.

*This work was, in part, supported by NASA

[1] D. Smith and P. Spanel, Int. J. Mass Spectr. Ion Proc. 129, 163 (1993)

DC-6 Flash X-ray Excitation of High Pressure Rare Gases,* E. ROBERT, A. KHACEF+, C. CACHONCINLLE and J.M. POUVESLE, GREMI, CNRS/University of Orléans, France, +LPMI, USTHB, Algiers, Algeria. High pressures rare gas (Rg) plasmas have been excited using an intense linear flash X-ray source specially developped for this experiment. Time resolved spectroscopy studies have been performed over a very wide pressure range (0.1-30 bars) in both pure rare gases and gas mixtures, thus providing an extended data base on the so-called third continuum of Rg radiating in the UV-VUV domain and attribuated to ionic excimers. These new data allow to understand some of the contradictory results previously reported in the litterature. They strongly suggest that different species may be at the origin of the fluorescence radiated in the domain covered by the third continuum. High repetition rate flash X-ray device appears as an very convenient apparatus for the production and study of high pressure plasmas, mainly leading to UV-VUV fluorescences. It is an excellent means for the production of excited ionic molecular species. In this work, we also report on the fluorescence of rare gas heteronuclear ions at high pressure.

*Work was suported in part by CNRS and in part by La Région Centre.

DC-7 Photofragmentation of the H_3 ($2s\ ^2A_1'$, $2p\ ^2A_2''$, $3s\ ^2A_1'$, $3d\ ^2E''$) Molecule,* U. MÜLLER, A. DYKMAN, and P. C. COSBY, SRI International, Menlo Park, CA--We investigated the dissociation of the $2s\ ^2A_1'$, $2p\ ^2A_2''$, $3s\ ^2A_1'$, and $3d\ ^2E''$ Rydberg levels of the H_3 molecule using SRI's fast neutral beam photofragment spectrometer. Fast metastable H_3 $2p\ ^2A_2''$ (N=K=0) molecules are generated by charge transfer of H_3^+ ions in Cs vapor. The neutral beam is crossed by a CO_2 laser beam in triple pass configuration which populates the $2s\ ^2A_1'$ state by stimulated emission pumping from the $2p\ ^2A_2''$ state. Alternatively, an intracavity dye laser beam is used to excite the $3s\ ^2A_1' \leftarrow 2p\ ^2A_2''$ and $3d\ ^2E'' \leftarrow 2p\ ^2A_2''$ transitions.[1] $H(1s) + H_2\ X^1\Sigma_g^+(v,J)$ photofragment pairs are detected in coincidence by a time- and position-sensitive detector. From the kinetic energy release spectra we obtain the rotational and vibrational population of the H_2 fragments. These distributions are compared with those predicted by the two-dimensional wave packet calculations of Orel and Kulander.[2]

*Research supported by NSF Grant PHY-91-11872.

[1]P. C. Cosby and H. Helm, Phys. Rev. Lett. **61**, 298 (1988).
[2]A. E. Orel and K. C. Kulander, J. Chem. Phys. **91**, 6086 (1989).

DD: CHARGED PARTICLE TRANSPORT AND ENERGY DISTRIBUTIONS

DD-1 **Nonstationary Treatment of Distribution Anisotropy in the Temporal Relaxation of Energetic Electrons,** R. WINKLER and D. LOFFHAGEN, *INP Greifswald, Germany* G. L. BRAGLIA, *University of Parma, Italy* — The study of the relaxation of the electron velocity distribution in collision dominated plasmas subject to the impact of an electric field is mainly performed by solving the nonstationary electron Boltzmann equation. Such investigations are almost generally limited to the first two terms of the distribution expansion in Legendre polynomials and to the quasi-stationary treatment of the distribution anisotropy. A comprehensive study of the relaxation of a group of energetic electrons based upon both these approximations indicated large discrepancies to results obtained by very accurate and time comsuming Monte Carlo simulations of the same relaxation process. To improve the accuracy of the solution of the nonstationary kinetic equation a new solution approach has been developed which allows for a strict nonstationary treatment of the distribution anisotropy as well as an extension to higher orders of the distribution expansion. Several results obtained with this approach on the relaxation of the electron distribution will be presented and the improvement in the relaxation treatment by this approach will be illustrated by comparisons with corresponding MC simulation results.

DD-2
Time Dependence of the Subexcitation Electron Distribution Generated by High-Energy Electrons* M. A. Dillon and M. Kimura, Argonne National Laboratory,
The time-dependent subexcitation electron distributions produced by the bombardment of argon and neon by keV electrons were calculated by using the *continuous slowing down approximation* (CSDA) in the energy transfer range below the first electronic excitation level. Solutions of the Spencer-Fano equation from the incident electron energy to the first electronic threshold were used as the boundary condition and as input to the continuity equation expressing the CSDA.

* Supported by the U.S. Department of Energy, Office of Energy Research, Office of Health and Environmental Research, under Contract W-31-109-ENG-38.

DD-3 **Modeling of Ion Transport on a Parallel Computer,** E. R. KEITER and W. N. G. HITCHON, *U. Wisconsin-Madison*, S. SHANKAR, and E. REID, *Intel Corporation* — An established kinetic ion model[1] based on the convected scheme formulation has been adapted for use on an Intel Paragon computer. A discussion of the algorithm and its implementation on a parallel machine will be presented, as well as a comparison with the non-parallel version of the code. Finally, some applications to a model of plasma source ion implantation (PSII) will be presented.

*Work supported in part by NSF grant #ECD–8721545
[1]W.N.G. Hitchon and E.R. Keiter, J. Comp. Phys. **112**, 226, (1994).

DD-4 **Monte Carlo Simulations of Electron Transport Across a Magnetic Filter,** A.A.GOLDEN and M.M. TURNER, School of Physical Sciences, Dublin City University, Ireland. -
The interaction of a Maxwellian eedf incident on a transverse magnetic filter field has been simulated computationally by the use of an elementary ballistic/kinetic electron algorithm, incorporating Monte Carlo collisions, in an ambient low pressure H_2 gas. Electron-electron collisions were included using the energy resolved electron fluid approach[1], and experiments with varying pressures, magnetic filters and voltage drops across the filter were undertaken. Results indicate that collisional cooling of the emergent eedf does indeed occur, with evidence that the filter plays an active role locally in the generation of negative ions. Further and more detailed modeling work is proposed.

[1]Y. Weng and M.J. Kushner, Phys. Rev. A 42, 6192 (1990).

DD-5 Spatially Resolved Energy Distribution and Transport Coefficients of Electrons between Absorbing Electrodes, H. ITOH, T. TANOUE, A. TAKEDA[A] and N. IKUTA[B], Chiba Inst. Tech., Shikoku Univ. [A], Tokushima Univ. [B], Japan. ---Precise calculation of spatially resolved transport coefficients and energy distribution of electrons in N_2 gas between two absorbing electrodes are carried out by using the SST-FTI method[1] at 20 and 300 Td. The N_2 cross section set of Phelps and Pitchford is used. Near the boundaries, the energy distributions in each spatial division show reasonable changes with the energy gain by displacement and the energy loss through inelastic collisions. Non-equilibrium and equilibrium regions in the energy distribution are observed in similar manner reported as the result of Monte-Carlo simulation[2]. However, this method can offer far stable results with less fluctuation corresponding to more than 10^8 electrons. Accordingly, spatially resolved velocity distributions, collision frequencies in respective kind of collisions, transport coefficients and related quantities are consistently obtained. This may be the first accurately analyses using the Boltzmann equation including absorbing boundaries.

[1]A. Takeda and N. Ikuta: Trans. IEE Jpn. 113-A, 618, (1993), (in Japanese).
[2]A. V. Phelps and L. C. Pitchford: JILA IFC Report 26, (1985).

DD-6 **Electron Drift Velocities in Mixtures of Helium with Argon, Krypton and Xenon,*** T. L. SMITH, D. C. LIPTAK and J. D. CLARK, Physics Department, Wright State University and R. NAGPAL, A. GARSCADDEN Plasma Research Group, WPAFB- Ramsauer-Townsend (R-T) rare gases are often used in low energy swarm experiments due to their sensitivity in drift velocity with small component mixtures. In the present experiment, the low mass Helium plays the same role as a small molecular component. A pulsed-Townsend technique measured electron swarm velocities at several mixture compositions ranging from 5% to 25% Helium in R-T rare gases with an E/N range of 0.002 to 10 Townsends. A change in drift velocity by a factor of ≈ 2 was observed with the addition of a small amount of Helium to the R-T rare gas. Comparison of the experimental data with Boltzmann calculations are used to suggest corrections for the R-T rare gas cross sections.

*Supported by Aero Propulsion and Power Directorate through the Southeastern Center for Electrical Engineering Education.

DD-7 **Electron Drift Velocity Measurements in SiF_4-Argon Gas Mixtures,*** T. L. SMITH, D. C. LIPTAK and J. D. CLARK, Physics Department, Wright State University and A. GARSCADDEN Plasma Research Group, WPAFB- A pulsed-Townsend technique measured the drift velocity profiles of several

mixtures of SiF_4 in Argon. Ten mixtures ranging between 0.1% to a maximum of 4.8% SiF_4 were used over a range in E/N of 0.07 to 16 Townsends. Negative differential conductivity was observed in all of the mixtures. Maxima in the drift velocity were measured with an increase over pure Argon of at least an order of magnitude. The maxima were observed to move progressively to higher E/N values with increasing concentrations of SiF_4. This data has been used to extract preliminary vibrational excitation cross sections for the electron scattering from SiF_4.

*Supported by Aero Propulsion and Power Directorate through the Southeastern Center for Electrical Engineering Education.

DD-8 **Electron Drift Velocities and Apparent Ionization Coefficients in Binary Mixtures of Argon, Carbon Monoxide, Carbon Dioxide and Nitrous Oxide,*** D. L. SCHWEICKART, R. NAGPAL and A. GARSCADDEN, Wright Laboratory, WPAFB- Measurements of electron drift velocities and apparent ionization coefficients were made in an original version of a pulsed-Townsend drift tube. These parameters were measured for various synthesized binary mixtures chosen from the three molecular gases (CO_2, CO, N_2O) and Argon. In most cases, the apparent ionization coefficients in binary mixtures are shown to scale linearly with the ratio of partial pressures in the mixtures. The rare gas-molecular gas mixtures of Ar/CO exhibited synergistic effects over the E/N range of 1 to 30 Td, which are attributed to the interactions between the respective elastic and inelastic collision processes. Boltzmann analysis of the ionization growth was carried out to provide a baseline for comparisons and interpretation.

*Work Supported by the Wright Laboratory.

DD-9 Mercury Diffusion in an AC Hg-Argon Low Pressure Discharge. M.W. GROSSMAN, OSRAM SYLVANIA INC.-Previously[1], the axial distribution of neutral mercury, n(x) was measured in a DC low pressure Hg-Argon discharge. A one dimensional diffusion model was used to describe n(x):

$$\frac{d^2n}{dx^2} - \alpha\frac{dn}{dx} = \frac{A^*}{D} \qquad (1)$$

Where D, A* , and α are the Hg diffusion coefficient, surface absorption (or desorption) parameter, and ratio of mean axial DC cataphoresis velocity divided by the diffusion coefficient, respectively. Now the experimental studies have been extended to include 60Hz applied discharge power We choose a time scale such that α=0 and the new model for the steady state n(x) is

$$\frac{d^2n}{dx^2} = \frac{A^*}{D} \qquad (2)$$

As reported earlier[1], the positive column model "Glow"[2] is used in conjunction with relative light output measurements in order to determine the absolute radially averaged value of Hg, i.e., n(x). Justification for the use of the "Glow" model is presented via comparison to published 60Hz data[3]. Also, analysis of the time dependent analog of equation (2) is utilized along with measured values of n(x,t) in order to determine the value of D under well defined but non-steady discharge operating conditions.

[1] M. W. Grossman 1993 Gaseous Electronics Conference, Montreal
[2] R. Lagushenko and J. Maya, J. IES, 306 (1984)
[3] C. W. Jerome J. IES, 205 (1956)

DD-10 Corelation of Anisotropies in Scattering and in Velocity Distibution on Electron Transport Properties, A.Takeda and N.IKUTA*, Shikoku Univ. and Tokushima Univ*: Tokushima, Japan ----The effect of anisotropy in elastic and inelastic scatterings on the electron transport properties in CF_4 are examined by using the extended FTI method. The residual components of incident velocity in anisotropic scattering in the laboratory frame are fully taken into account. Elastic momentum transfer and inelastic integral cross sections q_m, q_{ex}, respectively, are maintained constant regardless of the anisotropy. The forward dominated elastic scattering reduces the transverse diffusion coefficient D_T but does not change the drift velocity W and the mean energy $<\varepsilon>$. The forward dominated inelastic scattering increases W and $<\varepsilon>$ but does not change D_T so much. There is a large corelation between the anisotropies in inelastic scattering and in the velocity distribution, but the effect of anisotropic scattering is hardly observed in almost isotropic velocity distribution when assumptions above are maintained.

1) A.Takeda: J.Phys.Soc.Jpn.63-7(1994).
2) R.Yokoyama, H.Gotoda, K.Yamamoto and N.Ikuta: J.Phys. Soc.Jpn.63(1994)2594.

DD-11 Momentum and Energy Balance in the FTI Analyses of the Electron Transport, H.GOTODA, H.TANAKA and N.IKUTA Tokushima University, Tokushima 770, Jpn. ------ Electron trnsport properties under anisotropic scattering are accurately calculated by extended FTI method considering the residual velocity after scattering. In usual analyses so far carried out, the mean forward momenta gained in flights are treated to be lost with the momentum transfer collision frequency ν_m. In the extended FTI method, electrons collide with gas atoms with the integral collision frequency ν_0 but lose a fraction q_m/q_0 of the forward momenta mv_x' at collision, and leave a fraction $(1-q_m/q_0)$. When q_m is maintained independent of anisotropy in a system of elastic collision only, the momentum loss rates in each method are the same and give the same mean energy and the drift velocity with perfect balance of gain and loss rates of energy and momenta. Even including inelastic collisions, a good agreement between the gain and loss rates in five digits are obtained although the drift velocity and the mean energy change with the anisotropy. The results of the Boltzmann equation analyses so far been carried out might be erroneous in anisotropic scattering systems.

1) N.Ikuta et al.:J.Phys.Soc.Jpn.63 (1994)563.
2) R.Yokoyama et al.: J.Phys.Soc.Jpn.63(1994)2594.

DD-12
Electron Energy Distribution in Nitrogen at 1-2 kTd. S. Vrhovac, Z.Lj. Petrovic and B.M. Jelenković, Institute of Physics, Belgrade, Yugoslavia. - Electron energies were measured in N_2 in the parallel plate discharges at E/N = 1 - 2 kTd using retarding potential analyzer (RPA). The bulk energy distribution functions (EDF) as well as mean energies are calculated using Boltzmann code and Monte Carlo (MC) simulations assuming isotropic scattering, but different models of energy partitioning in ionizing collisions are applied. The experimental EDF are compared to the results of the MC calculations of the energy distribution of electrons passing through the anode aperture and accepted by an RPA. The effects of variations of the electric field[1] and gas density[2] on both sides of the aperture are being investigated. The experimental distributions show a low and high energy structure.

[1]B.E.Thompson et. al., J. Appl. Phys. 59, 1890 (1985).
[2]J.W. Coburn and E. Kay, J.Vac.Sc.Tech. 8, 738 (1971).

DD-13 **Coupled transport of Hydrogen ions at high E/N,** J.BRETAGNE, G.GOUSSET and T.ŠIMKO, Lab. Phys. Gaz Plasmas, Université Paris-Sud, F91405 Orsay Cedex, France
The coupled transport of H^+, H_2^+ and H_3^+ ions, at high E/N

reduced electric fields ($100 \leq E/N \leq 2$ kTd) was studied using a 1-D Convective Scheme simulation. Ion velocity distributions were obtained assuming a local source of H_2^+ ions. Results show that H_3^+ are dominant up to about 1.5 kTd and that the three ion species are strongly coupled. We do not clearly observe the presence of runaway H_3^+ ions even for $E/N \geq 700$ Td contrarily to the results of Phelps[1]. Nevertheless, our results indicate the presence non-equilibrium H_3^+ ions which influence the recovering of H^+ and H_2^+ ions through H_3^+/H_2 collisions. Finally, it is clearly shown that the three ion species cannot be in equilibrium with rapidly varying electric fields typical of cathode fall regions.

1. Phelps A V 1990 J.Phys. Chem. Ref. Data **19** 653

DD-14 Thermal Plasma Heat Transfer Characteristics for a Cylinder in Cross Flow, D. R. NOVOG, S. C. LI, J. S. CHANG, *McMaster Univ.* — The heat transfer characteristics from a thermal plasma to a cylinder in cross flow are investigated in order to produce an experimental correlation for these conditions. A DC argon plasma torch produces a thermal plasma jet which impacts on a 6.35 mm O. D. water cooled inconel flow tube. The coolant flow rate, torch power level, inlet coolant temperature, and argon flow rate are varied from 0.2 to 1.2 l/min, 3 to 5 kW, 20 to 90°C and 12.5 to 20 l/min respectively. A specially designed heat flux probe measured a temperature gradient of as much as 800 K/mm near the inconel tube surface. The local and total heat transfer rates are determined by the local heat flux probes and the heat balance of coolant flow. An IR thermo-image camera is used for surface temperature profile measurements. The results show a heat flux up to 0.16 MW/m^2 for a heat transfer area of 16.8 cm^2. The heat transfer characteristics for a cylinder in thermal plasma cross flow is presented as a function of the coolant Reynolds number, plasma gas Reynolds number, coolant Prandlt number, and plasma gas Prandlt number.

DD-15 The Ion Boundary layer in Strongly Ionized Thermal Plasmas, M. S. BENILOV, Universidade da Madeira, Portugal - The problem of a transition from the equilibrium (Saha) ionization in the plasma bulk to the boundary conditions at the wall or electrode surface is studied. The structure of the transition layer is determined by the ratio ϵ of the ion-neutral mean free path to the recombination length. In the case $\epsilon \ll 1$, the transition layer may be treated in the framework of the diffusion approach. This case is at present relatively well studied. However, in many practically interesting situations (for example, in arc discharges) ϵ is large. In the present paper a self-consistent theory for the case $\epsilon \geq 1$ is developed. It is shown that the motion of the ions is collision-dominated and may therefore be considered in a hydrodynamics multifluid approximation. In the case $\epsilon \ll 1$, the developed theory is consistent with a conventional diffusion approach. Numerical and asymptotic solutions of a stated problem are obtained. It is found that the problem is solvable only if the ionization degree does not exceed a certain value, which varies between approximately 0.6 and 1. Beyond this value, the equation of the pressure balance cannot be satisfied and the plasma as a whole cannot stay in a static equilibrium. A simple approximate formula for the ion flux is obtained.

DD-16 Loss processes of N_2 metastable molecules by CH_4, S. SUZUKI, H. ITOH, H. SEKIZAWA and N. IKUTA*, Chiba Inst. Tech., The Tokushima U.*, Japan. ---In order to study the importance of metastable nitrogen molecules $N_2(A^3\Sigma_u^+)$ for the ionization processes, the destruction processes of $N_2(A^3\Sigma_u^+)$ in Townsend discharge region were investigated[1]. The diffusion coefficient and the collisional quenching rate coefficient were determined along with the reflection coefficient of $N_2(A^3\Sigma_u^+)$ at the boundary[2]. In this paper, we study the destruction processes of $N_2(A^3\Sigma_u^+)$ in N_2/CH_4 mixture gas. The experimentally obtained values for $N_2(A^3\Sigma_u^+)$ were, 184 cm^2/s for the diffusion coefficient, 1.6×10^{-15} cm^3/s for the collisional quenching rate coefficient by CH_4, and approximately 0.3 for the reflection coefficient. However, the collisional quenching rate coefficient was values smaller than other investigators[3,4].

[1]S. Suzuki, H. Itoh, H. Sekizawa and N. Ikuta, :J. Phys. Soc. Jpn., 62, 2694 1993.
[2]S. Suzuki, H. Itoh, N. Ikuta and H. Sekizawa, :J. Phys. D(Appl. Phys.), 25, 1568, 1992.
[3]L. G. Piper, W. J. Marinelli, W. T. Rawlins and B. O. Green: J. Chem. Phys., 83, 5602, (1985).
[4]M. F. Golde, G. H. Ho, Wen Tao and J. M. Thomas: J. Phys. Chem., 93, 1112, 1989.

DD-17

Spatially Dependent EEDF by Solving Boltzmann's Equation Using Flux Corrected Transport for Low Pressure Plasma Reactors*–J. W. SHON, Sandia National Laboratories, and B. PENETRANTE, V. VAHEDI and T. D. ROGNLIEN, Lawrence Livermore National Laboratories, Livermore, California, M. J. Kushner, U. of Illinois, Urbana – Spatially dependent electron energy distribution function (EEDF) for inductively coupled rf discharges in Argon and Chlorine is studied using 2D (1D configuration / 1D velocity space) Boltzmann's equation (BE). The flux corrected transport (FCT), which solves BE by direct integration as an initial value problem using finite differences, is applied.[1] The static electric fields in the ICP reactor are computed from the quasi-neutrality. The effect of RF fields is included by velocity and space diffusion describing both collisional (Ohmic) and collisionless (Stochastic) heating.

*Work supported by SEMATECH and U.S. Department of Energy

[1]John V. DiCarlo and Mark J. Kushner, J. Appl. Phys. 66, 5763 (1989).

DD-18 Characteristic Energy and Ratio of Longitudinal Diffusion Coefficient to Mobility for Electrons in Hydrogen at Moderate E/N, W. ROZNERSKI and J. MECHLIŃSKA-DREWKO, *Faculty of Applied Physics and Mathematics, Tech. University of Gdańsk, 80-952 Gdańsk, Poland* — By means of an experimental procedure described earlier[1] the characteristic energy (D/μ) and the ratio of longitudinal diffusion coefficient to mobility (D_L/μ) over the reduced electric field E/N: $50 \leq E/N \leq 212$ Td have been determined. The present results of the D/μ are at least within the combined errors of this work and those by Crompton *et al.*[2] As to the D_L/μ our results agree fairly-well with those by Flecher and Reid[3] although over the E/N range: $80 \leq E/N \leq 150$ Td the data points of this work lie lower than those mentioned above and the difference between both data sets reaches about 25 percent at about 110 Td.

[1]W. Roznerski, J. Mechlińska-Drewko, and K. Leja, Joint Symposium (Gold Coast, 1991) p. 83.
[2]R. W. Crompton *et al.*, Proc. 7th ICPIG, Belgrade, 1965.
[3]J. F. Flecher and I. D. Reid, J. Phys. D. **13**, 2275 (1980).

WEDNESDAY MORNING

SESSION EA: MAGNETICALLY ENHANCED PLASMAS I
Wednesday morning, 19 October 1994
NIST Building 101
Red Auditorium, 8:00–10:00
M. Lampe, presiding

Contributed Papers

EA-1 The Role of the Plasma in the Chemistry of Low Pressure Plasma Etchers*, R. E. P. HARVEY, W. N. G. HITCHON and G. J. PARKER, Engineering Research Center for Plasma-Aided Manufacturing, U.of Wisconsin-Madison —A new procedure for the calculation of neutral transport at long mean free paths[1] is applied to describing plasma chemistry in a low neutral pressure high plasma density plasma reactor. This procedure is a novel 'propagator' technique. The calculation of propagators to allow for various effects such as variable mean free path and anisotropic scattering is demonstrated. The role of the plasma in determining the neutral species behavior is investigated in some detail. The main processes by which the plasma controls the chemistry involve the ionization of neutrals and the subsequent transport of the products to the walls. The transport and re-cycling of ions and hot neutrals are examined, allowing for different spatial distributions of ions striking the walls and different sticking coefficients on the wall. The plasma parameters are chosen to correspond to measured values but the critically improtant tail of the distribution has not been measured. The effects of truncating the hot tail of the electron distribution function and altering the spatial distribution of hot electrons are also calculated.

* Work supported by NSF Grant #ECD-8721545

[1] R.E.P.Harvey,W.N.G.Hitchon and G.J.Parker, J.Appl.Phys 75, 1940 (1994).

EA-2 Power deposition mechanisms in a helicon plasma source, Albert R. Ellingboe, Rod Boswell, PRL, R.S.Phys.S.E., ANU Australia - Time and spatially resolved optical emission spectroscopy has given insight into the power deposition in a helicon plasma source. A PIC code has been used to investigate the interaction between plasma electrons and the known plasma electric wave-fields. The standing-wave under the antenna is found to modify the electron energy distribution function in such a way as to increase the number of electrons that are able to interact resonantly ($\omega - k_{||} v_z = 0$) with the traveling wave leaving the source.

EA-3 Silicon transport properties in a Helicon Activated Reactive Evaporation, ANTOINE DURANDET, BEN HIGGINS and ROD BOSWELL, PRL, R.S.Phys.S.E., ANU Australia - The Helicon Activated Reactive Evaporation (HARE) is a deposition device that combines an evaporation source (Electron Beam) and a high density plasma source (Helicon plasma source), in a configuration where the evaporant material is transported through the plasma source. The transport of silicon vapor from the electron-beam evaporation source through argon and hydrogen gas at pressures near 1.0 mTorr has been studied. The flux-distance relationships for the diffusion of the evaporant through the device are found to vary with the type of filling gas. The investigation includes both a simple theoretical model and experiment. The results of each study are in good agreement. Cross-sections for the energy-averaged momentum transfer collisions of silicon with the filling gases at thermal energies have been determined. The effect of the plasma on the ionisation of the evaporant has been investigated.

EA-4 Characterization of Chlorine/Argon ECR Plasmas for the Etching of GaAs, C.R. EDDY, JR., S.R. DOUGLASS* and B. WEBER, Naval Research Laboratory - To assist in the development of a predictive model for ECR-based RIE, electron densities in electron cyclotron resonance argon and argon/chlorine plasmas used to etch GaAs have been measured by microwave interferometry using 140 GHz radiation and by Langmuir probes. Langmuir probe data was also used to calculate electron temperature and plasma and floating potentials. The effects of pressure, flow rate, microwave power, ECR volume (as determined by magnetic field profile models), and chlorine addition to argon on plasma parameters were investigated. In addition, effects of the rf-bias level and position of the substrate stage on plasma parameters will be reported. Langmuir probe density measurements exceed the non-intrusive interferometry measurements by a factor of 5-10 in the high magnetic field regions of the source. Electron densities increased with microwave power over the range from $2x10^{12}$ to $1x10^{13}$ cm^{-3} in the source region and from $1x10^{11}$ to $1x10^{12}$ cm^{-3} in the downstream region, as measured by Langmuir probes. Typical line averaged densities measured by interferometry for > 300W absorbed power were $8x10^{11}$ cm^{-3}. Electron densities are weakly dependent on pressure, flow rate, and ECR volume.
*National Research Council Associate

EA-5 Influence of the Static Magnetic Field Intensity on the Spatial Distribution of Excited Atoms in a Surface-Wave-sustained (SW) Magnetoplasma*, A. DALLAIRE, P. JONES, J. MARGOT, M. MOISAN AND M. FORTIN, Département de Physique, Université de Montréal - Using a tomography technique we have determined the 3-dimensional distribution of argon atoms in the $3p^5 6d$ configuration in a SW magnetoplasma. In particular, we have examined the influence of the magnetic field intensity B_0 and gas pressure. The results show that the radial profiles are drastically modified when B_0 is increased, yielding a relatively higher atom concentration near the plasma axis than without magnetic field. This profile contraction is the result of (i) a flatter radial distribution of the ionization frequency resulting from a deeper wave electric field penetration into the plasma bulk[1] and (ii) reduced radial diffusion losses with increasing B_0. The experimental results are compared with those predicted from a one-dimensional self-consistent model for the discharge, taking into account the three first moments of Bolztmann equation for both electrons and ions coupled with Maxwell equations.

[1] J. Margot and M. Moisan, J. Phys. D, **24**, 1765 (1991)
*Work supported by NSERC and FCAR

EA-6 A Study of Ion Velocity Distributions in an ECR Discharge, M.D. BOWDEN, N. MAYUMI, K. UCHINO, K. MURAOKA, M. MAEDA, M. YOSHIDA, Y. MANABE, and R.K. PORTEOUS, Kyushu U., Mitsubishi Heavy Industries, Matsushita Electric and Australian National U. A combination of experiment and simulation has been used to determine the main factors which affect the ion

velocity distribution function (IVDF) in an ECR discharge. The effects of gas pressure, magnetic field configuration and chamber shape on the IVDF were studied by a two-dimensional fluid/particle-in-cell hybrid model of an argon ECR discharge[1]. Laser-induced fluorescence measurements of the IVDFs of argon metastable ions in an ECR discharge were also measured. Comparison of the results of the simulation and the experiment indicated that the magnetic field configuration is an important factor in determining the spread of ion energies of ions in the downstream region of the discharge.

1. R.K. Porteous, H-M. Wu and D.B. Graves, Plasma Sources Sci. Technol. 3 (1994) 25-39

EA-7 A Process Model for ECR Plasma Processing, M. MEYYAPPAN, Scientific Research Associates - ECR plasma processing has been widely investigated in recent years for etching and deposition of semiconductor materials. It provides a high density discharge, large flux of low energy ions, radial uniformity and independent substrate bias control. We have developed a comprehensive process model for ECR to provide an understanding of mechanisms and study the effects of process variables on reactor performance. The model considers transport of electrons, ions and the neutrals together. The governing equations consist of continuity and energy equations for electrons, gas flow and gas energy equations and finally species conservation equations for each neutral and ionic species. These equations are solved in a coupled manner in the flow direction. ECR power deposition, gas heating effects, transition-regime flow characteristics, multicomponent diffusion, plasma and surface chemical reactions have been accounted for self-consistently. The code allows for downstream introduction of additional feed gases, common in deposition. Results have been obtained for argon, chlorine and CF_4 gases. Density profiles for electrons, ions and radicals in each case and gas flow characteristics are presented.

EA-8 Propagation of Helicon Waves away from an Antenna*, I.D. SUDIT, M. LIGHT, and F.F. CHEN, UCLA--Detailed mapping of plasma and wave properties has been made in an argon helicon discharge 5 cm in diam by 120 cm long. Density, T_e, and plasma potential measurements were made by rf-compensated Langmuir probes; local emission of the 488 nm Ar^+ line by a miniature optical fiber system; and wave magnetic fields by single-turn coax B-dot probes. KT_e falls from ~5 to ~2 eV in 70 cm, while n_e at first rises to keep pressure balance and then decays due to diffusion. In spite of these changes in parameters, the helicon B_z field maintains a fairly constant wavelength over 100 cm. However, the wavelength is twice as long for the standing wave than for the traveling wave component. It appears that the standing wave pattern results not from reflection of the wave from the far end, where the amplitude is small, but from a beat between two co-propagating waves of different k excited by the m = +1 helical antenna. The 488 nm light falls off too slowly to be consistent with the KT_e decay unless metastable Ar+ ions are assumed to exist. Excitation of these by the cool downstream plasma gives the observed light profile.

*Supported by SRC, Wisconsin ERC, and LLNL-PPRI.

SESSION EB: TRANSPORT AND ENERGY DISTRIBUTIONS
Wednesday morning, 19 October 1994
NIST Building 101
Green Auditorium, 8:00–10:00
J. Wu, presiding

Contributed Papers

EB-1 Numerical and Experimental Verification of the Nonlocal Approach to the Solution of the Spatially Inhomogeneous Boltzmann Equation
C. BUSCH, U. KORTSHAGEN, University Bochum, 44780 Bochum, Germany, L. L. ALVES, C. M. FERREIRA, CEL–IST, Lisbon Tech. University, Portugal
An important and usually very laborious part of self–consistent plasma models deals with the spatially resolved description of the electron kinetics. The development of accurate and efficient approaches to this problem is an important task. In the present contribution first results on the solution of the spatially dependent, kinetic equation for the isotropic part of the electron distribution function (EDF) within the two term approximation are presented. The situation of a positive column is addressed. The results of this method are compared to results obtained within the "nonlocal approximation".[1] Within this approach the EDF is determined from a spatially averaged kinetic equation *without* loss of the spatial information about the EDF. The results of both approaches are compared to spatially resolved measurements of the EDF.
[1] I. B. Bernstein and T. Holstein, Phys. Rev. **94**, 1475 (1954)

EB-2 Separation of Collision Term of the Boltzmann Equation, N.Ikuta Tokushima Univ. Tokushima 770,Jpn.
--- In the Boltzmann equation analyses of transport properties of electrons and ions, the collision term has been used in a combined form only to determine the net loss rates of velocity moments by using the momentum transfer and other integral cross sections. Such a treatment has been believed to be enough to calculate the accurate transport properties even in anisotropic scattering systems. However, anisotropy in scattering in the laboratory frame necessarily leave residual velocity components which give large influences on the electron and ion transport. In the flight time integral (FTI) method, the collision term is naturally separated into two terms, the starting and colliding rate distributions $\Psi_s(v_0)$ and $\Psi_c(v')$, respectively,[1] and the transport properties have been calculated accurately considering the residual velocity components. Obtained transport properties are significantly different from those without the residual velocity components.[2)3)] The data will be shown at the conference.

1) N.Ikuta, S.Nakajima: Trans.IEE Jpn.113-A(1993)83. (in Japanese) 「563.
2) N.Ikuta,Gotoda and R.Yokoyama:J.Phys.Soc.Jpn.63(1994)
3) R.Yokoyama et al.:J.Phys.Soc.Jpn.63(1994)2594.

EB-3 Diffusion Tensor in an Radiofrequency Electron Swarm,* K.MAEDA and T.MAKABE, Keio University, Yokohama
Temporal behavior of the diffusion tensor of electrons in gases under an radiofrequency field is investigated from the Boltzmann equation. Previous rf electron transport theory[1,2] is developed into a locally isolated swarm under the condition of hydrodynamic as-

sumption. A direct numerical procedure(DNP) of the Boltzmann equation is applied to the system.
The results for 100kHz-1GHz in Reid's ramp model gas are mainly discussed. Marked difference between D_L and D_T in a time modulation is found in an rf swarm, in addition to the appearance of a size difference in a dc swarm. As increasing frequency, the temporal profile of D_L approaches that of D_T due to the decrease in energy gain during a half period. The characteristics of ensemble average of energy in time is reflected on D_T.

*Work is supported in part by a Grant-in-Aid for Science Research No.B-05452106 from MESC.
[1]R.W.Crompton, M.Hayashi, D.E.Boyd, T.Makabe Edt, "Gaseous Electronics and Its Applications"(1991).
[2]K.Maeda and T.Makabe, Jpn. J. Appl. Phys. 33(7B) 1994.

EB-4 Electron Swarms in the Upstream Region of an Electron Source H Sugawara, Y Sakai and H Tagashira Dept. of Electrical Eng., Hokkaido Univ., Sapporo, Japan. — Exponential spatial growth of electron swarms under steady-state Townsend conditions may be observed not only in the downstream region of an electron source but also in the upstream region due to backward diffusion. This is caused by a large value of the relative electron density gradient coefficient. Relations between swarm parameters in the upstream region, deduced assuming an exponential spatial distribution for the electrons, were found to have interesting characteristics. For example, the sign of the diffusion modified electron drift velocity, $V_d \equiv W_s - \alpha D_s$, is positive when the gas is electro-positive, and negative when the gas is electro-negative. A propagator method modified for analysis in the upstream region is applied to quantitatively confirm this property. An example of the occurrence of backward diffusion is found in a steady-state Townsend experiment between parallel plane electrodes. In this case, the effect of electron absorption at the anode is transmitted towards the cathode by a mechanism similar to the backward diffusion of electrons.

EB-5 Electron Transport Coefficients in Methane - Rare Gas Mixtures, R.E.VOSHALL, Gannon University and J.L.PACK* - Drift velocity (W), transverse diffusion (DT/μ) and longitudinal diffusion (DL/μ) coefficients were calculated for 3 ppm to 10% CH4 in Ar, Kr, and Xe as a function of E/N from .001 to 100 Td at 300 K by a numerical solution of the Boltzmann equation. Sensitivity to ppm of CH4 in the three gases are similar; i.e. 3 ppm CH4 in Kr yeilds a 16% reduction in DT/μ at 0.01 Td and an increase of 3% and 5% respectively in W and DL/μ at the Ramsauer minimum. For 2000 ppm CH4 in Ar, the drift velocity W is in excellent agreement with Nagy et al[1] from 0.01 to 0.2 Td. A concentration of 10% CH4 in Kr results in a peak of $4x10^4$ m/s in W at 1 Td similar to the $1x10^5$ m/s peak for pure CH4[2]. Also, 97% or more of the electron energy is absorbed in two vibration bands of CH4 between 2 and 15 Td.

*Present Address: J.L.Pack, 3853 Newton Drive, Murrysville, PA 15668.

[1] T.Nagy, et al, Nu. Instr. & Methods, 8, 327(1960).
[2] Bernhard Schmidt,J. Phys. B: Mol. Opt. Phys. 24(1991) 4809-4820.

EB-6 Temporal Sheath Dynamics, MICHAEL S. BARNES, *Lam Research Corporation, Fremont CA* — Previous models of an rf sheath resolve the sheath dynamics in terms of a bimodal ion energy distribution function which tends towards unimodal distribution when the ion transit across the sheath is significantly larger than the rf period. In this work, the ions in a Monte Carlo based sheath model are resolved as a function of rf phase - both in terms of number and energy density. This along with a new scaling law allow a distinction to be made between an "ac" rf sheath and a "dc" rf sheath. The results suggest it might be preferable to operate clearly in one regime rather the transition between the two modes. The "ac" mode exhibits "dead" zones in the temporal energy density suggesting it might be preferable for plasma etching using selective chemistries requiring ion mixing of the etch surface. Finally, the results show that the average ion energy in the transition region far exceeds the time-averaged "dc" sheath potential.

EB-7 Langmuir Probe and Simulation Results on the GEC Reference Cell, M. J. BUIE, J. SONIKER, C. BUSH BROOKS, W. McCOLL[1)] and M.L. BRAKE, Department of Nuclear Engineering, University of Michigan - Langmuir Probe measurements are compared with PDP1[2)] simulations of pressure effects on the electron energy distribution function and the sheath of various RF glow discharges in the University of Michigan Gaseous Electronics Conference Reference Cell. EEDF measurements were made using a single probe which compensated for perturbations due to the RF.[3)] Measurements of sheath thicknesses were made from photographs. These results will be compared to particle-in-cell Monte-Carlo simulations, which give similar results.
1) Dublin College, Ireland
2) Vahedi, V., Ph. D. Thesis, U. C. Berkeley, 1993.
3) Overzet, L. J. and Hopkins, M. B., J. Appl. Phys. 74(7), 1993.

SESSION F: WILL ALLIS PRIZE LECTURE
Wednesday morning, 19 October 1994
NIST Building 101
Red Auditorium, 10:30–11:30
R. Flannery, presiding

Invited Paper

F-1 Development and Early Application of the Flowing Afterglow Technique for Low Energy Ion-Molecule Interactions, ELDON E. FERGUSON, NOAA/CMDL, Boulder, CO - The Flowing Afterglow Technique for thermal energy ion-molecule reaction studies was developed at the National Bureau of Standards in Boulder, Colorado in the period starting in late 1962. The technique has a unique versatility in regard to both the ion and neutral reactants which can be studied. It allowed the first thermal energy ion reaction rate constant measurements with radicals such as O, H and N atoms as well as reactive species such as O_3, N_2O_5, H_2O_2, HNO_3 and H_2SO_4. The early application led to a substantial understanding of atmospheric ion composition. The first measurements of negative-ion associative detachment reactions were obtained. The first ion-molecule reaction measured as a function of neutral reactant vibrational state was carried out. The first systematic studies of molecular

ion vibrational quenching were obtained. Useful thermochemistry was obtained, including electron affinities, ionization potentials, and proton affinities. A variable temperature FA was constructed which extended measurements to the temperature range 80-900 K. A drift tube was added extending measurements from thermal to ~2 eV CM energy.

SESSION G: BUSINESS MEETING
Wednesday morning, 19 October 1994
NIST Building 101
Red Auditorium, 11:30–12:00
J. Dakin, presiding

SESSION HA: INDUCTIVELY COUPLED PLASMAS I
Wednesday afternoon, 19 October 1994
NIST Building 101
Red Auditorium, 13:30–15:30
T. J. Sommerer, presiding

Contributed Papers

HA-1 Characteristics of Inductively Excited Plasmas in the GEC RF Reference Cell* P. A. MILLER, Sandia National Laboratories, B. P. ARAGON, Applied Physics, Inc., K. E. GREENBERG and P. D. POCHAN, University of New Mexico - We describe performance of an inexpensive modification to the Reference Cell that enables generation of high-density plasmas by inductive coupling. Langmuir-probe data showed that plasma electron densities from 10^{10} to 10^{12}/cm^3 were obtained in 1.3 Pa (10 mTorr) of argon for deposited powers from 20 to 300 W. Bulk electron temperatures were typically 4 to 5 eV. Although no electrostatic shield was used between coil and plasma, capacitive-probe data showed ≤ 2-V oscillations in plasma potential. Microwave interferometry at 80 GHz indicated that electron densities in 1.3 Pa of chlorine were typically a factor of two to three lower than in argon at the same power level. While ion and electron densities in argon were peaked on the Cell's centerline, the polysilicon etch rate in chlorine was radially very uniform.

* Work supported by the U.S. Dept. of Energy and by SEMATECH.

HA-2 Ion Energy Distribution Functions in an Inductively Coupled RF–Discharge
U. KORTSHAGEN, M. ZETHOFF, University Bochum, 44780 Bochum, Germany
Recently inductively coupled RF–discharges using a planar, spiral induction coil have attracted growing attention. These discharges seem to be well suited for providing high density plasmas at simultaneously low ion impact energies. In the present contribution ion energy distributions (IED's) measured at a floating electrode in a RF induction plasma are presented. The parasitic capacitive coupling is suppressed by the use of an electrostatic screen. The measured peak ion energies are below 20 eV. The formation of the IED's is interpreted in terms of a kinetic model for the electrons. The strong dependence of the IED's on the non–thermal electron distribution is pointed out. It is demonstrated that for the explanation of the measured ion energies knowledge of the actual non–thermal electron distribution is necessary. The assumption of a Maxwellian distribution of the electrons leads to considerable deviations from the experimental results.

HA-3 Electron Distribution in an Inductively Coupled RF Discharge*, V.I.KOLOBOV and W.N.G.HITCHON, ERC for PAM, U.of Wisconsin, Madison - The non-local Boltzmann equation in two-term approximation is solved numerically for a given distribution of RF and space charge electric fields. For trapped slow electrons the problem is effectively reduced from three to *one* dimension since the electron distribution function (EDF) is only a function of *total* electron energy [1] in the range of parameters studied. The EDF of fast electrons depends on spatial coordinates as well. The shape of the EDF and spatial distribution of the ionization rate are calculated as functions of pressure and plasma density for different spatial profiles of the ambipolar field. The results are compared to experiment [1] and used for self-consistent modeling [2].

* Work supported in part by NSF Grant ECD-8721545
[1] V.I.Kolobov, D.F.Beale, L.J.Mahoney and A.E.Wendt, Appl. Phys. Lett. **65**, 1 August 1994
[2] D.F.Beale, W.N.G.Hitchon, V.I.Kolobov and A.E.Wendt, this conference

HA-4 Electric Probe Characterization of a Multidipole-Confined RF Inductively-Coupled Plasma Etching Source*, C. LAI and R. CLAUDE WOODS, The Engineering Research Center for Plasma-Aided Manufacturing, U. of Wisconsin, Madison, - A planar rf inductively-coupled plasma etching system has been constructed. The plasma is confined by an external multidipole magnetic bucket made of strong Nd-Fe-B magnets. A single-sided planar Langmuir probe was used to measure electron velocity distribution functions (EVDFs) radially and axially for both Ar and N_2 plasmas with rf powers up to 1 kW at lower pressures (≤ 10 mTorr). By rotating the single-sided planar probe we found that the EVDFs are noticeably anisotropic. The values of the plasma potential, which were highly uniform radially, were independent of the probe orientation, but those of the floating potential depended strongly on it. The magnitude and radial uniformity of the plasma potential were confirmed by measurements using an emissive probe. The Langmuir probe measurements showed some deviations from Maxwellian EVDFs for both Ar and N_2 plasmas. Because of the multidipole confinement, the plasma densities are quite uniform axially, and the radial uniformity improves as the axial distance from the quartz window increases. The system was further characterized using a capacitive probe and an electromagnetic (B-dot) probe.

*This work was supported by the National Science Foundation under Grant ECD-8721545

HA-5 Effects of Chamber Aspect Ratio on Uniformity in a Low Pressure Planar Inductive Argon Discharge,* J. STITTSWORTH and A. E. WENDT, Engineering Research Center for Plasma-Aided Manufacturing, U. of Wisconsin-Madison — Spatially resolved Langmuir probe measurements of electron density have been employed to examine the effects of chamber geometry on plasma uniformity in an argon planar inductive discharge. The plasma is confined to a cylindrical volume 14" in diameter bounded on top by the quartz window (separating the antenna from the vacuum chamber) and on the sides and bottom by a grounded conducting surface. The induction antenna is a single turn circular loop 11" in diameter. The bottom plate position can be adjusted to allow for chamber heights varying from 1" to 5". The operating conditions are 500 W power at 13.56 MHz (measured at the power supply) and 5 mTorr argon. Preliminary profiles of electron density in the *r-z* plane show an off-axis density peak for a squat aspect ratio, consistent with a plasma production maximum near the radial location of the antenna. As the

reactor height increases, diffusion effects increasingly dominate the density profile and the density maximum shifts to the axis of symmetry.

*Work supported by NSF Grant #ECD-8721545 and Olin Summer Project Grant Program

HA-6 Simulations of real-time feedback control of 2-dimensional features in inductively coupled plasmas P.L.G. VENTZEK Y. SAKAI, H. TAGASHIRA, Dept. of Electrical Eng., Hokkaido University, Sapporo, Japan, and K. KITAMORI, Dept. of Industrial Eng., Hokkaido Institute of Technology, Sapporo, Japan. - Design of a real-time control scheme for the control of etch uniformity in reactive plasmas is complex because there is usually not a simple measurable and controllable variable which describes this 2-dimensional parameter. A conventional feedback control system is proposed in which the controller simply corrects deviations from the operating point by knowing only process derivatives (e.g. species production rates). In particular, control of a density mesurement based plasma uniformity using two independently powered and controlled coils will be presented. Stability limits and the utility of the control system on etching time scales will be investigated using a simplified hybrid computer model taking into consideration issues such as diagnostic response time, sampling rate, and robustness.

HA-7 **Scaling of Inductively Coupled Plasmas,*** Joseph M. BARICH and Mark J. KUSHNER, University of Illinois, Dept. of Elect. and Comp. Engr., Urbana, IL 61801 USA - Inductively coupled plasma (ICP) reactors are being developed for high plasma density, low gas pressure etching of semiconductors and flat panel displays. We have developed a 2-dimensional hybrid model for ICP reactors (< 10-15 mTorr, $>10^{11}$ cm^{-3} plasma density) with which we are investigating the scaling of these devices to processing large area substrates (> 0.1 m^2). The model has electromagnetic, electron Monte Carlo, plasma fluid, neutral hydrodynamic and external circuit modules. The validation of the model will be discussed using electron densities measured using microwave interferometry.[1] We have investigated the effects of reactor and coil geometry on producing uniform plasma sources. The effect of substrate topography (sacrificial surfaces, focus rings, discontinuities in material properties) on the directionality of the ion flux and uniformity of the radical flux will be demonstrated. We will discuss results for radially dependent ion and radical fluxes in rare gas/chlorine mixtures.

* Work supported by Sandia National Laboratory, SRC, NSF and the University of Wisconsin ERC for Plasma Aided Manufacturing.

1 K. Greenberg, Sandia National Labs, 1994.

HA-8 **A 2-D Model of Polysilicon Etching in an Inductively Coupled Plasma Source***, D. P. LYMBEROPOULOS AND D. J. ECONOMOU, U. of Houston - We have developed a two-dimensional model of polysilicon etching with chlorine in an inductively coupled high density plasma reactor. The model consists of a set of modules: The electromagnetic field distribution is calculated by solving Maxwell's equations. The power deposited into the plasma determines the electron energy and hence the electron-impact reaction rate coefficients. Species balance equations solve for the density of charged and neutral species. The self-consistent space charge field is found from the Poisson equation. Information is cycled among the modules until a converged solution is obtained. The model has been used to study etch uniformity as a function of gas pressure, flow rate, power and frequency. The chlorine discharge is moderately electronegative at these low pressures (1-10s of mtorr) and high powers (100-1000s of W). The negative ions present a challenge in the simulation. Results show that judicious manipulation of operating conditions can result in uniform etching over large (200 mm diameter) wafers.

* Work supported by Sandia/Sematech and the National Science Foundation.

SESSION HB: ELECTRON-MOLECULE SCATTERING
Wednesday afternoon, 19 October 1994
NIST Building 101
Green Auditorium, 13:30–15:30
I. I. Fabrikant, presiding

Invited Papers

HB-1 **Low-energy (E < 20 eV) electron-molecule scattering: comparison of ab initio calculations with recent measurements,** ASHOK JAIN, *Physics Department, Pennsylvania State University, Wilkes-Barre Campus, Lehman, PA 18627* — We review the recent advances in theoretical *ab initio* calculations for low energy electron scattering with molecules. Particular emphasis is given on the differential cross sections (DCS), which are very sensitive to the theoretical model, and where recent measurements are available for a variety of molecules. We discuss our recent results on several molecules such as the CH_4, SiH_4, CF_4, SF_6, H_2O, NH_3, H_2S, C_2H_2, etc., where several measurements on the DCS are available for comparision. We also discuss various discrepancies between theory and experiment.

HB-2 **Absolute generalized oscillator strength measurement of valence and inner-shell excitations of Freons.*** K. T. LEUNG, *Department of Chemistry, University of Waterloo, Waterloo, Ontario N2L 3G1, Canada.* In the past two decades, electron scattering has become a powerful technique for determining "absolute" cross sections of dipole excitations in the VUV to soft X-ray region. By controlling the so-called momentum transfer parameter in an electron scattering process, it is also possible to determine precise absolute generalized oscillator strengths (GOSs) of multipole (or dipole-forbidden) transitions and to observe new dissociative pathways (in favourable cases). We will present some recent results on the non-optical excitation spectroscopy and electron-induced chemistry of Freon molecules ($CF_{4-n}Cl_n$, n=0-4) in the valence and inner-shell regions. The non-dipole components of the $n \rightarrow \sigma^*$ (HOMO $\rightarrow$ LUMO) transitions, most of which are found to be predissociative in nature, appear to increase with increasing fluorination. Furthermore, predominantly dipole components are observed for the low-lying pre-ionization-edge Rydberg transitions. Finally, the possibility of site-specific investigation of the excited states by GOS measurement of excitations from localized inner-shell orbitals will be discussed.

* Work supported by the Natural Sciences and Engineering Research Council of Canada.

Contributed Papers

HB-3 **Formation of H_3^+ by Electron Impact on CH_4 and NH_3***, S. K. SRIVASTAVA, K. FUJII AND J. W. McGOWAN, J. P. L. AND CALTECH - Utilizing a crossed beams electron-molecule collision geometry and a time-of-flight mass spectrometer cross sections for the formation of H_3^+ have been measured for the first time at electron impact energies of 30 and 70 eV. Recorded mass spectra consist of H^+, H_2^+ and H_3^+. The same instrumentation was also used to measure thresholds of formation of all three species. These thresholds were then used to predict the pathways for the formation of these species. Implications of these results in the interpretation of mass spectra obtained by mass spectrometers on the Pioneer Venus atmospheric probe mission will be discussed at the time of presentation of the paper.

*Work supported by the Planetary Atmospheric Office of NASA and AFOSR.

HB-4 **Electron-Impact Ionization of CH_x (x=1-4),*** V. TARNOVSKY, A. LEVIN, and K. BECKER, City College of CUNY, USA - Absolute partial cross sections for the ionization and dissociative ionization of the CH_4 molecule and the CH_x (x=1-3) free radicals have been measured using the fast-neutral-beam technique. The break-up of CH_4 and the subsequent reactions of the CH_x radicals play an important role in the plasma-assisted deposition of diamond films as well as in many planetary atmospheres. While there have been several previous measurements of the CH_4 ionization and dissociative ionization[1], we report the first studies of the ionization and dissociative ionization of the CH_x radicals (aside from some earlier work[2] on CD_2 and CD_3). Great experimental care had to be exercised to ensure the full separation of the parent ion signal from the various fragment ion signals for each target species. The measured cross sections range from 0.5 to 2 x 10^{-20} m^2 at 70 eV.

*Work supported by NSF, NASA, ACS-PRF and NATO.

1. O.J. Orient and S.K. Srivastava, J. Phys. B 20, 3923 (1987) and references therein to earlier work
2. F.A. Biaocchi et al., Phys. Rev. Lett. 53, 771 (1984)

HB-5 **Dissociative Electron Attachment to Chloroalkenes,*** T. UNDERWOOD-LEMONS, J. H. MOORE, and J. A. TOSSELL, U. of Maryland at College Park- Dissociative electron attachment can be used to probe electron transfer between functional groups in a molecule.[1] In this work, we examine electron transfer between π^* and σ^*(C-Cl) orbitals located on opposite ends of n-chloro-1-alkenes (n = 2 to 6). Chloride detachment signals the decay of the temporary negative ion state formed by the resonant capture of an electron into the π^* orbital. The ejection of the chloride fragment indicates electron transfer facilitated by coupling between the π^* and σ^* orbitals. We find that, with one exception, the cross section for dissociative electron attachment associated with electron capture into the π^* orbital diminishes as the number of intervening CH_2's increases; while, the resonance energy changes only slightly. For 3-chloropropene, the cross section increases by a factor of 3.5 and the energy decreases by 0.45 eV relative to vinyl chloride.

*Work supported by the National Science Foundation Grant No. CHE-91-20504.

[1] J. K. Olthoff, J. A. Tossell, and J. H. Moore, J. Chem. Phys. **83**, 5627 (1985); D. M. Pearl, P. D. Burrow, J. J. Nash, H. Morrison, and K. D. Jordan, J. Am. Chem. Soc. **115**, 9876 (1993).

SESSION J: POSTER SESSION
Wednesday afternoon, 19 October 1994
NIST Building 101
Lecture Rooms A and B
and Employee Lounge, 15:45–17:30
J. K. Olthoff, presiding

JA: MICROWAVE DISCHARGES

JA-1 **Kinetics of Formation and Loss of S_2 in a Pure SF_6 Microwave Magnetoplasma**, C. BARBEAU, F. CHATAIN*, L. ST-ONGE, J. MARGOT, M. CHAKER**, J.P. BOOTH* and N. SADEGHI*, U. de Montréal – Formation and loss mechanisms of molecular sulfur S_2 in the ground state are investigated using laser-induced-fluorescence spectroscopy in a surface-wave-sustained SF_6 plasma at 2.45 GHz, submitted to a static magnetic field. The plasma is operated at low gas pressure (1–10 mtorr) near ECR conditions. The relative importance of surface and volume reaction paths for S_2 formation under specific plasma conditions is determined from the space dependence of S_2 density as a function of the distance from different substrates (Si, W, Al, stainless steel). The relative density of atomic fluorine has also been measured in order to underline the effect on S_2 formation of the presence in the plasma of a F atom-consuming material. Moreover, measurements of the S_2 density decay in the post-discharge of a pulsed plasma allow the characterization of S_2 losses to reactor or substrate walls.

* LSP, U. Joseph-Fourier, Grenoble (France)
** INRS-Énergie et Matériaux, Varennes (Québec)

JA-2 Si and SiH_3 Radicals in On-Off Modulated ECR SiH_4 Plasma*, M.HORI, Y.YAMAMOTO, M.HIRAMATSU* and T.GOTO, Nagoya Univ. and Meijyo Univ.* - The Si and SiH_3 radical densities in ECR SiH_4 plasma have been measured using ultraviolet absorption spectroscopy (UVAS) and infrared diode laser absorption spectroscopy (IRLAS), respectively. The microwave power was modulated with on-period of 10 ms and off-period of 20 ms. The radical measurements were carried out at 27 cm below ECR plasma region. In the SiH_4(50%)/H_2 plasma, Si and SiH_3 radical densities were $3x10^9$ cm^{-3} and $2x10^{10}$ cm^{-3}, respectively, at the SiH_4 flow rate of 6 sccm, the microwave power of 400 W and the total pressure of 1.3 Pa. The SiH_3 radical density increased up to around 1.5Pa and then decreased as the total pressure increased, while the Si atom

density decreased as the total pressure increased. The mechanisms of these behaviors in the ECR plasma have been investigated.

*Work supported by a Grant-in-Aid for Scientific Research on Priority Area from the Ministry of Education, Science and Culture.

JA-3 Waveguide Based Field Applicator for Large Diameter Plasma Generation*, M. MOISAN, Z. ZAKRZEWSKI, R. GRENIER and G. SAUVÉ, Dépt. Physique, Université de Montréal - We describe a field applicator suitable to sustain plasmas in cylindrical vessels with diameters comparable or large with respect to free-space wavelength. It is based on a circularly bent rectangular waveguide with an inwardly directed power leaking aperture. This aperture comprises a resonant array of centred inclined slots in the wide wall of the waveguide terminated with a fully reflected load to create standing wave pattern to which the slot positions are correlated. We have built and investigated such an applicator operating at 2.45 GHz and fed directly from a WR-430 waveguide to sustain plasma in tubes of approximately 130 mm diameter. It was used to generate argon and helium plasmas in the pressure range 0.5-10 torr and at input power up to 1 kW. Over this range of pressure and power, the power reflection coefficient at the applicator input, operated with no tuning elements, does not exceed 0.05 provided the input power is larger than some minimum value (less than 100 W for argon, less than 300 W for helium).

* Supported by NSERC (Canada) and Academy of Sciences of Poland

JA-4 Electromagnetic Performance of a Surfatron-based Coaxial Microwave Plasma Torch*, M. MOISAN, R. GRENIER and Z. ZAKRZEWSKI, Dépt. Physique, Université de Montréal - Low power microwave plasma torches are of particular interest to analytical chemists. The torch design investigated is based on the known surfatron structure[1] with an interchangeable coaxial transformer section added before the nozzle at the tip of which the discharge occurs. We have carried a series of experiments to illustrate some important aspects of the electromagnetic performance of this coaxial microwave plasma torch operating at 2.45 GHz and with input power 10-160 W. A specially devised slotted coaxial line with a movable probe arrangement can be inserted into the torch in place of the transformer section enabling direct, in situ, measurements of the plasma impedance. Using results from these measurements, we show ways to control the shape of the tuning characteristics of the torch to improve power transfer to plasma and stability of operation, and to simplify the torch design. The procedures presented have a general character and can be applied to various torch configurations.

* Supported by FCAR (Québec) and KBN (Poland).

[1] M. Moisan, Z. Zakrzewski, J. Phys. D: Appl. Phys. **24**, 1025 (1991)

JA-5 Behavior of Lithium in a Microwave Resonant Cavity Discharge* CYNTHIA BUSH BROOKS , RAMI A. KISHEK, R. M. GILGENBACH AND M. L. BRAKE, Department of Nuclear Engineering University of Michigan; Ann Arbor, MI 48109. An Asmussen-type microwave resonant cavity ion source[1] will be used for laser-enhanced isotope enrichment of lithium-6 in natural lithium. Lithium is introduced to the system in the form of lithium chloride, which is then heated by a background argon discharge allowing dissociation of lithium and chlorine. The dissociation is evidenced by the observation of strong Li-I lines in the discharge using optical emission spectroscopy. Several methods of introducing the LiCl will be presented and their effectiveness compared. Behavior of the discharge with varying initial amounts of LiCl and argon gas pressures will be shown. Methods of collecting processed lithium will be discussed as well.

* Work supported by DOE DE-FG02-92ER75789

[1] L. Mahoney and J. Asmussen, Rev. Sci. Instrum. **61**(1), 285 (1990).

JA-6 The Ring-Resonator - A New Concept for the Microwave-Excitation of Gas-Discharges,* A. HUNSCHER, J. MENTEL, Ruhr-Universität Bochum, AEEO, Germany - A new resonator-concept for the MW-excitation of gas discharges is presented. MW-energy is coupled into a ring build up by R32 waveguide components. Usually two travelling waves are excited in the ring superposing to a standing wave. However, with a tuning element in the ring (EH-tuner) by positive and negative interference with the incident wave a travelling wave in only one direction with an enhanced electric field can be realized. A plasma tube is inserted in the direction of the waveguide on one side of the ring, so that the electrical field (H-mode) is perpendicular to the tube-axis. The impedance of this ring-resonator is matched to the MW-generator (2.45 GHz magnetron) by another tuning element (EH-tuner). We solve with this resonator-concept the problem of low MW-power absorption of gas discharges combined with the the advantages of a travelling wave excitation. We reach high power dissipation (more then 90 % of the incident power) and homogeneous discharges in several gases in a wide pressure range (10-10^5 Pa). We realized with this structure, for our knowledge for the first time, a MW-excited He-Cd^+-laser oscillating on the blue 441.5 nm line.

*Supported by the CEC, Copernicus-Programme CIPACT 93-0219.

JB: MAGNETICALLY ENHANCED PLASMAS II

JB-1 Measurement of Electromagnetic Wave Structure in Novel Geometry Helicon Source, RUSTY JEWETT[1], A. J. PERRY[2], R. W. BOSWELL[2], H. M. ANDERSON[1], *1. Chemical and Nuclear Engineering, 209 Farris, University of New Mexico, Albuquerque, New Mexico 87131, U.S.A. and 2. Plasma Research Laboratory, Research School of Physical Sciences, The Australian National University, Canberra, ACT 2601, Australia.* - **B**-dot probes were used to examine electromagnetic wave structure parallel to magnetic field lines in an argon plasma, powered by a novel geometry helicon source. Wavelengths of ~10cm were observed at low pressure with a density of 2 x 10^{12} cm^{-3}, and an average static field of 100 Gauss. Results for a variety of operating conditions are presented, and compared with the dispersion relation in finite geometry.

JB-2 Observation of non-thermal electron tails in novel geometry helicon plasma, R. F. JEWETT[1], H. PERSING[2], R. W. BOSWELL[2], H. M. ANDERSON[1], *1. Chemical and Nuclear Engineering, 209 Farris, University of New Mexico, Albuquerque, New Mexico 87131, U.S.A. and 2. Plasma Research Laboratory, Research School of Physical Sciences, The Australian National University,*

Canberra, ACT 2601, Australia.-Non-thermal electron tails have been observed in an argon plasma, powered by a novel geometry helicon source. Data can be accurately described by a two-temperature electron population model. The presence of only 2% of 18eV electrons in a 3eV Maxwellian background increases the number of electrons with enough energy to ionize argon by 100 times. Measurements are shown for a variety of probe positions and operating conditions.

JB-3 Quasineutral Particle Simulations of ECR Plasma Processing Devices*, G. JOYCE, M. LAMPE, W. MANHEIMER, AND S. SLINKER, Naval Research Laboratory -- Because of the disparity of time scales (from 10^{-10} sec for electron plasma oscillations and gyrations to 10^{-4} sec for heavy particle equilibration), it is quite difficult to perform particle simulations of low-pressure plasma processing devices using standard techniques. We are developing a quasineutral particle simulation for an ECR discharge. In this formulation, which avoids the fast time scales, the internal electric field is determined by the requirement of quasineutrality, rather than by solving Poisson's equation. The electrons are modeled as guiding center particles that are constrained to move only along the field lines. The ions move in three dimensions under the influence of the external magnetic field and the self-consistent electric field. The electrons are heated by the microwave fields and collide with the neutrals, leading to ionization, dissociation, and isotropization of the electrons. The plasma sheath potentials are determined from a two-dimensional generalization of the "logical sheath" condition[1]. Simulations of simple axisymmetric ECR reactors are presented.

*Supported by ONR.

1. S.E. Parker, et al., J. Comp. Phys. **104** 41

JB-4 Simulation of the cathode fall region of a cylindrical magnetron discharge, T.A VAN DER STRAATEN, N.F. CRAMER, I.S. FALCONER and B.W. JAMES, School of Physics, U. of Sydney, Australia - A DC magnetron discharge between concentric cylindrical electrodes has been simulated using a one-dimensional, electrostatic particle-in-cell code, with electron and ion collisions with the filling gas being modelled using Monte-Carlo techniques. The model incorporates non-periodic boundary conditions and an external circuit, and the electric field is calculated self-consistently from the charge density profile until a steady-state has evolved. This model has been used to examine a steady state discharge for a range of magnetic field strengths, discharge currents and gas pressures for helium and argon. The spatial structure of the discharge is shown to be heavily determined by the relative values of the electron and ion cross-field mobilities. Electron and ion energy distributions have also been calculated at several radial positions within the discharge. The results of preliminary Langmuir probe measurements of the radial potential distribution in a laboratory magnetron are presented and compared with the predictions of the model to determine if the code realistically models a magnetron discharge.

JB-5 Modelling helicon plasma wave fields using ANTENA, Albert R. Ellingboe, Rod Boswell, PRL, R.S.Phys.S.E., ANU Australia - Detailed comparison between plasma wave fields calculated using ANTENA (B.McVey, Plasma Fusion Center, MIT, 1984) and measured in the experimental apparatus WOMBAT are made. A Boswell type (double saddle coil) antenna and a double-half-turn antenna have been used. The comparison is found to be good, both under the antenna (where there is a standing wave) and downstream from the antenna (travelling wave).

JB-6 Thomson Scattering Measurements of Spatial Profiles of T_e and N_e in an ECR Discharge, H. MUTA, H. TANAKA, M. YOSHIDA, M.D. BOWDEN, K. UCHINO, K. MURAOKA, M. MAEDA, Y. MANABE and R.K. PORTEOUS, Kyushu U., Mitsubishi Heavy Industries, Matsushita Electric and Australian National U. - We have previously reported incoherent Thomson scattering measurements of electron temperature T_e and density N_e in the source region of argon ECR discharges[1,2]. In this paper, we report measurements of radial profiles of T_e and N_e in both the source and downstream regions of an argon ECR discharge. Measurements were made for a variety of gas pressures and magnetic field configurations. These measured profiles were compared to the profiles calculated with a two-dimensional fluid/particle-in-cell hybrid model of the plasma[3] in order to determine the important influences on the density and temperature for different discharge conditions.

[1]M.D. Bowden *et. al.*, J. Appl. Phys. 73, 2732 (1993)
[2]H. Muta *et. al.*, 46th GEC Meeting, Montreal, October 1993.
[3]R.K. Porteous *et. al.*, Plasma Sources Sci. Technol. 3 (1994) 25-39

JB-7 Breakdown, steady-state and decay regimes in pulsed oxygen helicon diffusion plasmas, C. CHARLES* and R.W. BOSWELL, PRL, R.S.Phys.S.E., ANU, Australia, *Laboratoire des Plasmas et Couches Minces, IMN-CNRS, France - Continuous and pulsed oxygen helicon diffusion plasmas have been characterized (ion energy distribution function -IEDF-, plasma potential, floating potential) by using an energy selective mass spectrometer and a Langmuir probe situated in the silica covered aluminum diffusion chamber of a helicon SiO_2 deposition reactor. In the continuous case, the IEDF of the O_2^+ ions escaping from the plasma to the sidewalls of the chamber consists of a single peak at an energy corresponding to the plasma potential in the chamber (≈32Volt). In the pulsed case, the IEDF exhibits two additional peaks at high (≈60Volts) and low (≈15Volts) energy as a result of different states of the plasma during the pulse period. Analysis of plasma breakdown, steady state, and decay has been made. The wall potential appears as a critical parameter.

JB-8 Comparison between plasma potential and ion transport in an extended Helicon source/diffusion chamber system, R. BOSWELL*, N. SADEGHI, F. CHATAIN and J. DEROUARD, Labo. de Spectrométrie Physique, Université J. Fourier Grenoble I, FRANCE--Previous measurements in low pressure diffusion plasmas have shown that the ion energy distribution function can have a high energy component presumably originating from ions created in the source and accelerated in the self consistent electric field generated by the expanding plasma. We present correlated measurements of plasma potential (Langmuir probe) and ion drift velocity (Laser Induced Fluorescence) along the axis of an extended Helicon source/diffusion chamber system. The

results are compared with ion energy distribution functions measured in the diffusion chamber with a multi grid analyser. Although the plasma potential in the source remains high (50 V) the transport of ions is critically dependent on the magnetic field configuration in the source region (uniform or cusp) and whether the plasma is in the low (pre jump) or high (post jump) density mode.

***Permanent address : PRL, Australian National University, ACT (Australia).**

JB-9 **Negative Ion Measurements In ECR Plasmas By Using Omegatron Mass Analyzer* :** GON-HO KIM, NOAH HERSHKOWITZ, EN-YAO WANG**, JOHN MEYER, and SARAH GROSS, Engineering Research Center for Plasma-Aided Manufacturing, University of Wisconsin-Madison, Madison, WI 53706 - An omegatron mass analyzer was modified and employed in detecting the negative ions in Electron Cyclotron Resonance (ECR) plasmas. In applying the omegatron to negative ion measurement, plasma is permitted to flow through a floating aperture along the magnetic field and the end plate is biased negatively. The electron and the negative ions emerging from the aperture encounters an transverse rf electric field applied inside the omegatron chamber, while most positive ions are collected at the end plate. Negative ion and electron separation occurs as the result of ion cyclotron resonance. Preliminary results show H^+, H_2^+, and H_3^+ and H^- in hydrogen and O^+, O_2^+, O^-, and O_2^- in oxygen ECR plasma. From the observation of the peak values, it is estimated that the negative ion concentration increases with pressure decreases and power increases. Experiments with CF_4 plasmas are planned.

* Work supported by the National Science Foundation Grant No. ECD-8721545.
** On leave from Southwestern Institute of Physics, Leshan, Sichuan, China.

JC: POSITIVE COLUMNS

JC-1 **Response of the Electron Velocity Distribution Function on the Impact of Spatially Dependent Electric Fields,** R. WINKLER and F. SIGENEGER, *INP Greifswald, Germany* — The study of the electron kinetics in spatially inhomogeneous plasma regions presents an important subject of current research on real discharge plasmas. To improve the understanding of the complicated behaviour of electrons in such plasma regions an accurate and very efficient approach has been developed for the solution of the one-dimensional inhomogeneous electron Boltzmann equation under the impact of a spatially dependent electric field and the action of elastic and inelastic electron collisions with gas atoms. This new method is used to investigate the reponse of the velocity distribution function, of relevant macroscopic quantities and of the power and momentum balance of the electrons in model and inert gas glow discharge plasmas on the impact of spatially embedded transitions and disturbances of the electric field. In addition to the representation of the main aspects of the new solution technique the resultant very different (nonperiodic and periodic) space dependencies of the electron distribution, the lengths for the establishment of the distribution into homogeneous states and the remarkable deviations from the local field approximation are illustrated and discussed.

JC-2 **Energy Distributions of Charged Species in the Volume and Incident on the Walls of Electropositive and Electronegative DC Positive Column Discharges,*** Fred Y. HUANG and Mark J. KUSHNER, University of Illinois, Dept. of Elect. and Comp. Engr., Urbana, IL 61801 USA - We previously introduced a modeling technique which equivalently treats transport of electrons, ions, and excited states. This model has been incorporated as the kinetic portion of a hybrid Monte Carlo-fluid model for positive column discharges. Densities and electric fields are obtained from the fluid module, while sources, transport coefficients, energy distributions, and angular distributions are computed in the Monte Carlo module. We have used this model to obtain energy and angular distributions for all species incident on the radial wall of the discharge, as well as to obtain volumetric velocity distributions. Diffusion heating and cooling effects will be discussed, as will the anisotropy of electron velocity distributions near the sheaths. The parametric dependence of these quantities as a function of p·d (pressure · diameter) and current densities will be discussed for electropositive (He/N_2) and electronegative (He/CF_4) mixtures.

* Work supported by SRC, NSF, and the University of Wisconsin ERC for Plasma Aided Manufacturing.

JC-3 Measurement of the XeI 147 nm Resonance f-value,* S. D. BERGESON, H. ANDERSON, D. A. DOUGHTY, and J. E. LAWLER Univ. of Wisconsin-Madison & General Electric CRD-Schenectady--Atomic xenon (Xe) is a candidate for replacing Hg in fluorescent lighting discharges because of environmental concerns over Hg. A highly quantitative understanding of resonance radiation transport in Xe is needed. To facilitate this, we report an accurate absorption f-value of 0.264 ± 0.016 for the 147 nm resonance line. This f-value is measured using absorption spectroscopy with an experiment designed to produce equivalent widths on a particularly well understood part of the curve of growth. Equivalent widths of 1 cm^{-1} to 10 cm^{-1} are measured using a 3 m vacuum monochromator with both accurately determined cell lengths and gas pressures (in the 0.1 to 1.0 Torr range). This very direct and accurate new measurement is compared to other f-values in the liturature.

*Supported by the General Electric Company and by NIST under the Advanced Technology Program.

JC-4 Radiation Trapping Simulations for the XeI 147 nm Resonance Line,* J. E. LAWLER, H. ANDERSON, S. D. BERGESON, and D. A. DOUGHTY Univ. of Wisconsin-Madison & General Electric CRD-Schenectady--Atomic xenon (Xe) is a candidate for replacement of Hg in fluorescent lighting discharges because of environmental concerns over Hg. A highly quantitative understanding of resonance radiation trapping in Xe is needed. We have developed a Monte Carlo code which includes angle-dependent partial frequency redistribution. Our code represents an improvement over earlier work in that both numerical integration and "look-up" tables have been eliminated.[1] This code, when used with a our value of 0.264 for the 147 nm absorption f-value, accurately reproduces experimental trapped decay rates from 2 mTorr to 1 Torr.[2]

[1] J. S. Lee, Astrophys. J 255, 303 (1982).
[2] F. Vermeersch et al., in Optogalvanic Spectroscopy, Inst. of Physics Conf. Ser. 113, 133 (1991).

*Supported by the General Electric Company and by NIST under the Advanced Technology Program.

JC-5 Simulation of the Angular Distribution of Resonance Radiation from a Positive Column Discharge,* D.A. DOUGHTY, GE Corporate Research and Development - A Monte Carlo simulation of radiation transport is used to determine the angular distribution of resonance radiation emanating from a positive column discharge. With the specification of the oscillator strength, absorption/emission profile, gas density, spatial distribution of radiating atoms, and boundary geometry, the angular distribution of photons arriving at the wall of the discharge is obtained. The ratio of the integral of the angular distribution to that for a diffuse, Lambertian surface is on the order of one-half for the parameter space studied here. The angular distribution is found to be insensitive to the density of absorbing atoms, but strongly dependent on the spatial distribution of emitting atoms. When combined with a measurement of the absolute intensity at one angle, this distribution provides a means of determining the radiant emittance of the source when the actual measurement of the distribution is problematic.

*Work supported in part by NIST Advanced Technology Program, cooperative agreement 70NANB3H1372.

JD: PLASMA PROCESSING-ETCHING AND DEPOSITION

JD-1 Models for Plasma Etching by Bombarding Ions,* B. ABRAHAM-SHRAUNER and C. D. WANG, Washington University- Pattern transfer by glow discharge plasmas to semiconductor wafers is modeled for etch rates proportional to the ion energy flux.[1] In the etching of long semiconductor trenches the etch rates are given by approximate analytical expressions with the ion distribution functions modeled as drifted Maxwellians. The aspect ratio dependence of the etched trenches is examined as a function of the ratio of the ion bulk speed to the thermal speed as well as two parameters that model the mask etch. Also models for etching with threshold values in the ion energy flux[2] for onset of etching are given.

1. B. Abraham-Shrauner, 46th GEC Conf. 1993.
2. D. Dane & T. D. Mantei, Appl. Phys. Lett. (July, 1994, in press)

*Support in part by National Science Foundation.

JD-2 Plasma Chemistry Effects on SiO_2 to Si Selectivity in a High Density Fluorocarbon Plasma, K. H.R. KIRMSE, A. E. WENDT, R. A. BREUN, J. Z. WU, I. C. ABRAHAM, S. B. DISCH, J. A. MEYER, R. C. WOODS, N. HERSHKOWITZ, Engineering Research Center for Plasma-Aided Manufacturing, University of Wisconsin-Madison - SiO_2 to Si selectivity is an important control parameter in etching processes. The goal of this study is to determine how changes in the chemistry at the wafer influence the SiO_2 to Si selectivity in high density fluorocarbon plasmas. To do this, Si and SiO_2 etch rates in an ECR source were measured with an *in-situ* HeNe interferometer under a variety of etching conditions. Initial results show that the SiO_2 to Si selectivity in $C_2H_2F_4/O_2$ can be varied from over 30 to < 1 by varying the percentage of oxygen in the source gas. The decrease in selectivity is roughly proportional to changes in the $[CF_2]$ to [F] ratio measured for the same conditions using an infrared diode laser absorption system and actinometry, respectively. These data were correlated with ion chemistry data taken over the same parameter space which was obtained using an in-line, differentially pumped quadrupole mass spectrometer. The spectrometer orifice was mounted directly beneath a substrate holder with a sampling hole that admits ions and neutrals incident at the substrate surface. The effects of chemical species present at the wafer surface on selectivity control in high density plasmas will be discussed.

Work supported in part by NSF Grant # ECD-8721545.

JD-3 Mass Spectrometric Studies Of High Density Inductively Coupled Plasmas for Selective Oxide Etch. J. WINNICZEK, J. FLANNER and J. COOK, Lam Research Corp. - The stringent requirements of high etching selectivity of SiO_2 over Si, coupled with a high and very uniform etch rate, and vertical profiles for high aspect ratio 0.35 mm geometries, have led to the development of a low pressure high density inductively coupled plasma source. The ability of the fluoro-hydro-carbon plasma to form rather specific polymer films has a great effect on the etch results. Measurements of refractive indices and thicknesses of these films indicate that the composition of the film rather than its deposition rate determines the selectivity. High refractive index films correspond to more selective processes; the high index is indicative of a higher F/C ratio in the polymer. The plasma precursors that form the films and etch the SiO_2 are probed with a mass spectrometer with plasma ion detection capability as ions play a major role in oxide etch. It also vital to take account of the many neutral species present in the plasma. Electron energy scans of the mass spectrometer ionizer facilitate generation of appearance potential curves (APC). We demonstrate that the APC is necessary in order to distinguish between fragments generated in the plasma and those generated in the ionizer of the spectrometer.

JD-4 Measurement of Deposition Uniformity in PECVD of Silicon Nitride and Silicon Oxide,* C. B. FLEDDERMANN and K. N. WROBLEWSKI, Center for High Technology Materials, U. of New Mexico, and D. RUBY, Sandia National Laboratories- Plasma deposited silicon nitride and silicon oxide are commonly used for passivation of silicon surfaces. The uniformity of the deposition both across the wafer and in different positions in the reactor is dependent on reactor conditions such as input gas ratio, pressure, substrate temperature, and rf power. Measurements of deposition rate and index of refraction for nitride and oxide films deposited using a modified Pacific Western Systems Coyote PECVD reactor operating at 13.56 MHz will be presented. Silicon nitride is deposited using a silane/ammonia mixture, and silicon oxide is deposited using a silane/nitrous oxide mixture. These measurements show that growth rate and index of refraction drop off rapidly with distance away from the gas inlet, indicating a rapid consumption of the parent gases. Film thickness is generally very uniform across individual wafers for nitride films, but is not uniform across the wafer for oxide films. The index of refraction varies between 1.36 and 1.96 for nitride films, and 1.79 and 2.17 for oxide films. Comparisons of these results with models of PECVD of nitrides and oxides reported in the literature will be presented.

*Work supported by Sandia National Laboratories under contract AG-3855.

JD-5 Plasma Process Uniformity in a High Density System: Experiment and Modeling, M. SURENDRA, C. R. GUARNIERI, G. S. SELWYN, and M. DALVIE, IBM T. J. Watson Res. Ctr. Yorktown Heights, NY – Experiments have been carried out in a high density, rf inductively coupled system with a rf capacitively coupled substrate. By changing the spatial

variation of rf coupling to the substrate alone, we are able to vary the wafer scale etch rate uniformity of SiO_2 on blanket wafers from a profile that is ~ 20% higher in the center to one which is ~ 10% lower in the center. The effect of spatially altering rf coupling impedance to the substrate is dependent on substrate resistivity and applied frequency. Situations where substrate rf coupling is unintentionally nonuniform, e. g. wafer bowing due to backside cooling gas pressure, are also examined. Process rate uniformity has been modeled with two dimensional analytic models of the plasma source and rf sheaths, coupled to an equivalent circuit element discretization of the electrode assembly, substrate, plasma source and sheath. Results from the model are in reasonable agreement with experimental measurements.

JD-6 Submicron Anisotropic Etching of Tungsten at Moderate Low-temperature using a Large Diameter Microwave Magnetoplasma, F. BOUNASRI, E. GAT*, M. MOISAN, J. MARGOT, M. CHAKER* and M. EL KHAKANI*, U. Montréal - Anisotropic etching of W over silicon substrates was investigated at temperatures around -20°C and floating potential, in SF_6 in the 0.25 to 1.5 mtorr pressure range. Plasma was supplied into a 280 mm dia. reactor from a surface-wave sustained discharge under electron cyclotron resonance conditions using an axially uniform static magnetic field. The microwave power density was 0.1 W/cm^3 and the substrate was at 35 cm from the wave launching gap. This study was carried out at low ion energy (~ 15 eV), no external biasing voltage being applied to the substrate. Etch rates of SAL 603 resist, Si, W and a-SiC:H are reported as functions of pressure at -23°C. Ion current density and relative concentration of fluorine atoms were measured *in-situ* in the SF_6 plasma using a Langmuir probe and an argon-based actinometry technique. Submicron (0.2-1 μm) pattern transfer into W was also investigated using resist or nickel as masks. To provide insight into submicron etching phenomena, correlations between ion and fluorine fluxes, and the lateral and vertical etch rates of W were examined.

* INRS-Énergie et Matériaux, Varennes, Québec

JD-7 Relationship between the plasma and the electronic, mechanical and structural properties of C_2H_2 polymerized by RF discharge*, R.P. MOTA, E.F. LUCENA, R.C. DOMINGOS S.M.H.O. CRUZ, and M.A. B. DE MORAES**, UNESP-FE/DFQ-Guaratinguetá, Brazil. Actinometric optical emission spectroscopy was used to follow trends in the plasma concentration of the CH species (431.4nm) as a function of the RF power operation from 5 to 35W. Infrared spectroscopy was employed to characterize the molecular structure and the C-H bond density of the polymeric material. The deposition rate was determined by optical interferometry resulting in a 10 to 300 nm/min, its dependence on the operation power of the glow discharge polymerization was in good agreement with the behaviour of the C-H bond in the films and the behaviour of the CH species in the C_2H_2 plasma. The electronic properties of the films were calculated presenting optical gap from 2 to 3eV and the refractive index from 1.8 to 1.6. We studied the residual mechanical stress σ, of the polymer films. Measuerments of the stress were carried out by the bending method, using a HeNe laser , showing values ranging from 50 to 220MPa.

*Work in part supported by CNPq, FAPESP and FUNDUNESP
** IFGW/UNICAMP-Campinas, Brazil.

JD-8 Plasma Polymerization of Ethane, Propane and Acetylene: a Comparative Study of the Discharge and Film Properties*, R.P. MOTA, M.A.B de MORAES** and S.F. DURRANT**, UNESP-FEG,DFQ, Guaratinguetá, SP, Brasil- By glow discharge polymerization, films were deposited from acetylene, ethane and propane in rf polymerization system. The influence of two important system parameters - gas feed pressure and applied power - on both the plasma properties and the deposited material was examined. Actinometric optical emission spectroscopy was used to determine trends in the electron density ρ_e and electron temperature T_e as well as the relative concentration of the radical CH, as a function of the two system parameters. Films grown under various conditions of feed pressure and applied power were characterized by infrared spectroscopy. Deposition rates were determined by optical interferometry. Plasma CH concentration and the activity of the plasma, which depends on ρ_e and T_e, were found to be directly related to the composition and rate of deposition of the films. These relations indicate why, under the same conditions, acetylene polymerizes at much higher rate than the other two monomers.

* Work in part supported by CNPq, FAPESP and FUNDUNESP.
** IFGW/UNICAMP- Campinas, SP, Brazil

JD-9 The properties of a microwave-generated plasma for the deposition of polycrystalline diamond films, I.S. FALCONER, V.L. HUMPHREYS, M.I. IBRAHIM, B.W. JAMES, J. KHACHAN, B.L. MATTHEW, J.R. PIGOTT, and M.J. WOUTERS, School of Physics, U. of Sydney, Australia - Although microwave assisted chemical vapour deposition is a valuable plasma source for the deposition of thin films of polycrystalline diamond, difficulties in measuring plasma parameters limit our understanding of the deposition process. Probably the most important parameter for understanding the essentially "chemical" deposition process is the gas temperature, which we have measured from the relative intensity of rovibronic components of an electronic transition of CN, CH_2 and N_2, and laser interferometry. Plasma parameters, which are critical to energy transfer and radical formation in the plasma, have been estimated using double Langmuir probes and from the relative intensity of the hydrogen Balmer lines. The interpretation of these diagnostics presents difficulties as the electron energy distribution function for the plasma deviates from Maxwellian.

JD-10 Spectroscopy of a Diamond CVD Reactor using Synchrotron Radiation,* M. A. CHILDS, K. L. MENNINGEN, L. W. ANDERSON, AND J. E. LAWLER, University of Wisconsin. - Several atoms and molecules have been detected in a hot-filament assisted diamond CVD reactor using absorption spectroscopy at the UW Synchrotron Radiation Center. Synchrotron radiation from 115 to 185 nm is used to make measurements of the absorption profiles of H, vibrationally excited H_2, C, CH_4, and C_2H_2. Density determinations are presented for C, H and C_2H_2. Spatially resolved measurements from the filament to the substrate allow us to study the effects of varying reactor parameters (filament temperature, substrate temperature, input CH_4 fraction and input flow velocity). The observed hydrogen dissociation fraction is higher than reported in the literature.

*Work supported by the Army Research Office and a grant from the NSF to the Synchrotron Radiation Center.

JD-11 Study of Diamond Growth From a Variety of Input Gases,* K. L. MENNINGEN, M. A. CHILDS, C. J. ERICKSON, L. W. ANDERSON, AND J. E. LAWLER, University of Wisconsin. - The gas phase densities of CH_3 and CH and the hydrogen dissociation fraction are measured in a hot filament diamond deposition system using high sensitivity absorption spectroscopy. The H/H_2 ratio is obtained from the CH_3 and CH densities. The gas composition, crystal growth rate, and the appearance of the diamond grown from several different input gases are examined. The nature of the input hydrocarbon is relatively unimportant because fast gas phase reactions completely scramble the identities of the input carbon atoms. The addition of oxygen suppresses the CH_3 and CH densities and inhibits the graphitic poisoning of the filament surface. Small concentrations of atomic impurities in the gas phase are also detected using high sensitivity absorption spectroscopy. Fractional absorptions of 10^{-5} are detected in this experiment.

*Work supported by the Army Research Office.

JD-12 Oxygen and Iron Implantation of Glass for Nonmetallic Magnetic Hard Disks,* L. ZHANG, J.H. BOOSKE, R.F. COOPER, J.L. SHOHET, J.R. JACOBS, Plasma ERC, U. of Wisconsin-Madison, and G. WAS, U. of Michigan - Plasma source ion implantation (PSII) of oxygen into iron-doped magnesium aluminosilicate (MAS) glass and simultaneous implantation of iron and oxygen into calcium aluminosilicate (CAS) glass have been investigated for developing a fabrication process to produce a nonmetallic magnetic hard disk. The implant energy used in these experiments was 30 keV and the oxygen dose was estimated to be 1×10^{17} ions/cm^2. Some of the implanted samples were annealed at 700°C. The samples were analyzed by Rutherford backscattering spectroscopy (RBS), transmission electron microscopy (TEM) and X-ray photoelectron spectroscopy (XPS). The results show that PSII of oxygen into iron-doped MAS glass increased the iron ion binding energy, likely due to the valence state conversion of Fe^{2+} to Fe^{3+}. The post anneal yielded a thin two-phase layer near the surface, consisting of Mg-Fe-Si-O crystals and the glass matrix. The simultaneous implantation of iron and oxygen into CAS glass resulted in the formation of an iron oxide, Fe_2O_3. Simultaneous implantation of oxygen and iron into undoped MAS glass is also being investigated. Details of TEM, RBS and XPS analysis from the oxygen and iron implanted CAS and MAS glasses will also be presented.

* Supported by the NSF under grant ECD-8721545

JD-13 Microstructure and Corrosion Resistance of Nitrogen Plasma Treated Aluminum,* L. ZHANG, J.H. BOOSKE, J.L. SHOHET, J.R. JACOBS, Plasma ERC, U. of Wisconsin, and A.J. BERNARDINI, Litton Industries - The objective of this work is to explore the feasibility of using nitrogen plasma ion implantation treatment to improve corrosion resistance of 6061T aluminum. Nitrogen ions were implanted into flat Al samples at a target potential of 30 kV. The profiles of Al and N in the samples were examined using a scanning Auger microprobe. It was found that a surface layer of AlN was formed and the surface was saturated by an implant dose between 7.2×10^{16} and 2.2×10^{17} ions/cm^2. Further implantation after the saturation dose will increase neither the thickness of the AlN layer nor the concentration of N in the layer. A 500 hour salt water spray field test has demonstrated that only the sample with the lowest implant dose (7.2×10^{16}) has acceptable resistance. A possible explanation is that further implantation beyond saturation dose only creates more defects in the AlN layer and degrades the corrosion resistance of the layer. To justify the speculation, further study including a more quantitative evaluation of corrosion behavior and surface structure analyses is being conducted. Results of this study will be compared with the plasma treatment process conditions to optimize the processing parameters for reliable corrosion protection.

* Supported by the NSF under grant ECD-8721545.

JD-14 DC Magnetron Reactive Sputtering Model with Two Species of Ions. A.ERSHOV* and L. PEKKER, Photran Corp. - The model of DC magnetron reactive sputtering has been developed which includes for the first time sputtering by both buffer and reactive gases. Previous models include the sputtering by buffer gas only (see for example [1]) thus limiting the consideration to the small values of reactive gas partial pressure and small sputtering rates. Argon and oxygen have been chosen as buffer and reactive gases in the presented model. Steady-state assumption has been made. The direct electron impact ionization, step-wise ionization through argon and oxygen metastable states, as well as dissociation of oxygen have been taken into account to calculate the ion current. The model allows us to consider the sputtering process for arbitrary ratio of partial pressures of reactive and buffer gases. This gives a possibility to simulate reactive sputtering for large erosion rates of target material. The comparison with experimental results for silicon target has been made.

[1] S.Berg, H.-O. Blom, M.Moradi, and C. Nenberg, J. Vac. Sci. Technol. A 7(3),1225

*Michigan Technological University, Houghton

JD-15 Formation of Fluorocarbon Thin Films using Plasma CVD Assisted by Selective Radical Source,* M. INAYOSHI, K. YAMADA, M. HIRAMATSU, M. NAWATA, M. IKEDA‡, M. HORI‡ and T. GOTO‡, Meijo Univ., and ‡ Nagoya Univ. — In the case of film formation by utilizing the plasma CVD method, it is desirable to supply selectively reactive species suitable for the film growth onto the substrate. We report on the developement of a novel CVD system, which is composed of the parallel plate RF (13.56 MHz) discharge plasma assisted by the selective radical source using the remote microwave (2.45 GHz) discharge plasma, and a cw-CO_2 laser for substrate heating. By using this system with a mixture of C_2F_6 and H_2, a whisker-like fluorocarbon film was successfully formed on Si substrate at C_2F_6/H_2=0.3/13Pa, RF power of 100W, microwave power of 100W, and substrate temperature of 600℃.

Work supported in part by a Grant-in-Aid for Research from the Ministry of Education, Science and Culture of Japan.

JD-16 Electron Kinetics and Plasma Chemistry in Plasma Polymerization Coatings for Laser Fusion Targets*, B. M. PENETRANTE, R. M. BRUSASCO, and G. WILEMSKI, Lawrence Livermore National Laboratory -- At LLNL, a considerable effort has been made to develop plasma polymer coatings on hollow microspheres for use as laser fusion targets. Considerable success has been achieved using a helical resonator reactor, but it is clear that an improved fundamental understanding of the plasma polymerization process can make significant improvements in the performance of current and future coatings, not only for

laser fusion targets but also for other commercial applications. This work is an attempt to understand the electron energy deposition and the significance of various plasma species in the plasma polymerization process. Electron kinetics and plasma chemistry calculations, along with experimental data, will be presented for typical operation at a gas pressure of 70 mTorr, using a gas mixture containing 99% H_2 and 1% C_4H_8. To what degree do the processes leading to polymer formation take place in the gas phase as opposed to the surface on which the polymer is deposited? Are the reactions in the plasma dominated by neutral or ionic species? The main goal of this analysis is to understand the activation of the monomer by the discharge plasma.

*Work performed at Lawrence Livermore National Laboratory under the auspices of the U.S. Department of Energy under Contract Number W-7405-ENG-48.

JD-17 2D Modeling of Microwave Plasma Enhanced Diamond CVD., B. Lane, *Plasma Dynamics*, Belmont, MA 02178 and *ASTeX, Inc.*, Woburn, MA 01801, E. Hyman, K. Tsang and A. Drobot, *Science Applications International Corporation*, McLean, VA 22102, and Richard Post, *ASTeX, Inc.*. We present results from a 2D self-consistent numerical model of microwave plasma assisted CVD reactors for diamond deposition in the 1-100 torr regime. Such modelling requires the treatment of (a) the microscopic coupling of electromagnetic energy to electrons and thence to the neutral gas, (b) the local gas phase neutral and charged particle chemistry of hydrogen, carbon and oxygen, (c) the macroscopic diffusive flows, species densities and temperature profiles and (d) the macroscopic microwave field pattern in realistic cavity geometries in the presence of plasma, (e) a model for surface reactions. These processes are tightly coupled and thus requires a simultaneous, self consistent solution of all the above processes. We present 2D (R-Z) self-consistent simulations of the electromagnetic field pattern, electron density, temperature, and important hydrocarbon species densities in an ASTeX High Growth Rate (HGR) reactor and a hypothetical "pancake" plasma reactor to investigate the effects of the thermal boundary layer at the wafer. We emphasize in the analysis of these results the 2D hydrocarbon chemistry and transport. We find that the radial distribution of the flux of the precursor species CH3 to the wafer is relatively flat although the atomic hydrogen flux is peaked on axis.

JE: PLASMA CHEMISTRY

JE-1 **Physics and Chemistry Modeling in RF CH_4 Plasmas,** A. RHALLABI*, E. GOGOLIDES, D. MARY, G. TURBAN*, NCSR "Demokritos" GREECE, *IMN FRANCE - A combined and consistent physics and chemistry simulator is presented as applied for RF CH_4 plasmas used for diamond-like deposition[1]. It consists of an one-dimensional (1-d) fluid model for plasma physics calculations (electron densities, temperature, etc.), a public domain[2] Boltzmann solver for electron energy distribution function (EEDF) calculations, and a generalized 1-d gas-phase chemistry simulator for prediction of the radical species densities and profiles. At the 100mTorr range, electron density is of the order 10^9/cm^3 (10-100 that of negative ions), bulk electron energy is 4eV, and the EEDF has less electrons in the tail than the Maxwellian or Druyvensteyn at the same energy. The CH_3, CH_2, and H densities are of the order 10^{12}, 10^{10}, 10^{13} /cm^3 respectively, with profiles that become flater as pressure is reduced. Sensitivity analysis reveals the major reaction pathways, and important reaction constants. All the above results compare favourably with experiments[3].

[1]E. Gogolides et al, J. Phys. D: Appl. Phys. **27** (1994), 818
[2]W.L. Morgan, B.M. Penetrante, Comp. Phys. Com. **58** (1990), 127
[3]H. Sugai, H. Toyoda, J. Vac. Sci. Technol. A **10**(4) (1992), 1193

JE-2 Gas Phase Reactions of Fluorocarbon Radicals in CHF_3/H_2 and CHF_3/O_2 ECR Downstream Plasmas*, K.TAKAHASHI, K.MIYATA, M.HORI, S.KISHIMOTO and T.GOTO, Nagoya Univ. - The reaction mechanisms of the CF_x(X=1-3) radicals in CHF_3/H_2 and CHF_3/O_2 ECR downstream plasmas were investigated using infrared diode laser absorption spectroscopy(IRLAS). The H_2 and O_2 partial pressure dependences of the CF_x densities were measured at CHF_3 pressure of 0.4Pa and microwave power of 300W. The H_2 and O_2 were added from 0.01 to 1.33Pa and from 0.01 to 0.67Pa, respectively. The CF density decreased gradually with increasing H_2 partial pressure. The CF_2 and CF_3 densities decreased rapidly with H_2 partial pressures up to 0.13Pa and the CF_2 density remained constant with further addition of H_2. The CF and CF_2 densities decreased rapidly below the detection levels at O_2 partial pressure of about 0.4Pa. The CF_3 density increased by a factor of 1.5 with O_2 partial pressures up to 0.02Pa and decreased gradually with further addition of O_2.
*Works supported by a Grant-in-Aid for Scientific Research.

JE-3 Self-consistent electron and heavy-particle kinetics in N_2-O_2 plasmas, V. GUERRA and J. LOUREIRO, CEL - IST, Lisbon Tech. Univ., Portugal - We present the results of a self-consistent model for the electron and heavy-particle kinetics in stationary N_2-O_2 discharges. The electron energy distribution function, the vibrational distributions of $N_2(X\ ^1\Sigma_g^+, v)$ and $O_2(X\ ^3\Sigma_g^-, v')$ molecules, and the concentrations of $N(^4S)$, $O(^3P)$ and $NO(X\ ^2\Pi_r)$ were calculated self-consistently by solving the Boltzmann equation along with the rate balance equations for the $v-th$ and $v'-th$ levels, and for the N, O and NO species. The present formulation involves the independent parameters E/N, $\delta(O_2)$=$[O_2]/N$ (with $N=[N_2]+[O_2]$), $\delta_e=n_e/N$, and T_g. The degree of excitation of both vibrational distributions are characterised by the temperatures $T_v(N_2)$ and $T_v(O_2)$, with $T_v(N_2) \gg T_g$ and $T_v(O_2) \gtrsim T_g$, which increase both as δ_e increases. The linked dependences of the concentrations [N], [O] and [NO] on the independent parameters are discussed. The effects of the V-V(N_2-O_2) and the V-T(N_2-O_2; N_2-N) energy exchanges are discussed as well, in particular, it is shown that a small concentration of O_2 added to N_2 produces a strong decrease in the rate of dissociation of N_2.

JE-4 Population Inversion between $(A^3\Sigma_u^+, v'')$ and $(B^3\Pi_g, v')$ States in a Positive Column of Nitrogen Pulsed Discharge,* E. AUGUSTYNIAK and J. BORYSOW, Physics Department, Michigan Tech. University - Time transients of population difference between $A^3\Sigma_u^+(v''=0)$ and $B^3\Pi_g(v'=2)$ states were measured in a positive column of moderate-current nitrogen pulsed discharge. The population difference was evaluated from integrated high resolution laser absorption/gain profiles. Optical gain, due to the population inversion, was present during the first 3 - 6 μs of the discharge pulse. The population difference was 0.3 $\times 10^{12}$ at the peak current of 1 A. Experiments were done at 0.5 Torr pressure and current densities ranging from 0.6 to 16 A/cm^2. The postulated kinetic model, which includes collisions with electrons and molecular nitrogen, and takes into account vibrational excitation of $N_2(X)$, reproduces fairly the measured time transients of population difference.

*Work supported by The National Science Foundation and State of Michigan Research Excellence Fund.

JE-5 Spatially-Resolved Mass Spectroscopy of Hydrogen and Other Light Hydrocarbon Species in the Boundary Layer During the Deposition of Diamond Thin Films* K. R. Stalder, SRI International, Menlo Park, CA 94025 - We report on continuing mass spectroscopic investigations of high-pressure arcjet plasmas. In previous studies[1], we found a radial decrease in the flux of acetylene while the total gas flux increased. The latter result is due to significant gas cooling and consequent density increase at constant pressure away from the stagnation point. In addition to CH_3 (M/e=15) and C_2H_2 (M/e=26), the flux of atomic hydrogen onto a growing diamond surface is also very important because it strips hydrogen effectively from the surface, thereby providing sites for further carbon insertion. Our current efforts are focusing on measuring the hydrogen flux on the surface and its spatial variation. As in earlier reports, spatially-resolved mass scans are achieved by mounting the arcjet source on a large x-y-z translator that enables the arcjet's stagnation point to be scanned around the sampling orifice in the deposition substrate.

*Work supported by ARO under Contract DAAH04-93-K-0001.

[1]K. R. Stalder and W. Homsi, 46th Annual GEC, paper DA-16, 1993.

JF: HEAVY PARTICLE INTERACTIONS

JF-1 Absolute Cross Sections For Reactions of $O^+(^4S, ^2D, ^2P)$ With N_2 and H_2,* X.Li,G.D.Flesch and C.Y.Ng,Iowa St.U.and Ames Lab,USDOE- We have been able to prepare O^+ in its pure $^4S, ^2D, ^2P$ states by varying the octopole trapping field in the cell where O^+ is produced.Combined with the differential method[1],this has enabled us to measure the cross sections of the reactions of state-specific O^+ with N_2 and H_2 over the collision energy range of .2 to 70 eV (lab).We find the cross sections for N_2^+ are constant over the above energy range and are ~1,32,46 Å^2,respectively,for $O^+(^4S), O^+(^2D), O^+(^2P)$.For $O^+ + H_2$,we have measured the cross sections of OH^+,H^+ and H_2^+.Contradictory to Kim et al.'s predictions[2],we find the cross section for $O^+(^2D)+H_2 \rightarrow OH^+ + H$ is higher than that for $O^+(^4S)$,while that for $O^+(^2P)$ is lower.We do not find H^+ in $O^+(^4S)+H_2$,but we do find H^+ for $O^+(^2D)$ and $O^+(^2P)$, where the reactions become spin-allowed.

*Work supported by National Science Foundation grant.
[1]X.Li,Y.L.Huang,G.D.Flesch and C.Y.Ng, submitted to Rev. Sci. Instrument.
[2]J.K.Kim,L.P.Theard and W.T.Huntress,Jr. J. Chem. Phys. 62(1975) 45.

JF-2 Vibrational Relaxation of Ozone in Electron-Irradiated $O_3/Ar/N_2/O_2$ Mixtures, B.L. Upschulte and B.D. Green, Physical Sciences Inc., Andover, MA, W.A.M. Blumberg and S.J. Lipson, Phillips Lab, Hanscom AFB, MA -- Collisional relaxation of the coupled ν_3, ν_1 stretching modes of O_3 at 90 K has been investigated by monitoring time and pressure variations of the O_3 infrared emission at 9.6 μm in electron-irradiated $O_3/Ar/N_2/O_2$ mixtures. The gas mixtures were subjected to a pulsed 4.5 keV electron beam, and time-resolved spectra were recorded with a circular variable filter spectrometer. Spectral modeling was utilized to determine the temporal variations in the populations of each vibrational level, and a single quantum collisional relaxation model was used to evaluate total decay rates out of each vibrational level up to three vibrational quanta in this highly coupled system. Quenching rate coefficients were found to be in the range of 10^{-14} - 10^{-15} cm^3s^{-1} for O_2, N_2, and Ar collision partners. Vibrational Einstein coefficients for $O_3(\nu_3)$ with up to three quanta were also determined. This represents the first experimental determination for the two- and three-quanta states. These Einstin coefficients compare favorably with theoretical predictions.

This work was supported by the Air Force Office of Scientific Research and the Defense Nuclear Agency.

JF-3 Accuracy Issues in Surface Deactivation Measurements on Flowing Vibrationally Excited $N_2(X,v)$ Gas Using Coherent Anti-Stokes Raman Spectroscopy (CARS). J. W. PARISH and P. P. YANEY, U. of Dayton.* -- Studies have been carried out using a flowing-gas discharge tube to provide a range of molecular residence times of the gas at a specimen surface from more than 80 ms down to 4 ms. The most recent measurements have been made using excited gas from a 38-cm water-cooled discharge tube operated at 90 mA and 17 Torr. Deactivation coefficient values are typically obtained for $v=1$ through $v=4$ for the gas flowing through a known length (0 to 12 cm) of a specimen tube. Among the various accuracy issues are 1) saturation of the CARS signal due to the stimulated Raman process, 2) the contributions of homogeneous interactions to the observed decay constants, and 3) species present in the gas which can influence the transfer of excited $N_2(X,v)$ vibrational energy to the specimen surface. We have carried out various measurements in order to clarify these issues. The results of these studies will be presented.

* Supported by USAF Contract F33615-93-C-2303.

JF-4 Elastic and Inelastic Processes in Collisions of H^+ Ions with CH_4 Molecules below 1 keV.* M. KIMURA, Argonne National Laboratory, Y. Li, G. Hirsch, and R. J. BUENKER, Univ. Wuppertal, Germany. -- Elastic scattering and electron capture processes resulting from collisions of H^+ ions with CH_4 molecules are studied theoretically below collision energies of 1.5 keV. A molecular state expansion method within a fully quantum mechanical formalism is employed, where molecular states are obtained by the multireference double-excitation configuration-interaction method. Differential cross sections for electron capture show a strong dependence on molecular geometry in collision dynamics, and in the C_{2v} symmetry, the electron capture cross section is found to be larger by an order of magnitude than that for the C_{3v} symmetry.

* Supported by the U.S. Department of Energy, Office of Energy Research, Office of Health and Environmental Research, under Contract W-31-109-ENG-38 (MK).

JF-5 Excitation in the Products of Helium Metastable Reactions*, L. M. BABCOCK and N. G. ADAMS, U. of Georgia - Emissions have been detected from the reactions of helium metastable atoms, He^m, with N_2, O_2, NO, CO, CO_2, SO_2, NO_2, N_2O, H_2S and NH_3 using a flowing afterglow coupled with vuv to near ir monochromators. Emissions from metastable reactions have been distinguished from those generated in He^+ reactions by obtaining spectra without and with Ar added which destroys the He^m. Results for N_2, O_2, NO, CO, CO_2, SO_2 and N_2O are substantially in agreement with previous observations, although weak N_2^+ (A→X) emissions have also been detected for the N_2O reaction. SH^+ (A→X) has been detected with H_2S, N_2^+ (B→X) and O_2^+ (A→X) with NO_2, indicating the presence of N_2O_4, and the neutral emissions NH(A→X) and (c→a) from NH_3 indicating that neutral reactions are occurring in parallel with Penning ionization. Analyses of the data are proceeding to determine vibrational population distributions for the products.

* Work supported by NSF Grant No. AST-9023640.

JF-6 Electron Detachment and Charge Transfer for Collisions of Negative Ions with Ozone.* J. A. FEDCHAK, B. L. PEKO, L. K. KEYT, and R. L. CHAMPION, College of William and Mary -- Absolute total cross sections for electron detachment and charge transfer for collisions of O^- and various halogen anions with O_3 have been measured for collision energies ranging from near-threshold up to a few hundred eV. The experiments were performed with a well defined negative ion beam and a static target gas of ozone which was originally produced by condensing O_3 (from an oxygen discharge) at LN_2 temperature. The purity of the ozone is monitored during the experiments. Electron detachment is observed to be the dominant inelastic channel over most of the energy range and that cross section exhibits an energetic threshold which is several times the anion's electron affinity. The cross section for charge transfer is found to be relatively constant over the energy range of the experiments with a magnitude of $3 < \sigma < 5\text{Å}^2$; the results will be presented.

* Work supported in part by the U.S. DOE, Division of Chemical Sciences.

JF-7 **Distribution of Unimolecular Lifetimes in Ion-molecule Association Reactions,** A. D. Sen and V. G. Anicich, JPL, Caltech, and M. J. McEwan, U. of Canterbury - The distribution of unimolecular lifetimes of ion-molecule complexes formed in association reactions has been measured by ion cyclotron double-resonance. The mean unimolecular lifetimes of $(H_2C_6N_2^+)^*$ and $(CH_3CN.CH_3^+)^*$ were determined to be 180 μs and 140 μs respectively. A theoretical examination of the distribution of lifetimes of $(CH_3CN.CH_3^+)^*$ was conducted using a RRKM model. The RRKM distribution, when modified by experimental constraints, was found to be a good approximation of the experimentally determined lifetime distribution. The lifetimes for unimolecular dissociation and radiative relaxation, and the absolute efficiency of collisional relaxation are also reported.

JF-8 Positive Ion-Molecule Reactions in Methane,* J. de URQUIJO, I. ALVAREZ and C. CISNEROS, Instituto de Física, UNAM, México - Measurements of the mass spectra of secondary and tertiary positive ions of methane (with 200 ppm water vapour) have been made using a drift tube-mass spectrometer under swarm conditions. E/N was varied between 60 and 7500 Td, with drift distances, z, from 4.72 to 35.72 cm, and gas densitites, N, in the range $(2.07\text{-}32.9)\times10^{14}$ cm^{-3}. For $60<E/N<300$ Td, the variations of the relative abundance of CH_5^+, $C_2H_5^+$ and H_3O^+ with z and with the product Nz indicate that the first two ions undergo proton transfer wiht H_2O, favouring the production of H_3O^+. Above $E/N=300$ Td, the breakup of CH_5^+ and $C_2H_5^+$ becomes apparent by the presence of CH_3^+ and $C_2H_3^+$. At $E/N>2000$ Td, CH^+, CH_2^+ and $C_2H_2^+$ are produced in concentrations ranging between 3-20%.

*Work supported by DGAPA and CONACyT.

JF-9 Model Potentials for Rare Gas Metastable Interactions, D. F. Hudson, NSWC/White Oak - Progress is reported on a program to generate reasonably simple interaction potentials for Rg^m - Rg^m and Rg^m - Rg interactions which will be useful for modeling studies. The asymptotic and well minimum are treated by the methods of Tang et. al. [1] and Varandas and co-workers [2]. Various methods are used to determine the form of the repulsive wall. Results of the various formulations are presented and compared with experimental results for $He(2^3S)$ + $He(2^3S)$ and $Ar(^3P)$ + Kr.

1 Tang, K. T. and Toennies, J. P., J. Chem. Phys 66, 1496, 1977.
2 Varandas, A. J. C. and J. Brandao, Mol. Phys. 45, 857, 1982.

JF-10 Highly Rotationally Excited NO(v,J) in the Thermosphere due to Solar and Auroral Energy Deposition, P.S. ARMSTRONG[1], S.J. LIPSON, W.A.M. BLUMBERG, J.A. DODD[1], J.R. LOWELL, and R.M. NADILE, Phillips Lab, Hanscom AFB, MA, and [1]Stewart Radiance Lab, Bedford, MA -- Earthlimb spectra of thermospheric nitric oxide fundamental band emissions near 5.3 μm, obtained in the CIRRIS 1A Space Shuttle experiment, have been analyzed using nonlinear least-squares synthetic spectral fitting. Absolute NO(v,J) number densities have been determined in the 100 to 260-km altitude region. Daytime spectra in this region reveal far greater rotational excitation than predicted based on the local kinetic temperature, and the high rotational excitation is observed in auroral spectra as well. Compared to the daytime, representative quiescent nighttime number densities for the rotationally equilibrated component are lower by a factor of 2-6, while the J=82.5 vertex state populations are lower by more than an order of magnitude. For NO($v\geq3$), the rotationally excited component emissions are more important than those for the equilibrated component, and are calculated to dominate the $\Delta v=2$ overtone bands. These results provide clues concerning NO(v,J) formation from $N(^4S,^2D) + O_2$ reactions under sunlit and auroral conditions, as well as important inputs to models of the chemistry, radiative processes, and energy budget of the thermosphere.

This work was supported by the Air Force Office of Scientific Research and the Ballistic Missile Defense Organization.

JF-11 Collisionally Induced Subthermal Nitric Oxide Spin-Orbit Distributions in the Thermosphere, S.J. LIPSON, P.S. ARMSTRONG[1], W.A.M. BLUMBERG, J.A. DODD[1], J.R. LOWELL, and R.M. NADILE, Phillips Lab, Hanscom AFB, MA, and [1]Stewart Radiance Lab, Bedford, MA -- The populations in the two spin-orbit manifolds of nitric oxide in the earth's thermosphere have been found to depart by as much as a factor of two (or hundreds of degrees K) from the ratio expected from thermal equilibrium. Absolute spin-orbit specific column densities of NO($X^2\Pi$, v=1) have been determined from high-resolution (1 cm^{-1}) IR earth limb spectra obtained in the CIRRIS 1A Space Shuttle experiment for the 100-200 km region. Nonlinear least-squares synthetic spectral fitting was used to analyze the NO($\Delta v=1$) emissions near 5.3 μm. The sublevel population ratio represents a third degree of freedom, along with vibration and rotation, that is not in equilibrium with the local kinetic temperature. The subthermal distributions most likely result from NO(v=0) + O collisions, which are the major source of NO(v=1) in the thermosphere. Thus, the present measurements provide new information on NO + O collision dynamics and the dissociation of the NO_2 transition states, suggesting a relationship with subthermal NO sublevel distributions observed in NO_2 photodissociation. It may be possible to use observed spin-orbit population ratios as diagnostic probes of NO(v) collisional and chemiluminescent excitation mechanisms.

This work was supported by the Air Force Office of Scientific Research and the Ballistic Missile Defense Organization.

JF-12
Inelastic Processes in Collisions of $H^{\pm}$ Ions with C, N, and O Atoms at Collision Energies in the low keV Range*. M. Kimura, Argonne National Laboratory, J.P. Gu, G. Hirsch, and R.J. Buenker, Univ. Wuppertal, Germany --Electron capture resulting from collisions of H^+ ions with C, N, and O atoms was studied theoretically at collision energies below 0.5 keV. A molecular orbital expansion method within a fully quantum mechanical formalism was used to investigate collision dynamics, with molecular states obtained by the multireference single- and double-excitation configuration-interaction method. In this representation, transitions within the same spin manifold are driven by nonadiabatic radial and rotational couplings, while those within different spin manifolds are driven by spin-orbit coupling. We examined effects of metastable states of C, N, and O atoms.

*Supported by the U.S. Department of Energy, Office of Energy Research, Office of Health and Environmental Research, under contract W-31-109-ENG-38 (MK).

JF-13 Effects of Velocity Dependent Cross Sections on the Thermal Mobility of Ions in Gases, T.MIYAZAKI, S.OKUDA and N.IKUTA, Tokushima Univ.Tokushima 770, Jpn. ---- Transport properties of ions in model gases are analysed with the extended FTI method[1] taking into account the residual velocity after anisotropic scattering in the laboratory frame under the assumption of isotropic scattering in the center of mass frame. The cross sections proportional to the powers of of relative velocity v_r^n, n= -1, -1/2 and 0, are used at gas temperatures of 50 and 300K. The thermal mobility of ions depends not only on the reduced mass but also on the ion mass m itself and the mass ratio m/M since the acceleration is dependent on 1/m and the residual velocity after scattering depends on the ratio m/M. It is found that the thermal mobility of ions[2] is dependent on gas temperature as $T_g^{-(n+1)/2}$. It has to be flat with E/N, in principle, although some dips are found in the mobility curves in molecular gases. In order to find the true interaction potentials, the features of ion transport properties in the whole range of E/N and of relative energies have to be made physically clear.

1) N.Ikuta,H.Gotoda,et al.: J.Phys.Soc.Jpn. 63(1993)536.
2) N.Ikuta: Tokyo symposium on ion transport,(1994-5), (unpublished).

SESSION KA: FLAT PANEL DISPLAYS
Thursday morning, 20 October 1994
NIST Building 101
Red Auditorium, 8:00–10:00
W. Hofer, presiding

Invited Papers

KA-1 Low-temperature plasma CVD of As-Grown Polysilicon Films for TFT Applications, K. TACHIBANA and T. SHIRAFUJI, Kyoto Institute of Technology – Polycrystalline silicon thin films were grown on glass substrates at a temperature as low as 300°C in $SiF_4/SiH_4/H_2$ RF-discharge plasma under the power density of 500mW/cm^2, the pressure of 0.2Torr and the total flow rate of 20sccm. In situ spectroscopic ellipsometry revealed that the c-Si fraction reached up to 80% in $SiF_4/SiH_4/H_2$(=2/2/16), while it saturated at 50% if SiF_4 was not supplied. Sequential repetition of the deposition in SiH_4/H_2 plasma and the treatment in SiF_4 plasma gave the c-Si fraction of 63%, where the latter treatment was proven to work in etching of a-Si preferentially than c-Si. A gas-phase reaction simulation suggested that the dominant precursor for deposition is SiH_3 radicals while that of etching is F atoms. The estimated densities of SiF_2H and $SiFH_2$ were negligible in the present condition. Mass analysis was also performed, which supported the results of our simulation.

KA-2 The Large Screen Opportunity of Plasma Displays, LARRY WEBER, *Plasmaco, Inc.* — Plasma displays were one of the first flat-panel display technologies but they have recently been overshadowed by liquid crystal technology for portable applications. However a very large opportunity for plasma displays is on the horizon for display diagonals of 20 to 60 inches because such large sizes are not easily manufactured by other flat-panel technologies. Applications for these sizes include the large markets for computer workstations and high definition television. Plasma display products showing full-color television and VGA quality are now available with 21 inch diagonals and full-color prototypes as large as 40 inches have been demonstrated.

Color plasma displays utilize color phosphors excited by ultraviolet light from a xenon based gas mixture at half an atmosphere and discharge gaps on the order of 100 μm. The necessary small size of the pixels has restricted practical devices to use the negative glow. The desired high display luminance requires the discharge to exhibit an inherent memory characteristic which allows operation at a pixel duty factor of one. Pixels must be addressable at speeds of a few microseconds in order to obtain television update rates and full-color gray scale. The major remaining gas discharge challenges are to achieve high luminous efficiency and a long stable device life.

Contributed Papers

KA-3 Plasma Display Panel Pixel Dynamics,* R.T. MCGRATH, et al., SNL, W. WILLIAMSON, Jr., et al., U. of Toledo, P. FRIEDMAN, et al., Photonics Imaging - Collaborative work is ongoing to increase understanding of the plasma dynamics and plasma materials interactions important for plasma flat panel display (PFPD) pixel operation. Models have been developed to assist with design of both monochrome and color PFPDs. The tools developed and being applied include 1) a simple analytical model for scoping studies, 2) one-dimensional fluid plasma models for assessing breakdown, bi-stable operating margin and multi-pulse (address/sustain/erase) operation, 3) a two-dimensional fluid plasma code for assessing different pixel electrode configurations and multi-pixel interactions, and 4) a plasma kinetic code in one spatial dimension for assessing non-Maxwellian effects. The accuracy of the model predictions is critically dependent upon the atomic physics and materials data provided as input to the models. Experiments are being conducted to measure current/voltage characteristics and spectroscopic emissions from pixel discharges and from closely related discharge configurations using a variety of different inert gas mixtures. The experimental data collected is being used to calibrate and validate the computational models.

*This work was supported by the U.S. Department of Energy under Contract DE-AC04-94AL85000.

KA-4 Comparison of Fluid and Particle 1-D Simulations of AC Plasma Display Panels*, V. VAHEDI, T.D. ROGNLIEN, B.M. PENETRANTE and J.P. VERBONCOEUR, Lawrence Livermore

National Laboratory -- The level of sophistication used to describe the dynamics of the discharge in plasma display panels will determine how computationally intensive and how practical the model is. This is a critical issue especially when the discharge dynamics is coupled with a comprehensive set of plasma chemistry that describes the numerous production and loss processes which control the populations of the radiating states. For fluid simulations, assumptions are usually made regarding the dependence of the electron transport and rate coefficients on, for example, the local and instantaneous value of the electric field. The objective of this work is to test the local field approximation by comparing fluid simulations with PIC-MCC[1] simulations. Results will be presented for Ne-Xe mixtures in configurations typical of double-substrate AC plasma display panels.

*Work performed at Lawrence Livermore National Laboratory under the auspices of the U.S. Department of Energy under Contract Number W-7405-ENG-48.

[1] V. Vahedi, G. DiPeso, C. K. Birdsall, M. A. Lieberman and T. D. Rognlien, Plasma Source Sci. Technol. 2, 261 (1993).

KA-5 The Kinship of a GEC RF Refererence Cell and an ac-Plasma Display Cell*, W. WILLIAMSON, JR., P. J. DRALLOS, AND V. P. NAGORNY, Dept. of Physics and Astronomy, The University of Toledo, Toledo, OH 43606 - A short introduction of the physical differences between a GEC cell and an ac-PDP cell will be followed by a discussion relating to the characteristic operating regimes of each cell. The contrast between a typical discharge in the cells will be presented and a highlight of the codes and analytic theory under development at The University of Toledo for an ac-PDP cell will be presented.

* Work supported by the USDOE under contract No. DE-AC04-76DP.

[1] P. J. Hargis, Jr., et al., Rev. Sci. Instrum. **65**, 140 (1994).

[2] e. g. P. S. Friedman, Proc. of SID, **30/3**, 253 (1989).

KA-6 Kinetic Corrections for HD Simulations of AC-PDPs,* P.J.DRALLOS, V.P. NAGORNY, and W.WILLIAMSON, JR., Dept. of Physics and Astronomy, Univ. of Toledo, Toledo, OH 43606 - The micro-discharges that provide the glow for ac plasma display panels (ac-pdp) are inherantly transient, self-extinguishing, and not in thermodynamic or hydrodynamic equilibrium. A proper description of the discharge must rely on self-consistent, electron kinetics in order to provide reliable excitation and ionization rates which characterize the discharge. Kinetic simulations, however, are often prohibitively time consuming. Fluid simulations are more efficient, but can not self-consistently provide the electron driven rates. Instead they rely on a parameterization of the rates based on some local, bulk property. Using self-consistent Boltzmann simulations, we have compared the kinetically derived rates verses those obtained parametrically from a local field approximation (LFA). We found the variation between the kinetic and LFA rates to be nearly independent of time but strongly space-dependent. This allows the construction of a 'correction' curve that can be used to modify the LFA rates to be consistent with the kineticly derived rates and provide more realistic fluid simulations of the discharge.

* This work supported by the USDOE under contract No. DE-AC04-76DP00789.

SESSION KB: ELECTRON COLLISIONS
Thursday morning, 20 October 1994
NIST Building 101
Green Auditorium, 8:00–10:00
S. K. Srivastava, presiding

Contributed Papers

KB-1 Electron Impact Excitation of the Chlorine Atom. D. C. Cartwright and J.B. Mann, Los Alamos National Lab.-* Integral cross sections for electron impact excitation of the chlorine atom are important for the optimized design of chlorine containing plasma etch reactors to be used in the semiconductor industry. A program is under way to obtain accurate integral cross sections to all bound states from the ground and two low-lying metastable states of the chlorine atom, from their thresholds to 500eV. These inelastic cross sections will eventually be obtained using a distorted-wave-plus-distortion approximation, multi-configuration initial and final target states, unitarization, and the n^{-3} scaling of the excitation cross sections. Initial results will be reported for excitation from the chlorine ground state.

*Supported by the US/DOE

KB-2 Ramsauer Effect in Atoms with Incomplete p-subshell,* I.I. FABRIKANT, U. of Nebraska-Lincoln – The low-energy e-O, e–S, and e–Cl scattering phase shifts have been calculated using an extrapolation of potential parameters along isoelectronic sequences of positive ions and the associated neutral atom with the inclusion of the long-range polarization and the Pauli exclusion principle. Both doublet and quartet scattering lenghts are negative for the S and Cl atoms, which causes Ramsauer minima for both atoms. In oxygen only the quartet scattering length is negative, and being small in absolute magnitude, it does not produce the Ramsauer effect. There are certain similarities between e–O scattering and e–Ne scattering on one hand, and between e–S, e–Cl, and e–Ar scattering on the other hand. However, nonzero values of the quadrupole moments and higher polarizabilities of the atoms with incomplete p-subshell make corresponding cross sections higher.

*Supported by the National Science Foundation.

KB-3 Electron Excitation out of the Metastable Levels into the 3^3S, 3^3D, and 3^1D Levels of the Helium Atom.* JOHN B. BOFFARD, MARK E. LAGUS, L. W. ANDERSON, and CHUN C. LIN, U. of Wisconsin–Measurements of the cross sections for electron excitation out of the metastable levels of He into the 3^3S, 3^3D, and 3^1D levels have been made for electron energies up to 450 eV. A fast He^+ ion beam is passed through Cs atoms. The charge exchange into the metastable He(2^1S) and He(2^3S) atoms is nearly resonant so that the emerging neutral He beam contains primarily metastabale atoms. This is a significant improvement over the hollow cathode discharge target source[1] which cannot be used for electron energies above the

threshold of excitation of the ground level (~23 eV) because the metastable concentration is only about 1 part in 10^5 ground-level atoms. The metastable He atom beam is crossed by an electron beam and the emission intensities from the 3^3S, 3^3D, and 3^1D levels are measured to obtain the cross sections.

*Supported by the National Science Foundation.

[1] D. L. A. Rall, *et al.*, Phys. Rev. Lett. 62, 2253 (1989); R. B. Lockwood *et al.*, Phys. Lett. A 166, 357 (1992).

KB-4 Absolute Measurements of Optical Oscillator Strengths of Noble Gas Resonance Lines,* N. D. GIBSON and J. S. RISLEY, North Carolina State University - Raleigh, NC. - We have remeasured the optical oscillator strengths of eight noble gas resonance lines. The new measurements use a 900 eV collimated electron beam to excite the atoms. The transmission of the emitted radiation was measured as a function of the gas density. In the method of self absorption used here, the measured oscillator strengths are proportional to the distance between the electron beam and the fixed aperture of the spectrometer-detector system. We investigated and eliminated a possible systematic effect in the determination of the absorption length due to deflections of the electron beam. These measurements are performed at higher energies than our previous experiments[1] at 100 eV in order to keep the electron beam path better defined. The measured oscillator strengths are He I (58.4 nm) 0.2700±0.0076, He I (53.7 nm) 0.0737±0.0023, Ar I (106.7 nm) 0.0580±0.0015, Ar I (104.8 nm) 0.2214 ±0.0060, Ne I (74.4 nm) 0.1095±0.0032, Ne I (73.6 nm) 0.1432±0.0038, Kr I (123.6 nm) 0.1775±0.005, and Kr I (116.5 nm) 0.1416±0.0041.

*This work was supported in part by NSF grant no. PHY90-16986.

[1]R.C.G. Ligtenberg, *et. al.*, PRA, 49, 2363(1994).

KB-5

Momentum Transfer and Vibrational Excitation Processes in Electron Scattering with C_2F_6 and C_3F_8 Molecules* M. KIMURA, R.A. BONHAM AND M.A. DILLON, ARGONNE NATIONAL LABORATORY, H. TANAKA AND L. BOSTEIN, SOPHIA UNIV-- Momentum transfer and vibrational excitation processes in electron scattering with C_2F_6 and C_3F_8 molecules were studied theoretically and experimentally at collision energies below 100 eV. Theoretically, we employed the continuum-multiple-scattering method, which is well suited to describe these processes correctly in electron scattering from larger molecules. We observed several resonance features in intermediate energy regimes for both molecules, and we interpreted the origins of these resonances on the basis of molecular structure calculations.

*Supported by the U.S. Department of Energy, Office of Energy Research, Office of Health and Environmental Research, under Contract W-31-109-ENG-38 (MK, RB, and MD).

KB-6

Elastic Scattering and Vibrational Excitation Cross Sections for Electron Collisions with C_2F_6* T. Takagi, L. Boesten and H. Tanaka, Sophia U., Tokyo and M. A.Dillon, Argonne National Laboratory -- Absolute elastic cross sections for e-C_2F_6 collisions have been measured for impact energies of 2-100 eV and scattering angles of 10-130°. From these angular distributions, the integrated and momentum transfer cross sections were obtained by extrapolation and numerical integration of least square fits to a phase shift expansion modified for application to e-molecule scattering. The vibrational excitation functions show resonances at 4.3 eV and 8.5 eV. Energy loss spectra were measured for vibrational excitation in the range of stretching and bending modes. By decomposition of the loss spectra and symmetry analysis according to angular correlation theory, the resonances were assigned to a temporary trapping of the electrons in the a_{2u} (4.3 eV) and e_u (8.5 eV) antibonding orbitals of the molecule. The sequence of trapping orbitals was selected to correspond to previous observations of CF_4 excitation functions.[1]

*Supported by the U.S. Department of Energy, Office of Energy Research, Office of Health and Environmental Research, under Contract W-31-109-ENG-38 (MD), and by a Grant in Aid from the Ministry of Education, Science, and Culture, Japan.

[1] Boesten L, Tanaka H, Kobayashi A, Dillon M A, and Kimura M *J. Phys. B* **25** 1607-1620 (1992).

KB-7 Calibration of Cross Sections Derived From Swarm Data,* A. GARSCADDEN and R. NAGPAL, Plasma Research Group, WPAFB- New parametrizations of electron transport in Helium-Ramsauer rare gas mixtures are presented[1]. Boltzmann calculations for small additions (0-20%) of He in Ar, Kr, and Xe show that there is a large increase in the electron drift velocities in the gas mixtures (by up to a factor of three) over those in either of the constituent gases. It is shown that due to its smaller molecular mass, elastic collisions in He-Ramsauer rare gas mixtures play analogous roles to weak inelastic collisions in molecular gas-Ramsauer rare gas mixtures. The swarm analyses of electron transport in the above gas mixtures provide a unique estimate of the *slope* and the *magnitude* of the momentum transfer cross section at and around the Ramsauer minimum of the buffer rare gases, since the cross sections of He are accurately known. These corrections significantly impact the low energy inelastic cross sections of molecular gases derived from swarm data, including the hydrogen cross sections.

*Work Supported by the Wright Laboratory.

[1]R. Nagpal and A. Garscadden, submitted for publication.

KB-8 Techniques for Identifying Excited States Populated in E-I Recombination,* N. G. ADAMS and B. L. FOLEY, U. of Georgia- This flowing afterglow technique distinguishes optical emissions (120-800 nm) resulting from electron-ion rcombination from those generated in ion-neutral and helium metastable reactions and those resulting from other sources. It involves making spectral scansover the wavelength range of interest, without and with a small amount of gas added which rapidly attaches electrons (SF_6 and CH_3I have ben used). Thus e-i recombination is quenched. Both the difference between the spectra and their ratio clearly identify emissions from recombination, even weak emissions. The technique has ben applied to several recombinations including O_2H^+, N_2OH^+, CS_2^+ and CO_2^+. Emissions were observed from OH(A→X), NH(A→X), CS(A→X) and the spin forbidden CO(a→X) showing that the OH A, NH A, CS A and CO a states are populated. From these spectra, information on vibrational populations is obtained. Emissions are also observed from electronically excited N_2O^+ which is generated in He^+ and He^m reactions with N_2O.

* Work supported by NSF Grant No. AST-9023640.

SESSION L: POSTER SESSION
Thursday morning, 20 October 1994
NIST Building 101
Lecture Rooms A and B
Employee Lounge 10:15–12:15
E. Benck, presiding

LA: PLASMA TECHNIQUES FOR WASTE TREATMENT I

LA-1 The Effects of Argon-Ammonia Mixture Gas on the Reduction of NOx in a Combustion Flue Gas by Superimposing Surface/Silent Discharge Plasma Reactors, K.Urashima, T.Ito, Musashi Institute of Technology, J.S.Chang, McMaster University - The effects of Ar-NH_3 mixture gas on the reduction of NOx in a combustion flue gas by superimposing surface/silent discharge plasma reactors is experientally investigated. The experiments are conducted for the applied voltages from 0 to 28 kV, the flue rates from 0.5 to 10 l/min and Ar-NH_3 mixture gas flue rates from 0.1 to 0.5 l/min, where a simulated flue gas and mixture gas compositions are (N_2:O_2:CO_2 = 80:10:10) and (Ar:NH_3 = 97 :3) respectively. The results show that : (1) NOx reduction increases with increasing discharge power and argon-ammonia mixture gas flue rate (2) superimposing surface and silent discharge yields more NOx reduction than an operating plasma reactor with only surface or silent discharge mode, since this can contribute more power to the reactor ; (3) NOx reduction energy efficiency increases with increasing argon - ammonia gas mixture flow rate and decreases with increasing discharge power ; (4) trace amounts of HNO_3, O_3, H_2O, and N_2O are observed as well as NH_4NO_3 aerosol particles.

LA-2 Generation of Ammonia and Nitrogen Radicals by DC and RF Discharge Plasmas for NOx Reduction in a Semiconductor Process Flue Gas, M. ARQUILLA, J.S. CHANG McMaster University , F.E. BARTOSZEK Ontario Hydro Technologies, and J. GALLIMBERTI Universita' di Padova - The NOx destruction efficiency by activation of nitrogen and ammonia mixtures using DC and RF (450 kHz) discharges has been experimentally investigated and the energy efficiency of these processes is also studied both experimentally and theorically. The experimental apparatus consists of a DC and an RF capacitively coupled plasma generator, reaction chamber and gas sampling system. The experiments are conducted at a pressure from 2 to 7 torr, and a gas flow rate from 100 to 800 micromole/sec at room temperature. The results are the following: a) the energy efficiency for nitrogen radical production is almost thirty times higher for an RF than for a DC discharge. A simplified statistical model confirms that the RF discharge reduces more efficiently a given quantity of NOx; b) ammonia decomposition with excited nitrogen molecules is more efficient with RF discharges; c) mixture of nitrogen and ammonia radicals injected into flue gas effectively reduce NOx, while pure ammonia or pure nitrogen radicals injected only slightly decrease NOx concentration.

LA-3 Treatment of Gaseous Wastes in a Very High Voltage Dielectric Barrier Discharge, M. NIKRAVECH, V. MASSEREAU, O. MOTRET, J.M. POUVESLE, and J. CHAPELLE, GREMI, CNRS/ University of Orleans, France.

A very high voltage triggered dielectric barrier discharge has been developped for the treatment of polluted gases and hazardous organic wastes. Very high voltage (90 kV) short (20 ns) pulses were applied with adjustable frequency (1 to 60 Hz) on two coaxial electrodes separated by a quartz tube which defines physical dimensions of a plug flow reactor. The method has been tested on well-known reactions. Destruction of CH_4 and CO_2 has been measured in various mixtures to determine the efficiency of the process. Mass balance was determined by in-line gas chromatography. Experiments were carried out at atmospheric pressure and room temperature. Conversion rates up to 25% and 40% have been obtained in pure CO_2 and CH_4, respectively. It has been shown that CH_4 dissociates following a 2nd order reaction. Vibrational and rotational temperatures of excited species and electron temperature have been estimated using spectroscopic methods. The role of the UV photons is presently under study.

LA-4 Experimental and Mathematical Modeling of Gas-Discharge Methods of Troposphere Cleansing from Chlorofluorocarbons (CFC's),* G. A. ASKARYAN, G. M. BATANOV, S. I. GRITSININ, I. A. KOSSYI, E. G. KORCHAGINA, A. A. MATVEYEV, V. P. SILAKOV, N. M. TARASOVA, *General Physics Institute, Russian Academy of Sciences, Moscow* — Possible schemes for cleaning the environment from antropohenic contamination by CFC's (CF_2Cl_2, $CFCl_3$, etc) are described. The method consist in a freely localized discharges excitation in an atmosphere. An analysis of the plasma processes capable of destructing CFC's molecules was performed. The results of laboratory experiments and results of mathematical modeling are discussed. The efficiencies of CFC's molecules destruction were found. It was shown that in a region where the microwave discharge is localized the CFC's molecules are destroyed with extremely high efficiency (small value of energetic cost for destruction of CFC molecule). Observed phenomenon is associated with the peculiar behavior of the high pressure microwave discharge lie in the fact of ionization instabilities development with the attainment of strongly nonlinear stage. Analysis of theory and modeling results determines the energetic characteristics of suggested system for environment cleaning. Both a possibility of local clean-up of CFC's and possibility of global cleaning of troposphere are considered.

* Work supported by International Science Foundation.

LB: CORONAS, ARCS, AND BREAKDOWN

LB-1 Influence of Space Charge on the Dielectric Behaviour of SF_6 under Oscillatory Impulse Voltages, S. K. VENKATESH and M. S. NAIDU, *Dept. of H.V. Engg., Indian Institute of Science* — Experiments were carried out to study the breakdown behaviour of SF_6 under oscillating impulse voltages (OIV) using a point-plane electrode system with a gap distance of 15 mm and over pressure range of 0.1 to 0.5 MPa. The frequency of the OIV was 400 kHz with a front time of 0.8 μs. The results showed that the breakdown voltage under OIV was higher than under the standard lightning impulse (LI) voltage with both positive and negative polarities. Under highly nonuniform fields at 0.1 MPa, corona stabilization occurs only under negative polarity LI voltage. However, this is not as pronounced as that observed under OIV. Under these conditions relatively longer time lags occurred with breakdown taking place at the second or third peak of the OIV. This has been explained on the basis of drift of positive and negative ions and the space charge modified field.

LB-2 Electrode Effect on S_2F_{10} Production in Negative Corona Discharges*

C. PRADAYROL, A.M. CASANOVAS, A. BELARBI and J. CASANOVAS
URA 277, Université Paul Sabatier, TOULOUSE, France -

The influence of plane electrode material (aluminium, copper, stainless steel) on S_2F_{10} (and other main gaseous SF_6 by-products) formation was investigated in SF_6 (300 kPa pressure ; dry $\simeq$ 200 ppm_V H_2O or damp : 2 000 ppm_V H_2O) submitted to point-to-plane negative corona discharges ($\bar{I} \simeq 24$ μA ; $0 < Q \leq 10$ C). For S_2F_{10}, the most important effect was observed, whatever the water contents beyond a transported charge value of $\simeq$ 3C : the greatest yields being obtained for aluminum and the lowest ones for stainless steel. Investigations were also carried out to test the influence of electrodes conditioning and showed that, particularly under wet conditions, S_2F_{10} production increased with plane electrode passivation.

Work supported by D.E.R., Electricité de France.

LB-3 Positive and Negative Coronas in SF_6

G. R. Govinda RAJU and J. LIU, U. of Windsor, Canada -

Positive and negative coronas are studied in a 5mm gap between a hyperboloid needle and a plane electrode in SF_6 at $N = 2.12 \times 10^{24}$ m^{-3}. The initiation and development of successive avalanches are traced as a function of time after voltage is applied. The simulation provides a detailed structure of avalanches from which essential differences between positive and negative corona with regard to total field distribution, propagation of successive avalanches and ion distributions can be discerned. The development of electron avalanches and streamers are due to ionization and photoionization while they are quenched due to space charge field. In positive coronas the total field is depressed near anode and enhanced in the rest of the region. In negative coronas the total field is enhanced near both cathode and anode and depressed in the region in between.

LB-4 Production of S_2F_{10}, S_2OF_{10}, and $S_2O_2F_{10}$ from Spark and Glow-Type Corona Discharges in SF_6/O_2 Gas Mixtures, I. SAUERS, *ORNL*, R. J. VAN BRUNT, J. K. OLTHOFF, S. L. FIREBAUGH, *NIST*, R. Y. LAROCQUE, C. LAVERDURE, *IREQ* — The rates for production of S_2F_{10}, S_2OF_{10}, and $S_2O_2F_{10}$ have been measured in both spark and negative glow corona generated using point-to-plane electrodes in SF_6 and SF_6/O_2 mixtures containing up to 20% O_2 and for absolute gas pressures in the range of 100 to 200 kPa. In pure SF_6, the production rates for S_2OF_{10} and $S_2O_2F_{10}$ are an order-of-magnitude or more below that of S_2F_{10} in both types of discharges. With the addition of 1% O_2, there is a dramatic drop in S_2F_{10} yield from both discharges with a corresponding increase in S_2OF_{10} yield from the spark and $S_2O_2F_{10}$ yield from the corona. The results can be explained from considerations of the competition among the reactions of SF_5 radicals with SF_5, O_2, and O and the relative degrees of O_2 dissociation in the two types of discharges.

LB-5 Breakdown Time Statistics for an Electrical Discharge in Argon, M. Agache, V. Kudrle*, M. Fitaire, Univ.Paris Sud, France-

Time τ for electrical breakdown of argon comprised between two parallel plates spaced by 2 cm was measured for pressure ranging from 1 to 5 Torr and applied voltage V_a to the gap discharge from 300 to 1600 V. τ is the time elapsed between the application of V_a and the rising edge of the discharge current. The probability Q(t), that breakdown hasn't appeared before time t, calculated using τ measurements for different V_a , agrees with an exponential low as predicted by Wijsman[1] . The deduced mean values for τ at different E/p are of the order of 10^2 ms. A special cathode - a dielectric sheet (kapton) between a polarised conducting plate and a grounded grid - has then been used as an electron emitter and the breakdown time again measured for previous pressures and voltages. With the dielectric of the special cathode submitted to an electric field $E \sim 6 \cdot 10^5$ V/cm, the distribution of τ values is fitted by a Poisson curve. The mean values are at least 10^4 order of magnitude lower than they are with E=0.

*On leave from Masaryk University Brno, Czech Republic

1 R.A.Wijsman, Phys. Rev., 75, 833 (1949)

LB-6 Electrode Erosion in High Currents Arcs in Argon and Nitrogen, G.F.GOMES, M.E.KAYAMA, M.A.ALGATTI, E.A.ARAMAKI AND R.P.MOTA, Universidade Estadual Paulista, UNESP, Campus de Guaratingueta, SP, Brasil

The erosion rate of brass and tungsten in arc at 15 kA was measured during experiments in a linear pulsed discharge. The electrodes had hollow tube shape and the discharge was performed at their end region. The current waveform is a characteristic RLC under damped current profile with 16 μsec period, 0.8 μH inductance and 50 mΩ resistance. The discharges were performed in Argon and Nitrogen with pressure in the range of 40-200 mTorr. The material loss was measured after around 1800 shots at each condition. Magnetic field mapping showed either contraction or expansion of plasma column, depending on the balance of ohmic heating, thermal conduction and radiation losses to the magnetic field energy rate. The material loss rate was 180 μg/C for brass-air, 108 μg/C for brass-Argon and 15 μg/C for brass-Nitrogen. The tungsten erosion rate was low, less than 1.7 μg/C. These elements were observed in high resolution spectroscopy that indicated lines of NIII, ArIV, ZnII and CuII.

LB-7 Attractor Model for Breakdown Instabilities in Microwave-powered Gas Discharges

H.F.MERKEL, H.-P.POPP, Graduiertenkolleg Numerische Feldberechnung, Universität Karlsruhe

The reduced electrical field strength in microwave-powered plasmas exceed the thermal equilibrium limit even in high-pressure discharges due to microwave resonances in pre-breakdown conditions. The resulting breakdown patterns exhibit a stable or quasiperiodic fractal structure. The characteristic fractal discharge types are discussed in terms of attractors in a power balance PDE. Static dielectric breakdown (DB) fractals solve a Dirichlet condition on their ideally conducting surface. The fractals of microwave-powered discharges have to fulfil a boundary condition of mixed type on their surface and the fields are solutions of Helmholtz-PDEs. So a electromagnetic DB algorithm had to be developed to predict the dielectric function of the breakdown pattern. The dielectric function is used in the power balance to couple thermal conductivity and fractal dielectric properties. The combined model describes plasmas constricted by thermal conduction and cold breakdown patterns. A set of stable solutions and an attractor map is obtained varying the phase difference and the amplitudes of the applied electromagnetic fields.

LB-8 Solar Array Arc Dynamics in the Presence of Magnetic Field, S. POPOVIC, Weber Research Institute, Polytechnic University, Brooklyn, N.Y. - Consider a thin conductor of rectangular section, partially covered with layers of dielectric, so that a portion of conductor is exposed to vacuum and interface dielectric-conductor-plasma (triple junction) exists. Current is flowing through the conductor and the induced magnetic field at the surface is in the range .3 to 30 G. The surfaces are exposed to dilute plasma and charged negatively up to 500V with respect to the plasma. We studied the dynamics of charged particles in this system as another example of the diamagnetic Kepler motion and found the observable influence of the induced magnetic field to charging of the dielectric surfaces, onset of the enhanced current flow to the conductor and the rates of unsustained discharges in the vicinity of the triple junction. The results are combined with the electrostatic theory of the enhanced electric field emission, and applied to the solar array arcing phenomena.

LB-9 Nonstationary Behavior of Pulsating Point-Dielectric Discharges Due to Discharge-Induced Increase in Dielectric Surface Conductivity, R. J. VAN BRUNT and P. VON GLAHN, *NIST*, T. LAS, *Electrotechnical Inst., Warsaw* — Observations have been made of the nonstationary behavior of pulsating discharges generated using alternating voltage applied to point-solid dielectric gaps in air. The nonstationary behavior is manifested by time dependences of the discharge pulse amplitude and phase-of-occurrence distributions. In some cases there is a complete and permanent disappearance of discharge pulses on the positive half-cycle at a given time after initiation of the discharge. The changes in discharge behavior have been correlated with discharge-induced increases in the local dielectric surface conductivity which appear to be associated with acidic deposits. The changes in the stochastic behavior of the discharge can be predicted using a Monte-Carlo simulation that allows for an increase in the surface-charge decay rate with increasing conductivity and a decrease in the rate of electron ejection from the surface with decreasing surface-charge density.

LB-10 Spectroscopy of a Turbulent Rotating Plasma in SF_6, C. FLEURIER, S. CIOBANU, D. HONG, *GREMI, Univ. d'Orleans* — Emission and absorption spectroscopy coupled to time resolved photographs with spectral resolution performed a detailed diagnostic of a transient electrical arc rotating between two circular electrodes in a strongly turbulent SF_6 atmosphere. The gas turbulence was induced by the fast arc motion and gas convection. In addition, arc roots on the copper-tungsten electrodes produced intense but random emission of metal vapor. In first, a bright compact and homogeneous core emitting only SII or FI lines was observed in the plasma. A theoretical fit, using radiative transfer of the 685.6 and 687 nm FI lines yielded the electron density and temperature and also the average thickness of the plasma together with the emitting area. On the contrary, photographs spectrally centered on copper lines showed extreme inhomogeneties and random behavior in peripheral regions. These regions could be roughly separated in a very dense and cold part close to the electrodes and in a second one much less dense in the electrode gap. The total amount of copper was estimated from resonance line absorption using the very bright light of a Z-pinch discharge as a reference source. This spatially extended source turned out to be very convenient to overcome the problem of strong light beam deviation due to turbulence.

LB-11 Theory of Cathode Spots in Arcs in Thermal Plasmas, M. S. BENILOV and A. MAROTTA, Universidade da Madeira, Portugal and Universidade Estadual de Campinas, Brazil - A theory of quasistationary arc spots, developed previously[1,2] for cathode spots in vacuum arcs, is extended to cathode spots in an arc in an ambient gas. Since the dependence of the heat flux density from a thermal plasma to the cathode surface on the surface temperature is non-monotonic with a narrow maximum, the asymptotic approach[2] may be used. The theory is applied to the case of a zirconium cathode in a nitrogen plasma. In the range of the spot currents 30 to 200 A, the spot temperature is found to be 4000-4100 K, the ratio between the integral heat flux per spot and the integral electric current 1-2 V. These values agree quite well with available experimental data.[3] The average current density in the spot does not depend on the spot current, which also agrees with the experiment.[3]

[1] M.S.Benilov, Phys. Rev. E **48**, 506 (1993).

[2] M.S.Benilov, IEEE Trans. Plasma Sci. **22**, 73 (1994).

[3] M.F.Zhukov, A.V.Pustogarov, G.-N.B.Dandaron, and A.N.Timoshevskij, *Thermochemical Cathodes*, Novosibirsk, 1985 (in Russian).

LC: PLASMA DISPLAYS

LC-1 Spatio-Temporal Behavior of Excited Xe Atoms in a Discharge Cell of Plasma Display Panel Measured by Laser Spectro-Microscopy, K.TACHIBANA, N.KOSUGI*, and T.SAKAI†,Kyoto Inst. Tech., *Matsushita Electronics Corp.,†NHK Sci. Tech. Lab. – Further improvements are required in the luminocity and the electric efficiency to realize a commertially available color plasma display panel (PDP), a promissing candidate as a flat panel display for high definition TV. In oder to understand the discharge phenomena in a micro-scale cell of 500 x 300 μm square with 200 μm thickness, a method has been developed to measure the densities of excited atoms by using a tunable diode-laser absorption technique combined with an optical microscope. Two-dimensional behaviors of the excited Xe atom densities in the $1s_4$ and $1s_5$ levels have been measured under a spatial resolution of 20 μm and a temporal resolution of 5 ns in a discharge cell. For example, the maximum absorption by Xe($1s_4$) atoms in one pass ammounted 6%, which gave the density of 7×10^{12} cm^{-3}. Measured characteristics are discussed in a comparison with the results of a simulation by a fluid model.

LC-2 2-D Fluid Simulations of an AC Plasma Display Panel,* R.B. CAMPBELL, SNL, R. VEERASINGAM, Penn St. U., and R.T. MCGRATH, SNL - In order to reduce the development time of new panel designs, we are studying the behavior of an AC plasma display panel computationally in two spatial dimensions. The model consists of reaction-diffusion-convection equations for ions, electrons, neutral metastables, dimers, and excited species, solved simultaneously with Poisson's equation using a fully implicit Newton-Raphson algorithm to circumvent the Courant condition. The rate coefficients for electron driven processes are evaluated with a 0-D Boltzmann solver and parametrized as a function of E/N_g. We are presently examining techniques (e.g., multigroup Pn theory) to improve upon the local field approximation inferred from this parametrization. The code treats a single fill gas species, but

mixtures are currently being added. We are in the process of benchmarking the code results with experimental data of current pulse time behavior and light emission, obtained in special panels filled with both single species and mixtures. We observe that the evolution of 2-D features in the electrostatic potential has an important effect on the behavior of all the species, both during and after the light emitting phase of the discharge.

*This work was supported by the U.S. Department of Energy under Contract DE-AC04-94AL85000.

LC-3 1-D Multispecies Fluid Modeling of a He-Xe Plasma Display Panel Cell,* R. VEERASINGAM[1], R.B. CAMPBELL and R.T. MCGRATH, Sandia National Labs - An AC color plasma display cell is a glow discharge that is initiated in a gap of 100-500 microns between two orthogonally placed electrodes contained within a dielectric substrate. We have developed a 1-D multispecies fluid model for a He-Xe discharge. The model consists of continuity equations for neutral species of xenon and helium in various levels of excitation, helium ions, xenon ions and electrons. Poisson's equation is solved for the plasma potential. A model for charge buildup on the dielectric walls of the cell is included. The electron impact rates for ionization and excitation are obtained from a 0-D Boltzmann calculation and are parametrized as E/N^2. Multipulse behavior including address, sustain and erase pulses are modeled and compared to experimental V-J characteristics. Results will include bi-stable operation margin and time-space dependent profiles for the various species.

*This work was supported by the U.S. Department of Energy under Contract DE-AC04-94AL85000.

[1]The Pennsylvania State University, University Park, PA.
[2]P. Drallos, et al., these proceedings.

LC-4 The Dynamics of a Discharge in an ac-pdp Cell Near the Breakdown Threshold,* V.P. NAGORNY, P.J. DRALLOS and W. WILLIAMSON, JR, Dept. of Phys. and Astronomy, The U. of Toledo - An analytical theory of the gas discharge between two parallel electrodes covered with an insulator under the conditions meet in the typical plasma display panel (pdp) cell[1,2] is presented. The theory is applicable when the voltage applied to the cell only slightly exceeds the breakdown voltage of the cell. For this case the analytic expressions for the electric field, electron and ion current densities, as functions of time and space are given. A discussion of the stability conditions and the role of metastables in the discharge is included.

*Work supported by the USDOE under the contract No. DE-AC04-76DP

1 O. Sahni, C. Lanza, *J. Appl. Phys.* **49**, p.2365 (1978).
2 P.S. Friedman, *Proc. of SID*, **30/3**, p. 253 (1989);
T. Ohi et al., *Proc. of Japan Display*, p.139 (1992).

LC-5 Electron Driven Rates in HeXe Mixtures for Color PDPs,* P.J.DRALLOS, V.P. NAGORNY, and W.WILLIAMSON, JR., Dept. of Physics and Astronomy, Univ. of Toledo, Toledo, OH 43606 - Theoretical investigations and simulations of AC-PDP discharges are often limited to cases in which a pure source gas is used. This is because the many of the electron transport properties corresponding to the relevant mixtures is unavailable. We have performed space-independent, kinetic calculations to obtain electron transport and rate coefficients in pure helium, pure xenon and in He/Xe mixtures, where Xe is a minor component. A reduced set of effective atomic levels for helium and xenon was used in the calculations and will be discussed. The calculations were performed for E/N ranging from 1.0 to 1000.0 Td. Electron driven rates for 14 helium transitions and for 8 xenon transitions were calculated. Comparisons between the pure gas rates and the mixture rates have been made. Differences between the xenon rates, from pure Xe and HeXe mixtures, are particularly dramatic. Furthermore, although xenon comprises only a minor portion of the gas mixtures, we show that the majority of electron energy in the HeXe mixtures goes into exciting and ionizing the xenon. Electron energy distribution functions will also be shown to illustrate the effect of mixtures on the electrons.

* This work supported by the USDOE under contract No. DE-AC04-76DP00789.

LC-6

1D Modeling of AC Plasma Displays, J. P. VERBONCOEUR, J. N. BARDSLEY, E. A. CHANDLER, Y. T. LEE, B. M. PENETRANTE AND P. A. VITELLO, V Division, LLNL, Livermore, CA 94550 - The efficiency of UV production in a plasma display panel has been characterized using fluid and kinetic simulation. The sensitivity to parameters such as gas pressure, gas mixture, gap size, voltage pulse shape and secondary emission coefficients is described for a benchmark case. The operating margin voltage for a sustained discharge is obtained. Using kinetic simulation, we study the energy and angular distribution of the damage-inducing ions incident on the electrodes.

This work was performed under the auspices of the US Department of Energy by LLNL under contract no. W-7405-Eng-48.

LD: ELECTRON COLLISIONS

LD-1 On the Electron Impact Ionization of Tetramethylsilane (TMS)

P. KURUNCZI, K. BECKER, City College of CUNY, USA,
R. FOEST, R. BASNER, M. SCHMIDT, INP Greifswald, Germany,
H. DEUTSCH, E.M.A. University Greifswald, Germany.

TMS is an important compound used in plasma assisted thin f deposition techniques and is also observed as a reaction product more complicated silicon compounds (e.g.HMDSO)[1]. Here we pres results of electron impact ionization cross section measurements v quadrupole and double focussing mass spectrometers. Besides the b peak (73) and the small mol peak (88) we observe the small intensi of the known ions with the loss of 2 to 4 methyl groups along v the protonated forms of the latter. Also H_2^+ and CH_3^+ ions observed. The total ionization cross section (70 eV $1.6 \cdot 10^{-15}$ cm^2) compared with calculations from semiempirical formulas. The population of an Ar TMS RF discharge measured with a plas monitor at the chamber wall is discussed on the basis of the ionizat cross section measurements. The relation of the intensities of $Si(CH_3)_3^+$ ion to $Si(CH_3)^+$ is similar to the cross section measureme the increase of $Si(CH_3)_2^+$ ions and CH_3^+ ions is discussed on the b of secondary reactions.

[1] R. Foest, M. Schmidt, M. Hannemann, R. Basner, Proc.VII. I Symp. Gas. Dielectrics Knoxville 1994

LD-2 Electron-Impact Ionization of the SO_2 Molecule*

V. TARNOVSKY, A. LEVIN, AND K. BECKER, City College of CUNY, USA, R. BASNER and M. SCHMIDT, INP Greifswald, Germany, and H. DEUTSCH, University of Greifswald, Germany -

We report measurements of the absolute partial cross sections for the ionization and dissociative ionization of SO_2. SO_2-containing plasmas play an important role in planetary atmospheres, in the surface treatment of medical devices, and in the remediation of flue gas. Experiments were carried out using the fast-neutral-beam technique at City College and a Nier-type ion source in conjunction with a high resolution mass spectrometer at the INP. Both experimental techniques yielded similar parent ionization cross sections of slightly less than 3×10^{-20} m^2 at 70 eV which is about 35% smaller than the previously reported cross section[1]. Dissociative ionization cross sections were found to be comparatively small. The experimentally determined total SO_2 single ionization cross section is also compared to a theoretical prediction using a recently modified additivity rule[2].

*Work supported by NSF, NASA, ACS-PRF and NATO.

1. O.J. Orient and S.K. Srivastava, J. Chem. Phys. 80, 140 (1984)
2. H. Deutsch et al., Int. J. Mass Spectrom. Ion Proc., in press

LD-3 O(^{1}S) Production Following Electron Impact Dissociation of NO_x*, L.R. LECLAIR, J.M. DERBYSHIRE, and J.W. McCONKEY, University of Windsor, Ontario, Canada--We have obtained time-of-flight (TOF) spectra of O(^{1}S) atoms following electron impact dissociation (EID) of NO and NO_2. This was done by employing a novel detector which consists of a layer of solid Xe in the field of view of a photomultiplier. O(^{1}S) atoms impinging on the layer produce fluorescence predominantly in the red within a few microseconds of impact. This method of detection has been successfully used to monitor O(^{1}S) production from other gases.[1] Its advantage is selectivity for O(^{1}S) over all other possible metastable fragments. Released kinetic energy transforms of the TOF spectra, and excitation functions for O(^{1}S) production following EID of NO_x will also be presented.

* Research supported by the Natural Sciences and Engineering Research Council of Canada and the ACS-Petroleum Research Fund.

[1] L.R. LeClair and J.W. McConkey, J. Chem. Phys. 99, 4566 (1993).

LD-4 FRAGMENTATION OF ARGON CLUSTERS INTO NEUTRAL METASTABLE FRAGMENTS BY ELECTRON IMPACT* L.A. PASTORIUS, P.J.M. van der BURGT and J.W. M^{c}CONKEY, University of Windsor, Canada N9B 3P4. The formation of neutral metastable fragments following electron impact on Argon clusters has been studied using time-of-flight techniques. The supersonic pulsed cluster beam is produced from a pulsed piezoelectric valve arrangement and is then crossed by a pulsed electron beam. Time of flight spectra of the resultant fragments show evidence for a number of dissociation or evaporation processes. Fragments are produced with kinetic energies ranging up to more than 1 eV. At least four different metastable production mechanisms are observed probably including dimer dissociation via a $^3\Pi_u$ repulsive parent state.

* Research supported by the Natural Sciences and Engineering Research Council of Canada.

LD-5 VUV SPECTRA FROM RF DISCHARGES IN SF_6 AND CF_4* JAN LI and J.W. McCONKEY, Physics Department, University of Windsor, Canada N9B 3P4--Emission spectra from RF discharges in SF_6 and CF_4 have been obtained in the wavelength range 115-315 nm using a CCD detector coupled to a 1/2 meter Seya-Namioka spectrometer. Strong atomic emissions of S, F and C dominate the spectra but some molecular features are also observed. The intensities of the features as a function of RF power and discharge pressure have been investigated.

* Research supported by the Natural Sciences and Engineering Research Council of Canada.

LD-6 Electron-Impact Excitation of the the Second Positive Band System ($C^3\Pi_u$-$B^3\Pi_g$) of the Nitrogen Molecule* JOHN T. FONS, R. SCOTT SCHAPPE, and CHUN C. LIN, U. of Wisconsin–The cross sections for electron impact excitation of the (v',v") emission bands of the Second Positive Band System ($C^3\Pi_u$-$B^3\Pi_g$) have been measured for v'=0,1,2,3,4. Comparison of the relative intensities within each of the (v',v") series of a given v' to the theoretical values shows generally good agreement. By summing the (v',v") emission cross sections over v" for each v', we obtain the apparent cross sections for excitation from the ground vibrational level of the ground electronic state, $X^1\Sigma_g^+$(v=0), into the $C^3\Pi_u$(v') level. The relative cross sections for v'=0,1,2,3,4 are quite close to the corresponding Franck-Condon factors. The cross sections for the v'=3 and v'=4 levels are much smaller than those for the cases of v'=0,1,2. This suggests that the cascade component of the apparent excitation cross sections is much smaller than the contribution from direct excitation. The relative intensities of the Second Positive bands are also measured for discharge systems, and comparison with the emission cross sections are made.

*Supported by the Air Force Office of Scientific Research.

LD-7 Measurement of Electron Excitation Cross Section of the First Positive Band System ($B^3\Pi_g$-$A^3\Sigma_u^+$) of the Nitrogen Molecule by Fourier Transform Spectroscopy. * JOHN B. BOFFARD, R. SCOTT SCHAPPE, MARK E. LAGUS, and CHUN C. LIN, U. of Wisconsin–The First Positive Band System ($B^3\Pi_g$-$A^3\Sigma_u^+$) of the N_2 extends from the visible well into the infrared region of the spectrum. The optical electron-excitation cross sections for the First Positive bands of wavelength below 1.05μm have been measured previously by photomultiplier detection. We have extended the optical emission cross section measurement further into the infrared region using Fourier Transform (FT) spectroscopy similar to the general method of DeJoseph and Clark.[1] In our experiment an electron beam excites the N_2 molecules and the intensities of the First Positive bands are measured by a FT weak emission spectrometer. The relative cross sections for the visible/infrared bands are calibrated by making absolute measurements for the bands detectable by photomultipliers. This method is applicable to infrared emission of other atomic and molecular systems.

*Supported by the Air Force Office of Scientific Research.

[1] C. A. DeJoseph Jr. and J. D. Clark, J. Phys. B 23, 1879 (1990).

LD-8 Thermal Electron Attachment to Halocarbons, J. M. VAN DOREN, A. BERNARD, J. McCLELLAN, W. FOLEY, J. COONEY, Holy Cross Coll., A. D. KOWALAK, U. Mass.-Lowell, S. T. ARNOLD, T. M. MILLER, A. A. VIGGIANO, R. A. MORRIS,

and J. F. PAULSON, USAF Phillips Laboratory, Geophysics Directorate - We will summarize our studies of thermal electron attachment to a number of perfluorocarbon molecules, fluorinated aromatics, and chloroacetonitrile. Attachment rate constants (k_a) and ion products were determined using a flowing-afterglow Langmuir-probe apparatus, over the temperature range 300-550 K. Perfluoro-pyridine, perfluorotoluene, pentafluoroacetophenone, pentafluoro-benzonitrile, and trifluoro-*m*-tolunitrile were found to undergo efficient non-dissociative electron attachment ($k_a > 10^{-7}$ cm^3/s). Thermal electron detachment was observed for the pyridine and toluene species at elevated temperatures. $ClCH_2CN$ dissociates to Cl^- + CH_2CN upon thermal electron attachment, at a rate that is about 1/10th collisional. By contrast, many of the smaller PFCs do not attach electrons, or very slowly.

LD-9 Observation of Autoionization in O_2 by an Electron-Electron Coincidence Technique,* J. P. DOERING and J. YANG, Johns Hopkins U. -- A strong transition to an autoionizing state has been observed in O_2 at 16.83 ± 0.11 eV by means of a new electron-electron coincidence method. The method uses the fact that electrons arising from autoionizing states appear at a constant energy loss corresponding to the excitation energy of the autoionizing state rather than at a constant ionization potential as do electrons produced by direct ionization. As a consequence, the autoionization peak appears to move in the spectrum as a function of secondary electron energy when the data are displayed as intensity vs. ionization potential. Comparison of the present data with previous photoionization studies suggests that the autoionizing O_2 state is the same state deduced to be responsible for abnormal vibrational intensities in the O_2^+ $X^2\Pi_g$ ground state when 16.85 eV Ne(I) photons are used. These electron-electron coincidence experiments provide a direct new method for the study of autoionization produced by electron impact.

*Work supported by NSF Grant ATM-9222344.

LD-10 The Covariance Mass Spectrum of Hexamethyldisiloxar (HMDSO) at an Electron Impact Energy of 40 eV. M. R. Bruce and R. Bonham, Department of Chemistry, Indiana University, Bloomington, IN 4740 The time of flight spectra of both ions formed in the break up of doubly charg molecules of HMDSO formed by electron impact using 40 nanosecond pulses 40 eV electrons have been recorded. Ten correlation features were observed. Tl parent ion peak is suppressed having only $\frac{1}{100}$ the area of the most intense featur $(CH_3)_3$ Si *O* $Si(CH_3)_2^+$. This observation, coupled with the observation by Beck [1] that little or no fluorescence is observed from the parent molecule under ele tron bombardment suggests that this molecule, like CF_4, dissociates on bei excited. An ion of mass 28 (Si^+, CO^+, or $C_2H_4^+$) is correlated with ions of ma 45 (CH_3CHOH^+, $CH_3SiH_2^+$, or $SiOH^+$), 59 ($(CH_3)_2SiH^+$, CH_3SiO^+, or SiH_3^+), ($(CH_3)_3Si^+$), 86 (CH_3SiOSi^+), 103 ($(CH_3)_3SiOCH_2^+$ or $(CH_3)_3SiOCH_3^+$), and 1 ($(CH_3)_3$ Si *O* $SiCH_2^+$ and/or $(CH_3)_3$ Si *O* $SiCH_3^+$). The peak at mass 103 sho a strong diagonal correlation band stretching to or near mass 45 which sugge that the heavier of the two ions is breaking up with a lifetime in the micro seco time range and ending up with the charged portion having a mass of 45. Eviden is also present for correlations between mass 45 and masses 59 and 73 as well mass 59 with mass 73. It should be noted that von Seefelt et al. [2] have assign mass 45 as $CH_3SiH_2^+$, mass 58.5 as $(CH_3)_2SiH^+$, mass 73 as $(CH_3)_3Si^+$, and ma 130.3 as $(CH_3)_3$ Si *O* $SiCH_2^+$ in addition to other assignments.

[1] K. Becker, Private communication.
[2] R. von Seefelt, W. Möller, and M. Schmidt, Z. Phys. Chemie Leipzig 26 797 (1985).

LD-11 **Simple, Effective Model for Electron-Impact Ionization of Atoms and Molecules**, Y.-K. KIM, NIST and M.E. RUDD, U. of Nebraska-Lincoln--Binary-encounter theory and the Bethe theory have been combined to provide a simple yet effective model to calculate electron-impact ionization cross sections for atoms and molecules. The model, referred to as the Binary-Encounter-Dipole (BED) model,[1] offers formulas to calculate the singly differential ($d\sigma/dW$, W=ejected electron energy) and total (σ_i) ionization cross sections for a subshell (or a molecular orbital) using its occupation number, binding energy, average kinetic energy ($U=\langle p^2/2m \rangle$), and differential dipole oscillator strength (df/dW). The BED model reproduces known σ_i for H, He, He^+, Li^{++}, Ne, and H_2 to within 10% from threshold to a few keV in incident energy (T). When df/dW is not readily available, we have a simpler version of the model that still leads to reasonable estimates of σ_i, though not necessarily the details of $d\sigma/dW$. This simplified version leads to σ_i of H_2O within 15% for $T \leq 10$ keV. We found that the angular distribution of ejected electrons ($d^2\sigma/dWd\Omega$) can be expressed by a Lorentzian shape with a correction in the backward angles.

[1] Y.-K. Kim and M.E. Rudd, submitted to the Phys. Rev. A.

SESSION MA: DIAMOND FILMS
Thursday afternoon, 20 October 1994
NIST Building 101
Red Auditorium, 13:30–15:30
B. Lane, presiding

Invited Papers

MA-1 Gas-phase Reaction Kinetics in the Chemical Vapor Deposition of Diamond, Wen L. Hsu and Ciaran Fox, Sandia National Laboratories, Livermore, CA 94551 — Molecular beam mass spectrometry is used to measure the gas composition near the growing diamond surface under a variety of chemical vapor deposition environments. This technique detects radical and stable species with sensitivities better than 10 ppm. In conjuction with these experimental studies, we model the process using a numerical code that includes mass and heat transport effects in addition to homogeneous and heterogeneous reaction kinetics. These tools allow us to arrive at an in-depth understanding of the complicated chemically reacting environment. In this paper we show that the gas-phase chemistry is driven by the concentration of H atoms. In turn, the H-atom concentration is strongly affected by surface catalysis, wall recombination, mass transport, and geometric effects. Using the hot-filament method for diamond growth, it was found that an inlet mixture of acetylene and hydrogen produces methane and methyl in the vapor with much higher concentrations than expected. This is consistent with the nearly identical growth rates that can be achieved with either methane or acetylene in the inlet gas. Using the microwave plasma method, the hydrogen concentration was found not to decay as a function of hydrocarbon feed, thus leading to a very different vapor phase composition as compared to the hot-filament method. Finally, we also investigate the use of fluorocarbons and discuss how it affects growth and the gas-phase chemistry.

MA-2 Total Cross Sections for Electrons Scattered from Atomic and Molecular Hydrogen* D.H. Madison and V.E. Bubelev, U. of Missouri-Rolla,--- Hydrogen plays a crucial role in diamond growth on surfaces. During the deposition phase, the concentration of hydrogen in the plasma determines the ratio of graphite to diamond deposited on the surface. After deposition, the amount of hydrogen trapped in the surface causes a reduction of diamond film quality.

Electron impact spectroscopy can be used to determine the hydrogen concentration in both cases. Consequently, it is important to know cross sections for electron scattering from both atomic and molecular hydrogen. In this paper, we will present a comparison of the latest theoretical and experimental results for this scattering process.

*Work supported by the NSF.

Contributed Papers

MA-3 **A helicon wave plasma source for the deposition of diamond-structure materials,** I.S. FALCONER, B.W. JAMES, J. KHACHAN, H-J. KIM, W.D. MCFALL, D.R. MCKENZIE, J.R. PIGOTT and H.B. SMITH, School of Physics, U. of Sydney, Australia R.W BOSWELL, A. DURANDET, A.J. PERRY and H.PERSING, RSPhysSE, ANU, Australia - A helicon wave plasma source has been modified by the incorporation of an electron beam evaporator to make an ion plating system for the deposition of thin films of diamond structure materials. A radiofrequency biased, heated substrate holder enables the energy of the ions incident on the growing film, which is critical to the formation of diamond-structure materials, to be controlled. Films of cubic boron nitride have been successfully deposited by evaporating boron into an Ar/N_2 plasma in this device. Transport studies of the flux of B atoms from the evaporator using both measurements of the deposition rate of B on glass slides and atomic absorption measurements demonstrate that an acceptable flux of evaporated atoms reaches the substrate, and that a substantial fraction of the B appears to be ionized in the plasma. Preliminary results from Langmuir probe measurements of plasma parameters will also be reported.

MA-4 **Intracavity Laser Spectroscopy of RF Plasmas of Methane and Benzene Used in Depositing Diamondlike Carbon Films,** J.J O'BRIEN and M.J. LIPP, U. of Missouri-St.Louis - Spatially resolved concentrations of excited atomic hydrogen (n=2) (H^*), generated from 13.56 MHz RF hydrocarbon discharges, are determined during film formation using intracavity laser spectroscopy. Intracavity laser spectroscopy enables number densities to be determined *in situ* and in real time in the RF discharge. Self-bias voltages and pressures of methane (25 and 100 mTorr) and benzene (25 mTorr) are selected so that diamondlike carbon films are deposited in the capacitively coupled symmetric discharges. The density of H^* varies substantially across the discharge region with values between $< 10^8$ cm^{-3} and $2x10^9$ cm^{-3}. In all cases, the minimum concentration occurs at the power electrode. Benzene produces the least amount of excited atomic hydrogen overall. Also observed are very different behaviors of the total pressure in sealed-off discharges for the different gases: the total pressure rises in a discharge of initially pure methane and decreases in a discharge of initially pure benzene. The results may have implications concerning the proposed impact induced fragmentation of hydrocarbon molecules during film growth using RF plasma discharges.

MA-5 Discharge Parameter Dependence of Growth Precursors in Thermal Plasma Assisted Diamond Film Deposition, H.J. YOON, P.G. GREUEL, D.W. ERNIE, and J.T. ROBERTS, U. of Minnesota - A system for mass spectrometric analysis of the growth precursor species impinging on growing films in high-pressure, high-power thermal plasma CVD[1] has been applied to the study of diamond film deposition onto molybdenum substrates from a 3.3 MHz inductively coupled torch operating between 50 to 400 Torr in $CH_4/H_2/Ar$ mixtures. Deposition of diamond films into the sampling orifice has verified the chemical integrity of the sampling technique. Measurements of the CH_4 and C_2H_x stable species, the CH_x unstable radical species, and the C_2/C_1 species ratio as a function of discharge parameters and film quality will be presented. It has been found that the boundary layer thickness has a significant effect on the C_2/C_1 species ratio. Experimental measurements will be compared with computer simulations of the chemical composition of the boundary layer. Implications of the results for diamond growth mechanisms will be discussed.

*Work supported by NSF Grant No. ECD-8721545, Engineering Research Center for Plasma-Aided Manufacturing.

[1] H.Y. Yoon *et. al.*, 46th GEC, Montreal, Paper DA-15 (1993).

MA-6 Relationship between atomic hydrogen concentration and the quality of diamond like carbon (DLC) thin films, R.C. CHESHIRE[1], V.KORNAS[2], H.F.DöBELE[2], K. DONNELLY[3], D. DOWLING[3], W.G. GRAHAM[1], T. MORROW[1], T. O'BRIEN[3]. 1. The Queen's University of Belfast, N. Ireland, 2. Universität GH Essen, Germany, 3. Forbairt, Dublin, Rep. Ireland. The presence of atomic hydrogen is of special importance in the production of diamond and diamond like (DLC) coatings using plasma assisted deposition techniques. It has been suggested there should be a correlation between the quality of the coatings produced and the concentration of atomic hydrogen present in the plasma during deposition. Here a two photon (205.1 nm) laser-induced fluorescence (LIF) technique is used to detect ground state atomic hydrogen in a 13.56 MHz rf plasma enhanced chemical vapour deposition (PECVD) system containing acetylene diluted in hydrogen. The LIF signal at 656.3 nm at constant laser energy is directly proportional to the H-atom concentration. In situ ellipsometry is used to measure the refractive index of the growing film which is a direct measure of the quality and hardness of the DLC film. Results show that the refractive index increases with increasing percentage dissociation of hydrogen. This work is supported by the EC BRITE EURAM program.

MA-7 **Quantitative Measurement of CH_3 Radicals in a Hot-Filament Reactor for CVD of Diamond Films by Cavity Ring-Down Spectroscopy (CRDS),*** P. ZALICKI, Y. MA, R.N. ZARE, *Chem. Dept.*, J.R. DADAMIO, E.H. WAHL, T.G. OWANO, C.H. KRUGER, *Mech. Eng. Dept., Stanford Univ.* — Methyl radicals in a hot-filament reactor for CVD of diamond films have been measured using the new optical diagnostics: cavity ring-down spectroscopy.[1] A reactor was filled with 20 Torr of hydrogen mixed with 5% of methane and operated with a tungsten filament at 2300 K. Diamond films were deposited on a molybdenum substrate 8 mm from the filament. The 216.4-nm absorption of CH_3 along a path parallel to the substrate was measured as a function of the distance from the substrate in a range of substrate temperatures from 650 K to 1600 K. We find that the CH_3 concentration in the space between the filament and the substrate is controlled by the substrate temperature. The CH_3 concentration peaks at substrate temperatures around 1200–1400 K. This behavior resembles the variation of the diamond growth rate with the substrate temperature reported by Kondoh et al.[2]

* work supported by DOE, grants DE-FG03-92ER14304 and DE-FG03-88ER13957, under the supervision of Dr. Oscar Manley.

[1] A. O'Keefe and D.A.G. Deacon, Rev. Sci. Instrum. **59**, 2544 (1988).
[2] E. Kondoh, T. Ohta, T. Mitomo, and K. Ohtsuka, J. Appl. Phys. **72**, 705 (1992).

SESSION MB: GLOWS
Thursday afternoon, 20 October 1994
NIST Building 101
Green Auditorium, 13:30–15:30
D. A. Doughty, presiding

Contributed Papers

MB-1 **Hydrogen Atom Density Measurement in H_2/N_2 Gas Mixtures in a GEC Reference Cell** B.N.GANGULY and P.BLETZINGER , Aero Propulsion and Power Directorate, WPAFB, Ohio-- The effects of direct electron impact and heavy particle internal energy transfer (not kinetic) induced dissociation[1] of H_2 have been measured in a GEC reference cell. The rf discharge was operated over 0.5 to 5 Torr pressure with H_2/N_2 gas mixtures and at 100 W nominal power (30 W into the plasma). A two-photon allowed LIF technique was used to measure collisional quenching corrected atomic hydrogen density for 100% to 10% H_2 in H_2/N_2. At 5 Torr, atomic hydrogen density is found to increase with a decrease in H_2 partial concentration to 60%; the plasma induced H_α emission intensity decreased monotonically with the decrease in H_2 partial pressure. This indicates that electron impact dissociation may not be the only process for the measured H_2 dissociation. At lower pressures, H atom density does not decrease significantly when H_2 partial pressure is varied from 100% to 10%. At pressures of 5 Torr and above, the discharge becomes unstable for H_2 partial pressures of less than 60%.

1. R. Nagpal and A. Garscadden, this conference.

MB-2 Two Dimensional Electromagnetic and Kinetic Analysis and Comparison with Experiments for Inductively Coupled *RF* Discharge. *** Chwan-Hwa "John" Wu and Fa "Foster" Dai, Department of Electrical Engineering, Auburn University, Auburn, AL 36849-5201.** For the planar inductively coupled plasma source, a 2-D electromagnetic model with closed-form solutions is developed. The calculated azimuthal E-field agrees with the self-consistent simulation results obtained by [1]. Based on the electromagnetic solutions, we further investigated the kinetic behavior of the wave-plasma interactions by solving the 2-D Boltzmann-Vlasov equation. It has been found that the induced E-field in the studied structure is dampened dominantly by a collisionless dissipation mechanism. On the basis of a closed-form solution, a novel 2-D coupled Landau damping mechanism is found in the inductively coupled plasma source. The instability of electron energy distribution function observed experimentally by [2] can thus be analytically explained by the presented model. Since the 2-D damping effect occurs when the electron thermovelocity is close to the *RF* wave phase velocity, appropriately adjusting the background pressure, *RF* frequency and power level, and the reactor geometry could result in efficient energy transfer to electrons for inelastic and ionization collisions with the background gas.

* This work is supported by NSF under ECS-9009395.

[1] P. L. G. Ventzek et al, *Appl. Phys. Lett.*, 63, 605, 1993.
[2] M. S. Barnes et al, *Appl. Phys. Lett.*, 62, 2622, 1993.

MB-3 **The Effect of Coil Configuration on Confinement of Plasmas in Remote Plasma Enhanced CVD Reactors,*** Irène PERES and Mark J. KUSHNER, University of Illinois, Dept. of Elect. and Comp. Engr., Urbana, IL 61801 USA - In Remote Plasma Enhanced CVD reactors the injected deposition gases are isolated from the plasma by confining the plasma in a narrow tube upstream of the deposition chamber. The plasma is sustained by an rf coil wrapped around the tube producing an inductively coupled discharge. Placement of the coils is important to confining the plasma due to the distribution of the inductive electric field and stray capacitive coupling. We have developed a 2-d hybrid computer model to investigate reactors which produce confined plasmas. The model has electromagnetic, Monte Carlo simulation (MCS) and fluid modules which are iterated until plasma properties converge. We found that for a given ratio of coil to plasma tube diameters there is a critical axial placement of the coils which ensures isolation of the plasma. The capacitive contribution to the plasma source also depends on which side of the coil is powered. We will also compare plasma properties obtained with the MCS and a modified local field model.

* Work supported by SRC, NSF, and the University of Wisconsin ERC for Plasma Aided Manufacturing.

MB-4 Modeling of a self-sustained discharge-excited ArF excimer laser -Effect of laser light on the discharge development-. H. Akashi, Y. Sakai and H. Tagashira Hokkaido Univ., Dep. of Elect. Eng., Sapporo Japan- The effect of laser light on the discharge development characteristics in the active medium of an ArF excimer laser is investigated using a one-dimensional fluid model including laser light induced photoionization and photodetachment processes. These processes are found to have a significant effect at times after the maximum in the laser output signal. For example, the laser light driven interactions increase the bulk electron number density by a factor of 2 and the electric field adjacent to the cathode by a factor of 1.5. Near the anode the field changes from slightly negative at early times to extremely positive near the end of the laser pulse resulting in an electron drift in the direction of the bulk plasma. The tendency of the field to change sign at the anode is not observed when photon processes are neglected. This strong field enhancement suggests the generation of a filamental instability at the electrodes as indicated by the experiments of Taylor [1].

1. R. S. Taylor Appl. Phys. B41, 1-24 1986

MB-5 **Dominant Dissociation and Ionization Channels in Nitrogen-Hydrogen Discharges,*** R. NAGPAL and A. GARSCADDEN, Plasma Research Group, WPAFB- Results from a systematic theoretical study of the electronic and heavy particle kinetics in glow discharges through $\%N_2 - \%H_2$ mixtures are presented. The calculations employ the solution of vibrational master equations of H_2 and N_2, self-consistent with respect to the electron energy distribution, current density and pressure. The results show that the collisional interactions between the excited electronic states and the vibrational manifolds of N_2, H_2 are highly non-linear and they strongly affect the dissociation, ionization, gas heating, discharge impedance and power loading. It is shown that the quenching of $N_2(A^3\Sigma_u^+)$, and of $N_2(a'^1\Sigma_u^-)$ by H_2, leading to the dissociation of hydrogen play critical roles in determining the strongly coupled dissociation and ionization balance in $\%N_2 - \%H_2$ discharges. The results demonstrate that the macroscopic information (in predicting the discharge characteristics) and the microscopic information (heterogenous collisional interactions) can be effectively used to orchestrate the plasma chemistry in molecular gas mixtures. The exper-

imental observations on rf excited $\%N_2 - \%H_2$ discharges are presented in a companion paper.

*Work Supported by the Wright Laboratory.

MB-6 **A model of the low current argon-xenon positive column*** TIMOTHY J. SOMMERER *Corporate Research and Development, General Electric Company, P. O. Box 8, Schenectady, New York 12301*—A model of the argon-xenon positive column has been constructed. The model assumes a functional form for the radial variation of the various ground state, excited, and charged species, and integrates the average densities forward in time to a steady state dc solution. The electrons are considered via a zero-dimensional Boltzmann model. The voltage-current characteristic predicted by the model is in good agreement with measurements when the current density is sufficiently high (say, >0.15 A in a 0.3 cm-radius tube), even when the pressure-radius product is low (0.03 Torr cm); however, the model overpredicts the electric field at low current densities irrespective of the neutral pressure. The discrepancy has been qualitatively attributed to the nonnegligible size of the sheaths in the radial direction at low current density. Methods will be described to account for this effect.

*Work partially supported under the NIST Advanced Technology Program, Cooperative Agreement 70NANB3H1372.

MB-7 Investigations of Single Filament Properties of Excimer Barrier Discharges in Krypton and Xenon*, R. KLING, M. NEIGER and R. SCHRUFT, LTI University of Karlsruhe, FRG - Dielectric barrier discharges are large area glow discharges at pressures near atmospheric. They consist of a large number of individual discharge filaments, although homogeneous forms have also been shown to exist at atmospheric pressure.[1] For both a good understanding of the filamentary microdischarges and their applications (ozone generation, UV- and VUV excimer lamps, plasma - chemical reactors), plasma properties and the scaling behaviour of individual microdischarges are necessary. We report on experimental and computer simulation results of single filament properties in Krypton, Xenon and Kr/Cl_2 barrier discharges as a function of pressure, gap spacing, operating frequency (sinusoidal) and electrical energy density.

*Part of this work was supported by the German Ministry of Research and Technology (BMFT)

[1]M. Neiger et al., BMFT final report 13 N 5695 (1991)

Invited Paper

MB-8 **Nature of the Normal Current Density Effect in DC and RF Glow Discharges**, YU. P. RAIZER, *The Institute for Problems in Mechanics, Russian Academy of Science* — In the normal dc glow discharge the current density value at the cathode is quite definite. This fact is known for almost a century. Half a century ago Von Engel and Steenbeck postulated that the state occurred which corresponded to the cathode fall minimum but the mechanism of this was given only recently. The paper presented explains this effect. Similar effect in rf discharge is also considered. It explains why the normal rf current density exists only at moderate pressures but never at low pressures.

SESSION N: POSTER SESSION
Thursday afternoon, 20 October 1994
NIST Building 101
Lecture Rooms A and B, 15:45–17:30
M. A. Sobolewski, presiding

NA: CAPACITIVELY COUPLED GLOWS

NA-1 A Two-dimensional Self-consistent Electron Monte Carlo, Ion Fluid (SEMCIF) Simulation of the Radio Frequency Discharge Benchmark Model, JYUN-HWEI TSAI, National Center for High-performance Computing (NCHC), Hsinchu, Taiwan 30077, ROC, and CHWAN-HWA "JOHN" WU, Electrical Engineering, Auburn University, Auburn, AL 36849 — A two-dimensional (2D) SEMCIF code was developed to simulate the radio frequency (rf) glow discharge benchmark model of the GEC Reference Cell. The SEMCIF model is based on the Monte Carlo simulation for electrons and the nonequilibrium fluid model for ions, and coupled with 2D Poisson's equation. The spatio-temporal result of the radial field near the radial wall reveal an influential radial sheath (the intensity is increased with the background pressure) that oscillates with respect to the rf driven voltage. The nonequilibrium radial transport due to the radial sheath significantly affects the ionization mechanism of the glow discharge, and consequently, causes nonuniform distributions of the plasma densities and higher electron mean energy and ionization rate in the sheath region near the radial wall. In this study, the time-averaged 2D (in *(r,z)* space) transport results, such as the plasma densities, electron mean energy, ionization rate, and the electric fields, in various background pressures will be shown and illustrated.

NA-2 **Modeling of ion flux uniformity in radio frequency discharges: effect of electrode topography**, M. Dalvie, M. Surendra, G. S. Selwyn, C. R. Guarnieri, IBM T.J.Watson Research Center, POB 218, Yorktown Heights, NY 10598.
Ion flux contribution to plasma process non-uniformity (particularly wafer edge exclusion) is studied here by means of a 2-d self-consistent fluid model of a radio frequency discharge. Time-dependent electron and ion mass, ion momentum, and electron energy balance equations are solved along with Poisson's equation. Simulation domain includes electrode topography that simulates clamprings and wafer edges. Results indicate that electrical property variation (e.g., conducting wafer to non-conducting clampring) causes the ion flux to fall off near the wafer edge. Effect of the topography is related to plasma parameters, e.g., pressure, through the sheath thickness. At high pressure (low sheath thickness), the ion flux is more sensitive to the topographical perturbation due to ionization rate enhancement in the corner. At low pressure, electrical property variation is more important. We compare results from the complete ion momentum balance to those from the drift-diffusion approximation.

NA-3 Measurements of the Electric Field in the Sheath Region of a Helium RF Discharge, M.D. BOWDEN, Y.W. CHOI, T. YAMASHITA, K. MURAOKA and M. MAEDA, Kyushu U.- The

electric field in the sheath region of a helium RF discharge was measured using a laser induced fluorescence technique[1]. This method was used to measure the electric field distribution in the plasma for a range of gas pressures and input powers. The time-dependence of the sheath electric field had to be considered in the interpretation of the measured fluoresence spectra[2]. The position where the electric field became zero was used to determine the width of the electric field sheath near the powered electrode. As expected, the width of the sheath near the electrode depends strongly on gas pressure. The measured sheath widths were compared with the widths predicted by published models of RF discharges.

1. K.E. Greenberg and G.A. Hebner, *Appl. Phys. Lett.* 73, p3282 (1993).
2. M.D. Bowden, Y. W. Choi, K. Muraoka and M. Maeda, *J. Appl. Phys.* (submitted) (1994).

NA-4 Non-Collisional Sheath Heating* M.E. RILEY, Sandia National Labs. Non-collisional or Fermi heating of electrons in a rf-driven plasma sheath has been studied by several investigators.[1] It appears that the estimates of the power transfer to the electrons is adequately described by the analytic formulae that result from the simpler models. The complication is that the most frequent circumstance in plasma processing is that of zero mean current due to a capacitively coupled surface in contact with the plasma. Thus an applied rf drive increases the electron power loss to the surface due to induced sheath motion. The net result is that rf drive almost always increases the electron power loss rather than heating the plasma for nominal voltages. Results of kinetic Boltzmann simulations will be presented.

*Work performed at Sandia National Labs and supported by US DoE under contract DE-AC04-94AL85000
[1]M.A. Lieberman, IEEE Trans. Plasma Sci. **16**, 638 (1988), V.A. Godyak and N. Sternberg, Phys. Rev. A, **42**, 2299 (1990), A.E. Wendt and W.N.G. Hitchon, J. Appl. Phys., **71**, 4718 (1992), M. Surendra and D. Vender, Appl. Phys. Letts. **65**, July 1994.

NA-5 Kinetic Energy Distributions of Ions Sampled from RF Glow Discharges in Helium, Nitrogen, and Oxygen, J. K. OLTHOFF, S. B. RADOVANOV, R. J. VAN BRUNT, and K. DZIERZEGA, *NIST* — Mass-analyzed kinetic-energy distributions of positive ions sampled through an aperture in the grounded electode of a GEC rf Reference Cell have been measured for radio-frequency discharges generated in helium, nitrogen, and oxygen. Distributions were measured for plasmas with an applied rf voltage of 200 V, and pressures ranging from 1.3 to 66.7 Pa. The "parent" ion (He^+, N_2^+, and O_2^+) of the carrier gas was observed to be the dominate ion for all conditions investigated here. Less abundant ions were also observed for each gas, such as He_2^+ and He_4^+ in helium, N^+, N_3^+, N_4^+, and N_2H^+ in nitrogen, and O^+ and O_3^+ in oxygen. Voltage and current waveforms, and vertical profiles of the optical emission were also measured for each plasma condition. Correlations of these data with the ion energy distributions and with known collisional cross sections provide insight into the ion-molecule reactions that influence the ion flux striking surfaces exposed to the discharge. The effects of electrode materials and conditions upon the ion energy distributions are also discussed.

NA-6 Kinetics of Formation and Loss of S_2 in a Pure SF_6 RF Discharge, L. ST-ONGE*, N. SADEGHI, J.P. BOOTH and J. MARGOT*, L.S.P., U. Joseph-Fourier, Grenoble – Using laser-induced-fluorescence (LIF) spectroscopy, we have investigated the kinetics of formation and loss of S_2 in a capacitively-coupled RF reactor operating with SF_6 at pressures ranging from 5 to 35 mtorr. The relative concentration of S_2, deduced from the LIF signal, is measured as a function of distance from either a plain or silicon-covered aluminium electrode. In this way, for each set of discharge conditions, we can determine which of surface or volume formation mechanisms are dominant. Formation of S_2 in the volume is observed to be dominant for high enough gas pressures (typically, above 20 mtorr) and when silicon is present in the reactor. Loss kinetics of S_2 at the reactor walls are investigated from its density decay in the post-discharge of a pulsed plasma. The characteristic decay time of S_2 varies linearly from 4.4 ms at 8 mtorr to 5.6 ms at 34 mtorr, independently of electrode material.

* U. de Montréal, Montréal (Québec)

NA-7 The Effects of a Small Transverse Magnetic Field Upon a Capacitively Coupled rf Discharge, D.A.W.HUTCHINSON, M.M.TURNER, R.A.DOYLE, and M.B.HOPKINS, School of Physical Sciences, Dublin City University, Dublin 9, Ireland. - A 7.5cm capacitively-coupled rf argon discharge at a pressure of 10mTorr has been studied both experimentally and using a one-dimensional particle in cell simulation with Monte Carlo collisions. A magnetic field is applied in the direction parallel to the capacitor plates. It was found that in the simulation as the magnetic field was increased such that the electron cyclotron orbit radius of the hot electrons became smaller than of the order of the discharge length, the electron heating in the bulk of the discharge increased. This was accompanied by a drop in the plasma density at small magnetic fields, which was also observed experimentally. A detailed discussion of the simulation results is presented drawing comparisons with the experimental results, with which there is good agreement, and a simple magnetohydrodynamic model for the bulk heating.

NA-8 Rf Discharge Simulations: GEC Reference Cell*, T.R. GOVINDAN and M. MEYYAPPAN, Scientific Research Associates - GEC reference reactor has been used in many laboratories as the benchmark experimental platform to gain insight into rf discharge characteristics and provide data for model validation. We have undertaken a detailed modeling study of the reference cell. We use a continuum model based on the three moments of the Boltzmann equation. The momentum equation is solved without making drift-diffusion approximations. The rate constants for inelastic processes are from a zero-dimensional Boltzmann solver which computes the EEDF for a given E/N. The one-dimensional code also accounts for the plasma asymmetry. Metastable transport is included self-consistently. A detailed parametric study varying operating parameters has been undertaken for an argon discharge and the results on current-voltage characteristics, density profiles and ion energy are compared against available experimental measurements for the reference cell.

* Research Supported by the Dept. of Commerce

NA-9 The observation of a double layer in a rf generated hydrogen plasma, K.F. AL-ASSADI and W.G. GRAHAM, The Queen's University of Belfast, N. Ireland. Langmuir probe measurements of plasma parameters, such as electron density and temperature and plasma potential as well as the electron energy distribution function have confirmed the visual observation of a double layer in a rf generated hydrogen plasma. The plasma system is a capacitively coupled 13.56 MHz single driven electrode system. The ground electrode is the chamber wall on average 100 mm from the driven electrode. The position and characteristics of the double layer are dependent on the particular operating conditions i.e. rf power and gas pressure. Plasma potential differences of typically 10 V between the bulk plasma and the middle of the double layer have been measured. Additional features in the eedf consistent with electron acceleration by such potential differences have been observed. This work is supported by the EC BRITE EURAM program.

SESSION NB: INDUCTIVELY COUPLED PLASMAS II

NB-1 Ion Energy Measurements in an Inductive, rf Plasma, with rf Bias JOHN TROW, Applied Materials - Ion energy spectra at the wafer surface in an inductive, rf plasma, with capacitive rf bias, have been measured with a small electrostatic energy analyser. The battery powered analyser is built into the wafer pedestal and is coupled to the outside via a fiber optic link.[1] The pedestal is covered by a blank silicon wafer. A hole through the wafer allows access to the analyser. This arrangement allows measurements to be made in near process conditions. The data, which show peak ion energies corresponding to the maximum negative voltage of the rf waveform, indicate that the ion motion across the sheath is in response to the instantaneous rf field and not to the dc potential established on the wafer. This is due to the lower bias frequency (1.8 Mhz) and higher plasma densities, hence thinner sheaths, than those obtained in previous plasma reactors.

1. A.D. Kuypers and H.J. Hopman, J. Appl. Phys. 63 (6), 1894 (1988)

NB-2 Wide Area (16") Radio-Frequency Induction Coupled Plasma Generation and its Applications,* Z. YU, D. M. SHAW and G. J. COLLINS, Colorado State University -- Radio-frequency induction coupled plasma (ICP) provides spatially confined high density plasmas. Most popular ICP processing systems have problems with coupler window erosion and plasma non-uniformity across its diameter. These problems becomes even greater when the device dimensions are scaled up. We have developed a large area ICP coupler with a uniform plasma over its entire 16 inch diameter coil. The thick dielectric coupling window has been removed in this new circuitry design. The deviation of photoresist ashing rate is 5% over the area of 16 inch diameter. The characteristics of the ICP will be presented, as well as its performance in thin film processing and large area electrodeless fluorescent lighting.

*Work supported in part by NSF Grant DDM - 9108531 and DDM - 9311697

NB-3 Stability of the Inductively Coupled Discharge System, M.SHINOMIYA, Matsushita Electric Works,Ltd. - A few years ago we reported[1] an inductively coupled mercury-rare gas discharge (H-discharge) operating at 13.56MHz. The plasma resistance of such a discharge has a negative V-I characteristic. Discussion of the stability of the H-discharge is still persisting. Eckert remarked the positive characteristic of the plasma due to the skin effect which occurs under high power conditions[2]. I showed H-discharge current is limited within the predetermined value when an impedance-inverter circuit is used[3]. I applied F-matrix analysis to the drive circuit under three assumptions: (1)The impedance loaded to the RF power source is the designed value under the nominal operation; (2)The circuit provides sufficient open voltage to start discharge; (3)When the plasma resistance decays by any reason, supplied power to the plasma do not exceed the power required to maintain the discharge. And I figured out the circuit conditions which gives stability of the inductively coupled discharge system whenever the plasma has a negative V-I characteristic.

1 Shinomiya,M. et al.: J. of the IES, 20-1, pp.44-49 (1991)
2 Eckert,H.U.: High Temperture Science, 6, pp.99-134 (1974)
3 Shinomiya,M. : J.Illum.Engn.Inst.Jpn. 78-2, pp.59-64 (1994)

NB-4 Measurement of Ar Metastable Concentration in a Planar RF Inductive Argon Discharge,* **A. A. PIERRE and A. E. WENDT,** Engineering Research Center for Plasma-Aided Manufacturing, U. of Wisconsin-Madison — **Although the plasma chemistry of argon is relatively simple compared to that of most gases used in plasma processing, there is still uncertainty about the role neutral metastable atoms play in argon discharge dynamics. Plasma uniformity as well as peak plasma density depends on whether plasma production is dominated by single step ionization from the ground state or by a two-step process involving metastables. We examine this issue through measurements of the absolute concentration of Ar metastables in a low pressure inductive discharge with a planar spiral antenna driven at 13.56 MHz, similar to systems used for semiconductor processing. Measurements are made by absorption spectroscopy using a xenon arc lamp as a broadband light source in a technique developed by Lawler *et al.*[1] The discharge is confined to a 20 cm diameter by 14 cm long cylinder for comparison of results to previous studies of electron energy distributions and optical emission on the same system.**

*Work supported in part by NSF Grant #ECD-8721545

[1]R. C. Wamsley, J. E. Lawler, J. H. Ingold, L. Bigio and V. D. Roberts, Appl. Phys. Lett. **57**, p. 2416 (1990).

NB-5 Discharge Physics Study of an ICP Source, M. MEYYAPPAN, T.R. GOVINDAN and J.P. KRESKOVSKY Scientific Research Associates - ICP sources have been receiving significant attention recently as a relatively simple means to generate high density plasmas with significant radial uniformity. Hence, they have promise for deposition and etching applications in integrated circuit manufacturing. We have undertaken a modeling study to investigate the discharge characteristics of an ICP source. The transport model consists of the three moments of the Boltzmann equation for both electrons and ions in (r,z) direction. An electromagnetic module is not included in this study; instead, known power profiles have been assumed as in Ref. 1. An argon discharge is investigated and results are presented in terms of two-dimensional profiles of electron and ion characteristics for various input power levels and operating pressures.

[1] R.A. Stewart, P. Vitello and D.B. Graves, J. Vac. Sci. Tech., B12, p. 478 (1994).

NB-6 **Modeling Inductively Coupled Electronegative Plasmas**, P. A. VITELLO, G. PARKER, J. D. BUKOWSKI*, M. D. KILGORE*, R. A. STEWART*, AND D. B. GRAVES*, LLNL and * U.C.Berkeley – Inductively coupled plasma (ICP) sources are regarded as one of the most promising technologies developed in recent years for use in sub-micron device manufacturing. ICP sources achieve large plasma densities with a high degree of anisotropy in the escaping ion flux. Electronegative discharges in high density, low pressure systems such as the ICP present a variety of issues concerning the effects of negative ions and molecular dissociation on the behavior of the plasma. We present results from a two-dimensional fluid model [1] of a Cl_2/poly-Si etching system. To simulate more electronegative gas mixtures, we allow the chlorine attachment rate to be enhanced by up to a factor of ten. Results are presented showing the variation in uniformity of the ion flux at the wafer substrate with the electronegativity of the plasma. We discuss also how strong attachment may lead to unstable discharge conditions.

*This work was performed at LLNL under the auspices of the U.S. DOE under Contract Number W-7405- ENG-48.

[1] R.A. Stewart, P. Vitello, D.B. Graves, E.F. Jaeger, and L.A. Berry, submitted to *Plasma Sources Science and Technology*, (1994).

NB-7 **A Hybrid Model of an Inductively Coupled Plasma**, E. R. KEITER, V. KOLOBOV, W. N. G. HITCHON, K. M. KRAMER, *U of Wisconsin-Madison*, S. SHANKAR, *Intel Coorporation* — A hybrid model of an Inductively Coupled Plasma (ICP) has been developed, which includes a kinetic ion module based on the convected scheme,[1] an electromagnetics module, an electrostatics module, and a calculation of the electron energy distibution. The electromagnetics module solves the wave equation, and the electrostatics module solves poisson's equation. The electron energy distribution function (EEDF) calculation is based on a two term expansion of the Boltzmann transport equation. The electromagnetic, electrostatic, and EEDF module are all based on a numerical package developed at Wisconsin.[2] Some preliminary results will be presented.

*Work supported in part by NSF grant #ECD-8721545

[1]W.N.G. Hitchon and E.R. Keiter, J. Comp. Phys. **112**, 226, (1994).

[2]K.M. Kramer and W.N.G. Hitchon, "A Highly Flexible Tool for Applied Physics Simulations," to be published.

NB-8 **Comparison of Ion Energy Distribution Functions in a Capacitively and Inductively Coupled RF-Discharge** U. KORTSHAGEN, M. ZETHOFF, University Bochum, 44780 Bochum, Germany

The inductive coupling of rf-power to a plasma using a planar coil geometry has attracted growing interest in the past few years. In contrast to the conventional parallel-plate etching devices this setup allows the production of large area high density plasmas with moderate ion impact energies. In this contribution the influence of capacitive and inductive coupling of the applied rf-power on the ion energy distribution (ied) is studied. The experimental setup allows the coupling of rf-power to the plasma via a planar induction coil or via an equally sized electrode. Additionally, an electrostatic screen is used to suppress possible capacitive coupling due to high potentials on the induction coil. The ied's are measured on the grounded electrode using a retarding field analyser. The observed ied's demonstrate effects of strong capacitive coupling in the planar inductive discharge. The experimental results are compared to PIC-MCC calculations, which account for the different heating mechanisms of electrons in the capacitive and inductive discharge.

NB-9 **Comparison of Langmuir probe characterization and model predictions in a high density ICP source**, P. WAINMAN, R. A. STEWART, M. A. LIEBERMAN, D. B. GRAVES, and P. VITELLO*, U. of California, Berkeley – An ICP source has been built and an argon discharge has been extensively characterized using a Langmuir probe. The ICP chamber design includes a planar stovetop coil and moveable pistons at either end, enabling the spacing between the top quartz window and bottom plate to be adjusted over a wide range. We report variation of peak plasma density, electron temperature and plasma potential with source power (50-400W) and gas pressure (2-20 mT) for chamber aspect ratios (R/L) ranging from 1.0 to 4.0. Radial plasma uniformity measurements are also presented versus pressure and aspect ratio. A 2D fluid model with self-consistent power coupling [1] has been used for comparison to predict variations in discharge parameters over the same parameter space as above. The model is also used to study how and to what extent the plasma is influenced by capacitive coupling from both an rf biased substrate and the rf coils.

*Lawrence Livermore National Laboratory

[1] R. A. Stewart, P. Vitello, D. B. Graves, E. F. Jaeger, and L. A. Berry, submitted for publication.

NB-10 **Self-Consistent Kinetic Modeling of a Low-Pressu Inductively Coupled RF Discharge***, D.F. BEALE, W.N.(HITCHON, V.I.KOLOBOV and A.E.WENDT, ERC for Plasm Aided Manufacturing, U. of Wisconsin, Madison - Results from tw dimensional numerical modeling of a planar inductive coupled R discharge in Argon are presented for a pressure range 10-50 mTo and plasma density range 10^{10}-10^{12} cm^{-3}. A flexible modeling packa allows the problem to be set up rapidly in different compact modul that solve quasi-steady Maxwell's equations for the RF fiel Boltzmann's equation for the electron distribution function[1], a flu equation for the ion density and Poisson's equation for the spa charge field. Quantitative comparison of the results of modeling experimental investigations[2] will be presented.

*Work supported in part by NSF grant ECD-8721545

[1]V.I.Kolobov and W.N.G.Hitchon, this conference

[2]V.I.Kolobov, D.F.Beale, L.J.Mahoney and A.E.Wendt, Appl. Phys. Lett. 65, 1 August 1994

NB-11 **Characteristics of a low pressure inductively coupled RF discharge**, B. COONAN, W. McCOLL and M. HOPKINS, Dublin City University, Dublin, Ireland - An investigation of the characteristics of a low pressure (<50mTorr) Argon inductively coupled rf discharge has been carried out. The plasma is powered through an antenna (inductance 1.5μH) placed inside the plasma chamber and driven at 13.56MHz with typical operating powers of between 20 to 200W. A movable tuned langmuir probe positioned over the middle of the antenna allows measurments of plasma characteristics to be taken. The magnetic field strength inside the plasma is measured using a magnetic field probe and allows the skin depth of the plasma to be determined. A collisionless heating mechanism for low pressure inductive discharges has been proposed by Turner [1]. An aim of the experiment is to test the prediction of the proposed collisionless heating mechanism. In a collisionless plasma (collision frequency < rf driving frequency), electrons can make a net energy gain from the antenna electric field if they pass through the electric field in a time less than one rf cycle, it is a warm plasma effect.

[1] M.M. Turner, Phy. Rev. Lett. 71, 1844, (1993).

NC: CATHODES AND SHEATHS

NC-1 Optical Spectroscopy, Etching and Deposition in Parallel Plate Hollow Cathode Discharges of Ar and Ar/N2, B.M. JELENKOVIC[+], A. CHELOUAH, and E. MARODE, LPD, SUPELEC, 91190 Gif-Sur-Ivette, France -

Spatial axial and radial profiles of Ar, N_2 and of sputtered Ti lines, in low pressure (< 0.1 Torr), high voltage (>1000 V) parallel plate hollow-cathode discharges were measured. The spatial profile of 1st negative emission of N_2^+ in the Ar/3%N_2 mixture was used to monitor high energy, i.e. ionizing electrons[1]. The later results were compared with PIC Monte Carlo simulation of electron ionization profiles. The intense heavy particle excitation of argon lines in the vicinity of cathodes and charge and energy transfer of Ar^+ to Ti in the glow region were observed. The etch rate of Ti cathodes in Ar and deposition rate of TiN in Ar/N_2 were 25 and 1.5 Å/s respectively.

[1] B.Jelenković and A.V.Phelps, Book of abstracts, 46th GEC(1993), p.37

[+] Permanent address: Institute of Physics, Belgrade, Yugoslavia.

NC-2 Oscillations and Constrictions for Cathode-Dominated, Low-Pressure Argon Discharges.* Z. Lj. PETROVIĆ** and A. V. PHELPS, JILA, U. of Colorado and NIST. - Quasi-steady-state voltage-current characteristics, voltage and current oscillations, and constrictions are reported for cathode-dominated, pulsed (5 ms at 20 Hz) discharges in low pressure Ar. Pressure times the separation of parallel-plane electrodes *pd* are 0.12 to 2 Torr-cm (area = 50 cm^2). The quasi-steady-state voltage decreases linearly with current up to the onset of self-sustained oscillations. Current growth rates obtained from frequencies of damped oscillations are 2 to 3 times predictions[1]. At 2 Torr-cm and currents of 0.3 to 4 mA nearly centered constrictions occur. Optical emissivities increase approximately linearly with current density for $2 \leq J \leq 150$ $\mu A/cm^2$ as for single-step excitation. Rotating ($\approx$ 4 kHz) constrictions form near the wall for *pd* = 0.12 and 0.2 Torr-cm at $\geq$ 10 and $\geq$ 1 mA, respectively.

* Supported in part by Air Force Wright Laboratories.

** Present address: Institute of Physics, Belgrade, Yugoslavia.

[1] A.V. Phelps, Z. Lj. Petrović, and B.M. Jelenković, Phys. Rev. E 47, 2825 (1993).

NC-3 Excitation of Ar lines near the cathode surface. K. Rozsa[+], A. Gallagher and Z. Donko[*]. Joint Institute for Laboratory Astrophysics, University of Colorado and National Institute of Standards and Technology, Boulder, Colorado 80309-0440.

Measurements of spatial intensity distribution of different Ar lines are reported for a flat cold cathode discharge in the j/p^2 range of 10^{-4} and 10^{-2} $Acm^{-2}mbar^{-2}$. In this range the cathode glow peak and the negative glow are well separated. With increasing j/p^2 as the heavy particle excitation increases the cathode glow intensity increases while the negative glow extends to larger area. The voltage, the pressure times length of the cathode sheath, and the fraction of the input energy which goes into the negative glow and the cathode glow have universal dependence with j/p^2, but the negative glow decay length times pressure does not.

The work was supported in part by NREL contract #DD-H1001-1.

[+] Permanent Address: Research Institute for Solid State Physics.
[*]Research Institute for Solid State Physics H-1525 Budapest, POB. 49 Hungary.

NC-4 Radial Spatial Distributions of Emission for Cathode-Dominated, Low-Current Discharges. B. M. JELENKOVIĆ* and A. V. PHELPS, JILA, U. of Colorado and NIST. - Radial spatial distributions of emission across the cathode for cathode-dominated discharges in low pressure Ar and H_2 are measured through a semitransparent anode. A photomultiplier allows measurements to much lower currents than the video camera of Ref. 1. Pressure times the planar electrode spacing *pd* are 0.2 to 9 Torr-cm for Ar and 0.3 to 4 Torr-cm for H_2. Currents are 0.1 to 10 μA (area = 50 cm^2). At some pressures the radial distributions of intensity are significantly asymmetric. At other pressures they are flatter than the predicted[2] symmetric, diffusion-dominated (Bessel function) radial solutions. For a given electrode aging in H_2, the asymmetric emission switches sides as *pd* varies across the *pd* for minimum breakdown voltage. This result is consistent with comparable nonparallel electrode (nonuniform field) and lateral diffusion effects. The emissivity is linear with current as for single-step excitation.

* Permanent address: Institute of Physics, Belgrade, Yugoslavia.

[1] Z. Lj. Petrović and A. V. Phelps, this conference (1994).

[2] V. I. Kolobov and A. Fiala, Phys. Rev. E (in press) (1994).

NC-5 Optical Investigation of Arc Spot Ignition in Noble Gas Atmosphere on Cold Cathodes,* J. SCHEIN, M. SCHUMANN, J. MENTEL, Ruhr-Universität Bochum, AEEO, Germany - For the investigation of arc spot ignition an arc is produced in a chamber filled with noble gas at atmospheric pressure. Perpendicular to the arc axis an electrode is positioned switched cathodically by an external applied constant voltage. The arc spot ignition on this cold cathodes is investigated optically. Emission spectroscopy and high speed photography are used simultaneously. The measurements are made in a spectral range from 400 nm - 700 nm imaging the electrode surface into the slit of the spectrograph. Looking at arc spot ignition in argon it turns out that the light during the current flow through an arc spot can be identified as the spectrum of argon ion lines. Material lines cannot be seen. Either the increasing of the exposure time of the OMA system or recording a larger area in front of the electrode leads to a spectrum looking like the continuum of a black body of about 5000 K. Having a look at high speed photography a plasma jet can be identified aiming from the arc right onto the electrode surface on which a bright plasma ball can be seen. The optical investigations will be combined with electrical measurement of the potential in front of the electrode and the current flow through it. Results will be presented for different electrode materials.

* Work supported by DFG-SFB 191/A3.

NC-6 Ferroelectric Cathodes for Pulsed Gas Discharge Triggering,* C. B. FLEDDERMANN, T. CAVAZOS, W. WILBANKS, and D. SHIFFLER, Dept. of Elec. and Comp. Eng., Univ. of New Mexico- Recent studies of ferroelectric cathodes have shown that emission of high fluxes of electrons is possible.[1] This electron emission is initiated by a rapid polarization change in the ferroelectric induced by a nanosecond time-scale electric field applied to a metal grid on the surface of the ferroelectric sample. This type of cathode could be readily used to sustain a gas discharge. In our experiments, a PLZT 9/65/35 bulk sample covered with a 20% transparent gold grid is used in a triode configuration. A cathode contact on the back of the PLZT wafer is grounded, and a dc voltage up to 20 kV is applied to the anode. The grid is pulsed with electric

fields up to 15 kV/cm. Electron emission is only observed when the PLZT sample is driven into saturation. In this work, a bias voltage is used to reset the ferroelectric to a known polarization before each shot. Typical emitted charge is 20-40 nC for grid fields between 10 and 14 kV/cm. The prospects for using this type of cathode for initiating breakdown in gas discharges will be discussed.

1. H. Gundel, J. Handerek, and H. Riege, J. Appl. Phys. 69, 975 (1991).

*Work supported by AFOSR grant #F499620-94-1-0087DEF.

NC-7 Studies of Plasma Source Ion Implantation (PSII) Sheath Expansion for Circular Planar Targets*, A. ONUOHA, D. DALLMANN, J.H. BOOSKE, R. BREUN, L. ZHANG, P. SANDSTROM, W.N.G. HITCHON, and E. KEITER, Engineering Research Center for Plasma-Aided Manufacturing, Univ. of Wisconsin-Madison. We report results of experiments and simulations investigating the effects of target geometry on sheath propagation. Specifically, circular planar targets of varying diameters were pulsed biased between -5 and -25 kV. Filament and RFI excitations were used to produce nitrogen plasma densities between 5×10^{11} - 2×10^{10} cm^{-3} and plasma electron temperatures between 0.3 and 3.0 eV. Sheath propagation times were measured using a Langmuir probe biased into electron saturation. Information on the sheath geometry and rate of expansion were extracted from both the Langmuir probe and target collected current waveforms. The experimental results are compared with predictions of 2D numerical simulations.

* This work supported by NSF grant ECD-8721545.

NC-8 **Self-Bias and Battery Effect at Moderate Pressure Coaxial RF Discharge**, YU. P. RAIZER and M. N. SHNEIDER, *The Institute for Problems in Mechanics, Russian Academy of Science* — The results of the first computer modeling of such situation will be given. They show how oscillating plasma never touches the larger electrode. There is a negative potential self-bias on the smaller electrode in the presence of a blocking capacity and dc current is formed for closed external circuit. The situation is quite similar to a low pressure rf discharges. The sheath breakdown at the smaller electrode is occurred at sufficiently high voltage. This effect violates the normal operation of the annular gas lasers with rf excitation.

ND: DUSTY GLOWS

ND-1 **Contribution of Short-Lifetime Radicals (Si, SiH_2) to Particulate Growth in Silane Plasmas,*** H. KAWASAKI, T. FUKUZAWA, M. SHIRATANI and Y. WATANABE, Faculty of Engineering Kyushu University - We have investigated particulate growth processes in silane RF plasmas using several methods.[1] Recently, to study contribution of short-lifetime radicals (Si, SiH_2) to the particulate growth, spatiotemporal profiles of the densities of the short-lifetime radicals and the size, size dispersion, density and refractive index of particulates have been measured. Particulate amount has been also measured by using a novel intra-cavity laser-light-extinction method, which offers higher sensitivity than usual laser light scattering/extinction methods. Close similarities among spatiotemporal profiles of Si emission intensity, Si density and particulate amount are revealed in wide discharge parameter ranges of 1~100%SiH_4, 11~20 Pa, and 40~100 W. Furthermore, when increasing RF power, the SiH_2 density linearly increases with the power until particulates become detectable and then saturates. The last feature suggests that SiH_2 may contribute importantly to nucleation and initial growth of particulates.

*Work supported by a Grant-in-Aid for Scientific Research by the Ministry of Education, Science and Culture of Japan.

[1]H. Kawasaki, T. Fukuzawa, H. Tsuruoka, T. Yoshioka, M. Shiratani and Y. Watanabe, Jpn. J. Appl. Phys. 33, No. 7B (1994).

ND-2 **Mie Scattering Measurement of Particulate Size*** G. PRABURAM, J. GOREE, *Dept. of Physics, Univ. of Iowa*

We have carried out a numerical study of an optical method of measuring size and density measurements of suspended particulates. Scattered laser light is detected at 90°, and the ratio σ of the $\parallel$ and $\perp$ polarized components is proportional to the fourth power of particulate size. The method has, however, some practical limitations, which we quantify using a Mie scattering code to compute σ as a function of particle radius and refractive index. We tested the sensitivity to the finite detector solid angle, the polarizer extinction ratio, and small errors in the scattering angle. Our calculations reveal that an error of 0.1° in scattering angle can cause more than 20% error in the size measurement, for example. To measure particle sizes < 200 nm, the detector solid angle should be $< 10^{-5}$ Sr and the extinction ratio of the polarizer must be $< 10^{-4}$.

* Work supported by NSF and NASA

ND-3 **Particulate Charging in RF Discharge Sheaths.** D. WINSKE and MICHAEL E. JONES, *Los Alamos Natl. Lab.*— Laser scattering measurements have shown that the charged particulates are present in rf discharges and tend to collect in certain well defined regions, while theory has demonstrated that the particulates are subject to a number of forces (the ion drag and electric forces usually being dominant) that tend to balance at the edge of the sheath. In this paper we discuss an extension to a one-dimensional force balance analysis at the edge of an rf sheath by the inclusion the effect of the finite charging time of the particulates compared to the period of the rf driven electrodes. We determine how the time averaged charge on the particulates is modified, as a function of the plasma, contaminants, and rf parameters. The corresponding modifications to the ion drag and electric forces acting on the particulates and resulting changes in their equilibrium positions are also presented. Results for spherical and nonspherical particulates, including the effect of the polarization force, are compared

ND-4 **Particles in Silane Discharges** B. JELENKOVIĆ*, A. LARACUENTE AND A. GALLAGHER- JILA U of Colorado and NIST

The occurrence of particles in pure silane rf discharges with parallel plate electrodes (52 x 95 mm) separated by 17 mm was investigated as a function of pressure (<0.5 Torr), power, and flow at 300 K. Gas was fed along the longer dimension. Mie scattering at 90° by particles

occurs at 0.2 Torr for 2mW/cm^3 and 10 sccm, mainly near the gas exit. As the flow decreases particle formation starts nearer the entrance and at lower power. In the region between electrodes dust formation shows pressure dependence with maxima between 0.25 and 0.3 Torr. After the rf power was turned on, Mie scattering reaches a maximum in a time interval of about 5 sec, followed by a slower decay to a lower steady state. A grounded electrode with side walls extended near the rf electrode (box reactor) enhances particle formation and trapping. Dust alters the spatial variation of emission by expanding and intensifying the glow region. A pressure increase and, to a lesser extent dust formation, make the discharge more resistive.

+ Permanent address: Institute of Physics, Belgrade, Yugoslavia.

ND-5 **A Correlation of Particle Growth and Spatio-temporal RF Plasma Structure**,* T.Kitajima, Y.Okabe and T.MAKABE, Keio University, Yokohama — Particle growth and subsequent decay in plasma reactors for surface processing is continuously studied in a parallel-plate rf discharge at 13.56MHz in Ar with sputter-etched (-CF_2CF_2-) as a particle source. The space-and time-variation of the plasma structure during a short time range is measured simultaneously with a long time variation of the particle size(density) by both spatiotemporally resolved optical emission spectroscopy and Mie scattering of Ar^+ ion laser.[1]
The slower process of particle growth in CF-Ar system enables us to analyze the change in the plasma structure due to the influence of the plasma-electron capture by massive dielectric particles. Numerical modeling including a submicron particle grwoth[2] shows the spatiotemporal profile similar to the observation.

*Work is supported in part by a Grant-in-Aid for Science Research on "Free Radical Science".
[1]T.Kamata, S.Kakuta, Y.Yamaguchi and T.Makabe, Plasma Sources Sci.Technol.(1994.8)
[2]T.Makabe, Y.Hosokawa and T.Kitajima, 3rd-AJW(1994.7).

ND-6 **Formation of a Coulomb Solid in a Dusty Plasma using a GEC Reference Cell** *
C. CUI, J. GOREE, R. QUINN
Dept. of Physics and Astronomy, Univ. of Iowa

Theoretical predictions of Coulomb solids of highly charged dust particles in a plasma have been experimentally verified, using a GEC reference cell with the top electrode removed. A cloud of polydispersive particles was levitated above the powered lower electrode in a 1-Torr Ar discharge. Grains were stratified at different heights (1 - 4 mm) according to their sizes. Video images using a horizontal sheet of laser light reveal grains fixed in a solid-like structure with a particle separation Δ that increases with particle size. The measurements show that $\kappa \equiv \Delta/\lambda_D$ increases from 0.8 to 2 (±30%) for grain sizes increasing from 1 to 20 μm, and that κ increases with Γ (the ratio of inter-particle potential energy to particle kinetic energy). The cloud of polydispersive charged particles includes some grains (<10%) that execute fixed circular orbits at 1 - 8 rev/sec rather than Brownian motion.

* Work supported by NASA and NSF

SESSION PA: INDUCTIVELY COUPLED PLASMAS III
Friday morning, 21 October 1994
NIST Building 101
Red Auditorium, 8:00–10:00
M. Barnes, presiding

Contributed Papers

PA-1 Thomson Scattering Measurements of Electron Temperature and Density in an RFI Discharge, M.D. BOWDEN, T. HORI, K. UCHINO, K. MURAOKA, M. MAEDA, Kyushu U., Recently, the technique of Thomson scattering of a high-energy pulsed laser has been applied to make measurements of electron temperature T_e and electron density N_e in processing plasmas[1,2]. In this paper, we report measurements of radial and axial profiles of T_e and N_e in a compact radio frequency induction (RFI) argon discharge made using this technique. The discharge chamber was designed specifically for Thomson scattering measurements and allows the measurement of spatial and radial profiles of plasmas variables without moving the position of the optics for the probing laser beam. The chamber also allows the separation of the planar RF coil and the substrate holder to be easily varied and T_e and N_e profiles for plasmas of different dimensions were measured.

1. M.D. Bowden *et. al.*, J. Appl. Phys. 73, (1993) p2732.
2. M.D. Bowden *et. al.*, J. Vac. Sci. Technol. 11, (1993) p2893.

PA-2 Strongly Radially Dependent Steady Potential in an Inductively Coupled Plasma at Low Frequency. F. A. HAAS, S. YANG and N. St. J. BRAITHWAITE. Oxford Research Unit, Open University, Oxford, U.K.- Considering a two-dimensional (r,z) configuration with a weakly coupled, externally wound, induction coil, the Maxwell equations are solved for vacuum fields Eθ, Br, Bz. Assuming exp (iωt) for time-dependence, electromagnetic fields are expressed in terms of Bessel and harmonic functions. Including collisions with neutrals, expressions are derived for electron and ion azimuthal velocities, ve, i. These are substituted into the time-averaged radial momentum equations. For appropriate conditions the electron fluid is shown to be maintained in equilibrium by $\langle v_e^2 \rangle$ inertial, magnetic pinch and space charge forces. Measurements on a 500 kHz argon plasma coupled via a thirty turn coil indicate potentials rising from a few volts in the central region to 60V or so at the edge are in qualitative support of the theory. Magnetic probes confirm the suitability of the model field structure.

PA-3 Neural Network Etch-Control of an Inductively Coupled Plasma Reactor, Ronald C. Caldwell and Harold M. Anderson, University of New Mexico, Roger D. Jones, and Kevin L. Buescher, Los Alamos National Laboratory, - Producing desired physical and electrical characteristics is of great importance for semiconductor etching. To investigate the control of an inductively

coupled plasma (ICP) reactor, we have developed a 2-dimensional plasma source and neural-network controller. The simulation consists of an azimuthal flat spiral-like excitation current-coil which induces a conduction current within the plasma. This induction current contains both an in-phase and an out-of-phase component with respect to the excitation current. The associated electric field is used for Monte Carlo tracking of particles to produce electron-energy distributions (EED's) for input into the neural network controller. Radical species etching semiconductors result from ionization of gas atoms by electrons; therefore, the EED histograms generated by this model provide real-time input into the neural network. Drift and random fluctuations are introduced and then stabilized by the neural network controller. Real wafer etch characteristics measured using a LAM 9600 reactor provide target values for the model.

PA-4 Ion Temperature in a 2-D Fluid Model of an Inductively Coupled Plasma, J. D. BUKOWSKI, M. D. KILGORE, R. A. STEWART, P. VITELLO†, and D. B. GRAVES, U.C. Berkeley and †LLNL – High density plasma sources such as the ICP are regarded as a promising technology for achieving high degrees of anisotropy in sub-micron device manufacturing. Profile evolution studies [1] indicate that deviations from anisotropy can be explained when ion heating in the presheath is taken into account. A fluid-particle hybrid model of an ECR reactor shows that ion temperatures of several tenths of an eV are achieved in high density sources [2]. We use a 2-D fluid model [3] of a Cl2/poly-Si etching system with ion and neutral energy conservation to predict ion temperature parallel and perpendicular to the drift velocity. We examine the effect of gas pressure and capacitive coupling on the ion energy transverse to etched surfaces. We compare the results from the fluid model to those obtained from Direct Simulation Monte Carlo / Ion Monte Carlo.

[1] J. Zheng and J.P. McVittie, *Proceedings of the Tenth Symposium on Plasma Processing*, ed. by M. Engelhardt, G.S. Mathad, and D.W. Hess, The Electrochemical Society, submitted 1994
[2] R.K. Porteous, H.-M. Wu, and D.B. Graves, *Plasma Sources Sci. Technol.*, **3** (1994) 25-39
[3] R.A. Stewart, P. Vitello, D.B. Graves, E.F. Jaeger, and L. A. Berry, submitted 1994

PA-5 Radially Dependent Ion Energy Distributions in Inductively Coupled Plasmas for Etching,* Robert J. HOEKSTRA and Mark J. KUSHNER, University of Illinois, Dept. of Elect. and Comp. Engr., Urbana, IL 61801 USA - High plasma density (10^{11}-10^{12} cm^{-3}), low pressure (< 10 mTorr) etching tools, such as inductively coupled plasmas (ICPs), typically use rf biasing of the substrate. The thinner rf sheaths at the higher plasma densities allow heavy ions to rapidly transit the sheath, thereby broadening the ion energy distribution (IED). We have developed a 2-dimensional Plasma Chemistry Monte Carlo Simulation (PCMCS) with which we are investigating spatially dependent IEDs in ICP etching tools. The PCMCS uses 2-d time dependent electric fields and source functions produced by a companion hybrid equipment model of ICPs. The PCMCS tracks the trajectories of ions and radicals while accounting for ion-neutral and ion-radical collisions. IEDs as a function of position on the wafer will be discussed for multicomponent chlorine gas mixtures for p-Si and metal etching; and fluorocarbon gas mixtures for oxide etching. The effect of electrode topography on ion angular distributions will also be discussed.

* Work supported by SRC, NSF, Sandia National Laboratory, and the University of Wisconsin ERC for Plasma Aided Manufacturing.

PA-6 Direct Simulation Monte Carlo (DSMC) of Plasma Flow in a High Density Source*, R. WISE, T. BARTEL, D. LYMBEROPOULOS and D. ECONOMOU, U. of Houston and Sandia National Laboratories - We present an axisymmetric, two-dimensional simulation of radical and ion flux uniformity in a high density plasma reactor. We employed the Direct Simulation Monte Carlo (DSMC) method, a particle based simulation technique, to handle the rarefied flow of radicals and ions at the low operating pressures (1-10s of mtorr). The spatial distribution of radical and ion production rate was calculated by using a glow discharge model. Ions were followed in the space charge field found by solving the Poisson equation. The etching of polysilicon in a chlorine discharge was selected as an example material system. Calculations were performed on a massively parallel supercomputer (n-Cube) using 2.5 to 5 million computation particles with specie dependent weights. Radical (Cl), product ($SiCl_x$) and ion (Cl^+, Cl_2^+) fluxes and their energy and angular distribution were obtained in addition to the etch rate along the wafer. A parametric investigation was conducted of the effect on etch uniformity of gas injector design, gas pressure, and wall recombination probability of Cl atoms.

* Work supported by Sandia/Sematech and the National Science Foundation.

PA-7 Numerical Solution of the Boltzmann Equation in Cylindrical Geometry, G.J. Parker, LLNL, W.N.G. Hitchon, U. of WI- Madison, R.A. Stewart, and P. Vitello, LLNL — A numerical procedure, the Convected Scheme (CS)[1], which provides a direct solution of the Boltzmann equation in cylindrical geometry with coordinates $(z, \rho, \vec{v})$ is discussed. Statistical methods such as Monte Carlo can be used but suffer from statistical noise and thus do not resolve low density regions well. Furthermore, the slow speed of pure Monte Carlo methods makes self consistent simulations quite difficult. The CS avoids these difficulties but suffers from errors due to finite size mesh effects. Judical choice of coordinates and propagator algorithms for solving the kinetic equation can eliminate some specific sources of numerical diffusion in cylindrical geometry. The velocity is represented as $(v_z, v_\perp, \mathcal{M})$, where $\mathcal{M}$ is a moment arm, $\mathcal{M} = \rho \sin\phi$ and ϕ is an azimuthal angle in velocity space (referenced to $\hat{\rho}$). The reasons for all the coordinate choices are discussed. A self-consistent kinetic model of a dc positive column is described as well as a hybrid solution of an ICP reactor.

1. W.N.G. Hitchon, G.J. Parker and J.E. Lawler, *IEEE Trans. Plasma Sci.* **21**, 228, (1993) and references within.

PA-8 A Fast, Self–consistent Two–dimensional Kinetic Model of an Inductively Coupled RF Discharge
U. KORTSHAGEN, University Bochum, 44780 Bochum, Germany, L. D. TSENDIN, St. Petersburg Technical University, 195251 St. Petersburg, Russia
Self–consistent plasma models are usually numerically laborious, in particular, if they involve a more than one–dimensional spatial description. Computation times of the order of hours or days on workstations or faster computers are typical. In this paper a fast, two–dimensional self–consistent kinetic model for an inductively coupled RF plasma is presented. The main simplification of this model is achieved by the spatially resolved treatment of the electron kinetics within the "nonlocal approach" to the solution of the spatially dependent Boltzmann equation. The static space charge potential is computed from a 2D fluid model, the RF electric field profile is calculated from Maxwell's equations. Computation times of about one hour on a usual PC (i486/33 MHz) are achieved. The theoretical results are compared to measured electron distribution functions. The measured spatial dependence of the electron distribution function proves the applicability of the nonlocal approach.

SESSION PB: PLASMA TECHNIQUES FOR WASTE TREATMENT II

Friday morning, 21 October 1994
NIST Building 101
Green Auditorium, 8:00–10:00
J. T. Herron, presiding

Invited Papers

PB-1 Microwave-induced Plasma Destruction of Organic Compounds,* T. R. Krause, Argonne National Laboratory - High-frequency plasmas in the radio and microwave range are being developed by various research groups as a candidate technology for the treatment of off-gas streams generated by environmental and production processes. At Argonne National Laboratory, we are investigating microwave-induced plasmas operating at atmospheric pressure for the destruction of volatile chlorinated compounds, such as trichloroethylene and trichloroethane, under oxidative and wet oxidative reaction conditions. Preliminary experiments have shown that destruction removal efficiencies ranging from 95 to >99% can be achieved with nearly quantitative conversion of the parent compound to CO_x and acid gases, such as HCl. In addition to our experimental program, an overview of the application of microwave-induced plasmas in environmental applications will be presented.

*Work supported by the Office of Technology Development within the U.S. Department of Energy's Office of Environmental Management under Contract W-31-109-ENG 38.

PB-2 Simultaneous Reduction of NOx and SOx from Combustion Flue Gas by Corona Discharge Radical Injection Techniques, J.S.Chang, McMaster University Canada - An experimental investigation has been conducted to reduce NOx and SOx from combustion flue gases by means of corona radical injection methods. In this process, pure or mixture ammonia, steam, hydrocarbon, nitrogen and oxygen radicals are generated by a flow stabilized corona discharge and injected to the combustion flue gas stream to convert acid gases to unharmful gases or reusable solid products. The laboratory and pilot plant test results show that this technique not only effectively reduces NOx and SOx up to 85 and 98% respectively but also reduces leak ammonia concentrations and ozone generations. Depending on flue gas flow rates, gas temperatures and acid gas concentrations, the energy efficiency of the process is approximately 10 to 50 g/kWh. Electron beam/corona radical injection hybrid system pilot test results will be discussed in detail.

PB-3 Energy Dissipation and Radical Yields in Non-Thermal Plasmas*, B. M. PENETRANTE, Lawrence Livermore National Laboratory -- Many types of non-thermal plasma reactors are being investigated for the disposal of a wide variety of gaseous pollutants.[1] Two critical issues restraining the commercial implementation of these reactors are electrical power consumption and byproduct identification. In non-thermal plasma processing, the electrons deposit the input electrical energy mainly through collisions with the dominant background gas molecules, thus producing radicals that in turn lead to the selective decomposition of the pollutant molecules. The type and amount of radicals produced in the plasma determine the electrical requirements and process byproducts for any given application. This talk will present an analysis of the energy dissipation and radical yields in non-thermal plasmas based on electron-molecule collision cross section data. Energy deposition calculations, along with an extensive survey of experimental data from various laboratories, indicate that the electron mean energy is the most important parameter controlling the radical production efficiency.

*Work performed at Lawrence Livermore National Laboratory under the auspices of the U.S. Department of Energy under Contract Number W-7405-ENG-48, with support from the Advanced Energy Projects Division of the Office of Energy Research.

[1]Non-Thermal Plasma Techniques for Pollution Control - Part B: Electron Beam and Electrical Discharge Processing, B. M. Penetrante and S. E. Schultheis, eds. (Springer-Verlag, Berlin Heidelberg, 1993).

Contributed Papers

PB-4 Radical Transport in Dielectric Barrier Discharges for Plasma Remediation of N_xO_y,* Ann C. GENTILE and Mark J. KUSHNER, University of Illinois, Dept. of Elect. and Comp. Engr., Urbana, IL 61801 USA - Dielectric Barrier Discharges (DBDs) are being investigated for remediation of toxic gases from atmospheric pressure gas streams. One important application is the removal of oxides of nitrogen (N_xO_y) from combustion exhaust produced by, for example, diesel engines. We have developed a plasma chemistry model to investigate the reaction mechanisms and radical transport during plasma remediation of combustion exhaust using DBDs. The simulation includes a circuit model, solution of Boltzmann's equation for the electron energy distribution and 1-d radial transport of radicals produced in the streamer channel. We have identified three time periods following the current pulse in which the dominant processes are radical formation, N_xO_y removal and redistribution of N_xO_y. The durations of these periods largely determine the energy efficiency of remediation and the production of undesirable species such as O_3 and N_2O. We will also compare the contributions of radical diffusion and advective transport to obtaining uniform processing of the gas.

* Work supported by NSF, and the Office of Naval Research.

PB-5 Effect of Vibrationally Excited Molecules in Non-Thermal Plasma Processing of Off-Gases*, C. GORSE and B. M. PENETRANTE, Lawrence Livermore National Laboratory -- For some applications such as mixed waste streams, a thermal plasma reactor, such as a plasma-arc furnace, may be the best approach to dispose of the complete waste, including the container. A non-thermal plasma reactor can then be used to treat the off-gas, which could contain high levels of NO_x when air is used as the torch and purge gas. Our analysis shows that in a non-thermal discharge plasma reactor, such as pulsed corona or dielectric barrier discharge, a large fraction of the input electrical energy is consumed in the vibrational excitation of molecules, rather than in the production of radicals. The purpose of this work is to determine whether it is possible to take advantage of these vibrationally excited molecules in the off-gas treatment by using the residual heat from the thermal plasma treatment stage. We will present calculations showing the effect of vibrationally excited molecules on the production of radicals in non-thermal discharge reactors for various air mixtures and gas temperatures.

*Work performed at Lawrence Livermore National Laboratory under the auspices of the U.S. Department of Energy under Contract Number W-7405-ENG-48, with support from the Advanced Energy Projects Division of the Office of Energy Research.

SESSION QA: INNOVATIVE PLASMA APPLICATIONS
Friday morning, 21 October 1994
NIST Building 101
Red Auditorium, 10:15–12:00
R. B. Piejak, presiding

Invited Papers

QA-1 Electrodeless Discharges for Lighting, D O WHARMBY, GE Lighting, Melton Road, Leicester, UK - A brief review of possible types of electrodeless lighting will be presented. Regulations concerning electromagnetic interference mean that the type of discharge excitation that is a commercial possibility at present is the inductively coupled discharge (ICD). Commercial types based on fluorescent lamp type discharges (Hg - rare gas) are now available and give benefits such as long life and compactness. These make use of an internal coil within a reentrant tube inside the bulb. The relationship between the discharge and the exciter coil characteristics will be discussed based on measurements and a 1-dimensional plasma-coil model[1]. The impedance of the coil when loaded by the plasma is the key quantity controlling the interaction of the discharge and the circuit. Unloaded coil impedance affects both coil losses and starting behaviour. Commercial lamps have to operate in fixtures which can act as a shorted turn to the exciter coil, affecting its loaded impedance and circuit operation: means for dealing with this problem will be discussed.

1. G.G.Lister and M.Cox, Plasma Sources Sci. Tech. **1**, 67 (1992).

QA-2 Microwave Excited Sulfur Lamp*
B.P. TURNER, M.G. URY and D.A. MACLENNAN, Fusion Lighting, Inc., Rockville, MD - Efficient (>130 lumens/watt), continuous, visible radiation with high color rendering (R_a=86) has been produced in microwave excited sulfur discharges. We will present recent developments in our understanding of the phenomena involved in these types of discharges. We propose a model for the efficient production of visible molecular radiation from selected Group VI elements. The deleterious effects of high order alletropes (S_6, S_8, S_{12}, etc.) and techniques to minimize these effects will be presented. We will also discuss the use of this novel light source for architectural and projection applications.

* Portions of this work have been supported by the following agencies: EPA, NASA, DOE.

Contributed Paper

QA-3 Electrodeless Alkali Flashlamps for Pumping Nd:YAG Lasers*, J. M. Richardson, J. Mangano, and A. Flusberg, Science Research Laboratory, Inc. Existing flashlamp-pumped Nd:YAG lasers employ standard tungsten-electrode xenon flashlamps. Such flashlamps produce a nearly continuous thermal spectrum of light much of which is not readily absorbed by solid state lasers such as Nd:YAG. Certain alkali vapors are capable of producing narrow-band radiation that is strongly absorbed by solid state lasers and thus could provide for a more efficient pumping method. A further important refinement is to excite the alkali vapor inductively, thus increasing the useful lifetime of the lamp. Inductive coupling also allows for a cylindrical geometry in which the flashlamp totally surrounds the laser crystal, improving overall efficiency. A brief review of this project will be presented along with recent developments and results.

* This work sponsored by Naval Air Warfare Center, Aircraft Division, under contract number N62269-93-C-0514.

Invited Paper

QA-4 X-Ray Lasers based on Capillary Discharges*, J.J.ROCCA, F. G.TOMASEL, V.SHLYAPTSEV**, O. D. CORTAZAR, and D. HARTSHORN, Colorado State University - We describe the first demonstration of soft x-ray lasing in a discharge created plasma. Soft x-ray lasing in plasmas generated by large laser facilities was first obtained in 1984. It has been recognized that direct discharge excitation could result in a significantly increased laser efficiency, increased simplicity and reduced size and cost. However, the problem of demonstrating large amplification at wavelengths below 100nm using discharge pumping had remained unresolved. We have utilized a fast capillary discharge, having nearly perfect initial symmetry and small initial radius, to create narrow plasma columns with the necessary conditions for soft x-ray lasing by collisional electron excitation. An amplification of $e^{7.2}$ was measured at 46.9nm in the J=0-1 line of Ne-like Ar in a 12 cm long plasma column generated by a compact discharge. The beam divergence was measured to be less than 9mrad.

* This work was supported in its different stages of development by N.S.F, D.O.E. and Air Force Wright Aeronautical Laboratories.

** P.N. Lebedev Physics Institute, Moscow

Contributed Paper

QA-5 Correspondence between Laser Excitation with ccrf Discharges and hollow cathode Discharges,* J. MENTEL, N. REICH, Ruhr-Universität Bochum, AEEO, Germany, J. MIZERACZYK, Inst. of Fluid Flow Machinery, Gdansk, Poland - It is supposed for many years that similar discharge conditions can be realized with transverse to the tube axis capacitively coupled radio frequency (ccrf) discharges and with hollow cathode discharges (hcd). The reason is the formation of positive space charge layers in front of the electrodes in both discharges. He-Kr^+, He-Ar^+ and He-Cd^+ lasers are realized with cw ccrf discharges by taking over the parameters of the corresponding hcd lasers from literature. To minimize sputtering they are operated in Al_2O_3-tubes. It is shown for the three lasers that for an optimized laser output the filling gas pressure, the portion of the lasing component of the gas mixture, the dependence of the voltage on the mixing ratio and the small signal gain per unit length is similar for both discharge types. Moreover it is demonstrated that the laser tubes for ccrf discharges are much simpler than those for hcds.

*Supported in parts by the European Commission, Copernicus Programme CIPA-CT 93-0219.

SESSION QB: DUSTY PLASMAS
Friday morning, 21 October 1994
NIST Building 101
Green Auditorium, 10:15–12:00
C. Cui, presiding

Contributed Papers

QB-1 Analysis of Coulomb-Solid Formation in Particle Plasma, K. TACHIBANA and Y. HAYASHI, Kyoto Institute of Technology - In a methane plasma a Coulomb solid was formed by spherical and monodisperse carbon particles grown from injected nucleus carbon soots.[1] By Mie-scattering ellipsometry[2] the solidification process has been precisely analyzed. From the discontinuities in the reduction rate of the particle density and the growth rate of the diameter, it was estimated that the liquid-to-solid phase transition occurred at 1530s after the injection of nuclus particles. At that time the diameter of particles was 1280nm and the density was $2.8 \times 10^5 cm^{-3}$. At the transition the particle charge is estimated to be more than 1000e, and the Coulomb coupling parameter defined by the ratio of the Coulomb potential energy to the thermal kinetic energy becomes more than 200, where the plasma mainly consists of negatively charged particles and positive ions. The dynamic arrangement of the particles is under investigation from the images taken by a CCD camera.
[1]Y.Hayashi, K.Tachibana: Jpn. J. Appl. Phys. 33(1994)L804
[2]Y.Hayashi, K.Tachibana: Jpn. J. Appl. Phys. 33(1994)L476

QB-2 Cluster Formation Mechanisms in Low-Pressure Plasmas,* A. SATHEESH KUMAR and A. GARSCADDEN, Plasma Research Group, WPAFB- Particle formation under low-pressure glow discharge conditions has been modeled invoking the ligand attachment process from nucleation theory. Nucleation occurs as an ion-induced sequence of clustering reactions. In inert gas sputtering plasmas, both ion-molecule capture and ion-ion recombination processes can be effective in building up the cluster whereas, in reactive gas plasmas ion-radical reactions may become significant. With graphite electrodes, the process gets an impetus by the fact that C_3 instead of the carbon monomer acts as the building block for cluster growth. The cluster grows rapidly via ion-assisted channels due to the induced dipole effects at molecular sizes and the Debye sheath around the charged clusters at sufficiently large sizes. Band structure and bulk properties become apparent at the transition region. The ion-assisted growth process dominates till the particle has grown up to sub-micron sizes. Calculations for the nucleation and growth-rates of particles will be presented.

*Work Supported by WPAFB and the National Research Council.

QB-3 **Particle Transport in the Afterglow of Electropositive Plasmas**, D. A. BROWN and S. M. COLLINS, SNL and U. of Arizona - Charge and transport properties of dust particles in the afterglow of an electropositive plasma are described. Using a pulsed RF power supply and a tuned Langmuir probe, the decay times of electrons and ions were measured in argon, krypton, and xenon discharges at pressures of 10, 100, and 250 mT and RF powers of 20 and 50 W. From these data, the particle charge as a function of time was computed for 0.5 μm particles (diameters on the order of the He-Ne laser wavelength). Trajectories of the particles were calculated from a net force model including gravity, the electric field, fluid flow, ion drag, and thermophoresis. Utilizing high-speed video with laser light scattering, trajectories in the afterglow were observed experimentally for each of the power and pressure combinations and at electrode surface temperatures between 15 and 75 °C. It was found that the ion decay time was approximately twice the time for electrons (≈ 100 μs). With typical particle charging times ≈ 1 μs, the particle charge decays continuously with the floating potential. In the low-flow regime, thermophoresis is found to be the dominant force, in excellent agreement with theoretical predictions.

QB-4 Photodetachment in a dusty SiH_4 rf discharge, W.W. STOFFELS, E STOFFELS, G.M.W. KROESEN, F.J. DE HOOG, TUE- Charging of microscopic particles in plasmas has been an unresolved problem due to lack of experimental data. In a low pressure SiH_4 rf discharge, nanometer scale clusters are formed prior to large particles, already after 100 ms of discharge operation. In this work we study the charging kinetics of these very fine clusters by means of laser-induced photodetachment. A pulsed high power laser detaches electrons from particles and negative ions in the plasma. The decay of the density of photodetached electrons after the laser shot is monitored by means of a microwave cavity method. The decay frequency of these electrons gives information about charging kinetics of clusters. In the first 10 ms of discharge operation (120 mTorr, 10 W, 5% SiH_4 in Ar with a cooled rf electrode) only a weak photodetachment signal has been found, most likely originating from negative ions; its decay frequency agrees with the attachment rate to SiH_4 (< 100 kHz). After about 50 ms of plasma operation the decay frequency of extra electrons becomes substantially higher (200 kHz) and it increases further up to 1 MHz at 1 s of plasma operation. At the same time the free electron density in the discharge decreases, while the height of the photodetachment signal increases. This shows that after 50 ms of plasma operation clusters start to acquire negative charge and their charging frequency rapidly increases as they become larger.
This work is supported by the European Commission under contract no. BE I 7328.

QB-5 **Plasma-Chemistry and Thin Film Deposition in Discharges, Excited by Powerful Pulse Microwave Beams** G. M. BATANOV, E. F. BOL'SHAKOV, N. K. BEREZHETSKAYA, A. A. DOROFEYUK, V. A. KOP'EV, I. A. KOSSYI, *General Physics Institute, Russian Academy of Sciences, Moscow* — There are presented the results of the studies of plasma-chemical applications for freely localized in space discharges excited by convergent powerful pulse microwave beams. The main properties of microwave discharges are described and their physical and mathematical models are discussed. Schemes are given of discharge excitation in both gas mediums and vacuum (a flare near the surface of target irradiated by powerful microwave beam). The main advantage of freely localized microwave discharges is the absence of any solid bodies in contact with the plasma. The discharge occupies the near-the-axis region of the vacuum chamber being located far from the chamber walls. Thus the main advantage of the scheme is the possibility to build, taking it as a basis, a plasma-chemical super-pure reactor, in which the level of contaminations of the reaction products is completely determined by the purity of reagents. The following reactions demonstrate the possibilities of the microwave beam method: (1) covering of dielectric and metal substrates by carbon-hydrogen or diamond-like films; (2) decomposition of CO_2; (3) production of SiC; (4) quartz (SiO_2) synthesis. The efficiencies of plasma-chemical reactions and the main chemical channels in a freely localized microwave discharge are determined.

Postdeadline Papers—Program of the 47th Annual Gaseous Electronics Conference 18–21 October 1994; Gaithersburg, Maryland

SESSION BA: NEGATIVE IONS IN PLASMAS
Tuesday morning, 18 October 1994
NIST Building 101
Red Auditorium, 10:15–12:00
L. G. Christophorou, presiding

BA-7 *Role of Negative Ions in Hydrogen Level Populations in the Recombining Expanding Plasma,* D.K. OTORBAEV, ZHOU QING, M. EERDEN, M.C.M. VAN DE SANDEN and D.C. SCHRAM, Eindhoven Univ. Techn., The Netherlands. - The absolute density of atomic hydrogen excited states in a magnetized expanding pure hydrogen cascaded arc plasma is measured using emission spectroscopy. The cascaded arc has been operated under low pressure $\simeq$ 30 Torr, and low hydrogen flow $\simeq$ 8 scc/s. In the expansion a population inversion is observed between the quantum states $3 \leq p \leq 7$. Comparing the measured population densities with the densities calculated on basis of the measured n_e and T_e (obtained by a Langmuir probe diagnostics), shows that purely atomic recombination can not account for the large population densities observed. It is argued that molecular induced recombination reactions in which the negative ion participates should be taken into account: H_2^+ $[H^+]$ + H^- $\rightarrow$ H_2 [H] + H^*(p). Negative H^- and positive ions H_2^+ either generated by the arc or formed in the reactions with the participation of rovibrationally excited $H_2^{v,j}$ molecules: $H_2^{v,j}$ + e $\rightarrow$ H^- + H, $H_2^{v,j}$ + H^+ $\rightarrow$ H_2^+ + H. Photodetachment techniques are employed to measure the negative ion density in plasmas.

SESSION J: POSTER SESSION
Wednesday afternoon, 19 October 1994
NIST Building 101
Lecture Rooms A and B
and Employee Lounge, 15:45–17:30
J. K. Olthoff, presiding

JE: PLASMA CHEMISTRY

JE-6 KINEMA: A User-Friendly General Purpose Plasma Chemistry Modeling Code, W.L. MORGAN, *Kinema Research & Software, P.O. Box 1147, Monument, CO 80132* — Due to the wide availability of desktop computers with processing speed and memory capacities exceeding those of mainframes of only a few years ago many large modeling calculations formerly performed on mainframes are now performed on personal computers. We have developed specifically for small computers a sophisticated plasma chemistry modeling code having a graphical user interface. This code incorporates a number of built-in models as well as user defined models. The key feature in dealing with low temperature non-equilibrium plasmas is the capability of reading in electron impact cross sections and either (1) constructing a table of Maxwellian rate and transport coefficients with an energy balance for electron temperature or (2) solving Boltzmann's equation on the fly for the non-Maxwell-Boltzmann electron energy distribution function [1] and associated rate and transport coefficients. Examples, demonstrations, and comparisons with Chemkin, another popular kinetics program, will be presented [2].

[1] W.L. Morgan and B.M. Penetrante, Comp. Phys. Comm. 58:127 (1990).
[2] W.L. Morgan and B.M. Penetrante, unpublished.

AUTHOR INDEX

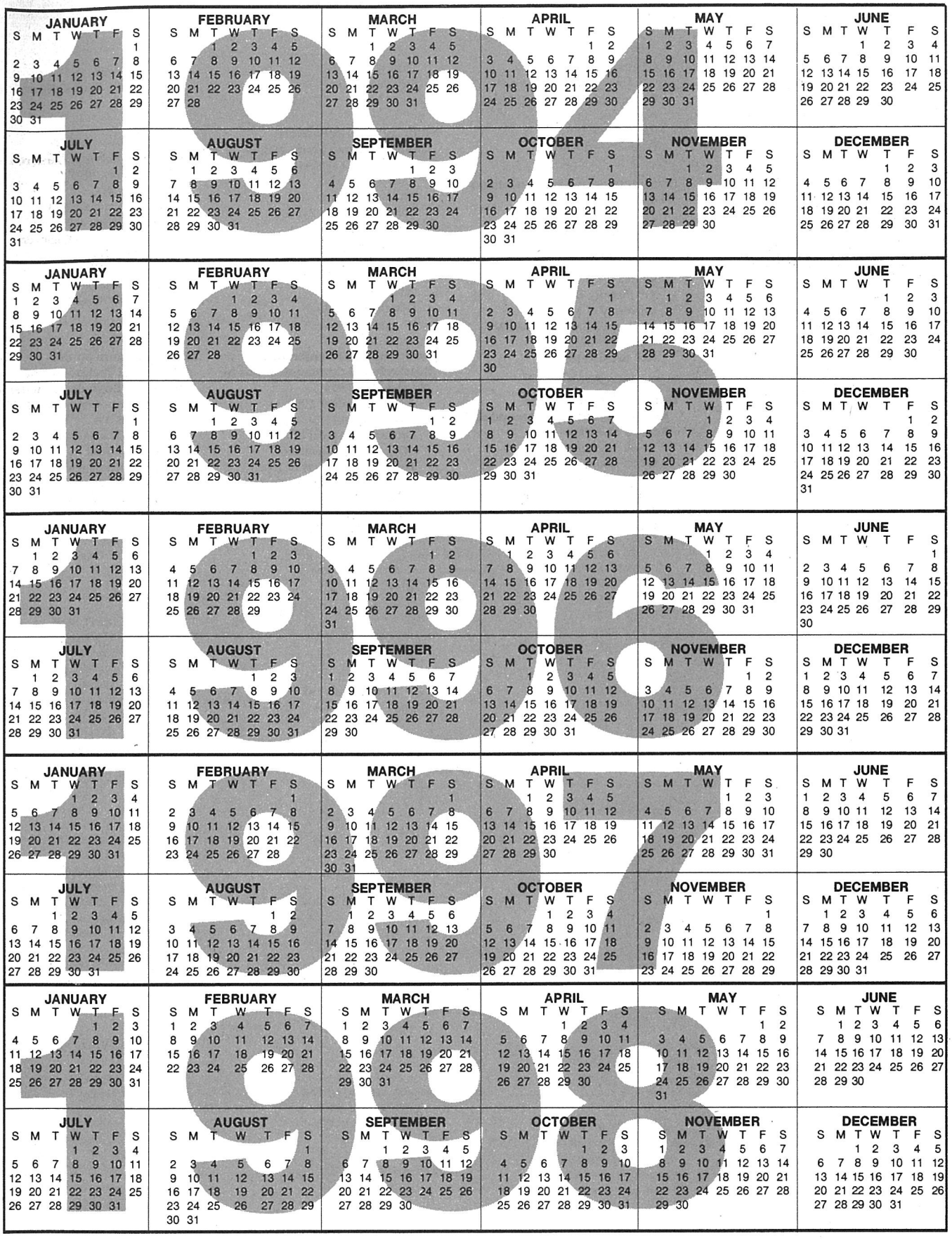

JANUARY

S	M	T	W	T	F	S
						1
2	3	4	5	6	7	8
9	10	11	12	13	14	15
16	17	18	19	20	21	22
23	24	25	26	27	28	29
30	31					

FEBRUARY

S	M	T	W	T	F	S
		1	2	3	4	5
6	7	8	9	10	11	12
13	14	15	16	17	18	19
20	21	22	23	24	25	26
27	28					

MARCH

S	M	T	W	T	F	S
		1	2	3	4	5
6	7	8	9	10	11	12
13	14	15	16	17	18	19
20	21	22	23	24	25	26
27	28	29	30	31		

APRIL

S	M	T	W	T	F	S
					1	2
3	4	5	6	7	8	9
10	11	12	13	14	15	16
17	18	19	20	21	22	23
24	25	26	27	28	29	30

MAY

S	M	T	W	T	F	S
1	2	3	4	5	6	7
8	9	10	11	12	13	14
15	16	17	18	19	20	21
22	23	24	25	26	27	28
29	30	31				

JUNE

S	M	T	W	T	F	S
			1	2	3	4
5	6	7	8	9	10	11
12	13	14	15	16	17	18
19	20	21	22	23	24	25
26	27	28	29	30		

JULY

S	M	T	W	T	F	S
					1	2
3	4	5	6	7	8	9
10	11	12	13	14	15	16
17	18	19	20	21	22	23
24	25	26	27	28	29	30
31						

AUGUST

S	M	T	W	T	F	S
	1	2	3	4	5	6
7	8	9	10	11	12	13
14	15	16	17	18	19	20
21	22	23	24	25	26	27
28	29	30	31			

SEPTEMBER

S	M	T	W	T	F	S
				1	2	3
4	5	6	7	8	9	10
11	12	13	14	15	16	17
18	19	20	21	22	23	24
25	26	27	28	29	30	

OCTOBER

S	M	T	W	T	F	S
						1
2	3	4	5	6	7	8
9	10	11	12	13	14	15
16	17	18	19	20	21	22
23	24	25	26	27	28	29
30	31					

NOVEMBER

S	M	T	W	T	F	S
		1	2	3	4	5
6	7	8	9	10	11	12
13	14	15	16	17	18	19
20	21	22	23	24	25	26
27	28	29	30			

DECEMBER

S	M	T	W	T	F	S
				1	2	3
4	5	6	7	8	9	10
11	12	13	14	15	16	17
18	19	20	21	22	23	24
25	26	27	28	29	30	31

JANUARY

S	M	T	W	T	F	S
1	2	3	4	5	6	7
8	9	10	11	12	13	14
15	16	17	18	19	20	21
22	23	24	25	26	27	28
29	30	31				

FEBRUARY

S	M	T	W	T	F	S
			1	2	3	4
5	6	7	8	9	10	11
12	13	14	15	16	17	18
19	20	21	22	23	24	25
26	27	28				

MARCH

S	M	T	W	T	F	S
			1	2	3	4
5	6	7	8	9	10	11
12	13	14	15	16	17	18
19	20	21	22	23	24	25
26	27	28	29	30	31	

APRIL

S	M	T	W	T	F	S
						1
2	3	4	5	6	7	8
9	10	11	12	13	14	15
16	17	18	19	20	21	22
23	24	25	26	27	28	29
30						

MAY

S	M	T	W	T	F	S
	1	2	3	4	5	6
7	8	9	10	11	12	13
14	15	16	17	18	19	20
21	22	23	24	25	26	27
28	29	30	31			

JUNE

S	M	T	W	T	F	S
				1	2	3
4	5	6	7	8	9	10
11	12	13	14	15	16	17
18	19	20	21	22	23	24
25	26	27	28	29	30	

JULY

S	M	T	W	T	F	S
				1	2	3
4	5	6	7	8	9	10
11	12	13	14	15	16	17
18	19	20	21	22	23	24
25	26	27	28	29	30	31

AUGUST

S	M	T	W	T	F	S
						1
2	3	4	5	6	7	8
9	10	11	12	13	14	15
16	17	18	19	20	21	22
23	24	25	26	27	28	29
30	31					

SEPTEMBER

S	M	T	W	T	F	S
			1	2	3	4
5	6	7	8	9	10	11
12	13	14	15	16	17	18
19	20	21	22	23	24	25
26	27	28	29	30		

OCTOBER

S	M	T	W	T	F	S
					1	2
3	4	5	6	7	8	9
10	11	12	13	14	15	16
17	18	19	20	21	22	23
24	25	26	27	28	29	30
31						

NOVEMBER

S	M	T	W	T	F	S
						1
2	3	4	5	6	7	8
9	10	11	12	13	14	15
16	17	18	19	20	21	22
23	24	25	26	27	28	29
30						

DECEMBER

S	M	T	W	T	F	S
	1	2	3	4	5	6
7	8	9	10	11	12	13
14	15	16	17	18	19	20
21	22	23	24	25	26	27
28	29	30	31			

JANUARY

S	M	T	W	T	F	S
						1
2	3	4	5	6	7	8
9	10	11	12	13	14	15
16	17	18	19	20	21	22
23	24	25	26	27	28	29
30	31					

FEBRUARY

S	M	T	W	T	F	S
					1	2
3	4	5	6	7	8	9
10	11	12	13	14	15	16
17	18	19	20	21	22	23
24	25	26	27	28		

MARCH

S	M	T	W	T	F	S
					1	2
3	4	5	6	7	8	9
10	11	12	13	14	15	16
17	18	19	20	21	22	23
24	25	26	27	28	29	30
31						

APRIL

S	M	T	W	T	F	S
	1	2	3	4	5	6
7	8	9	10	11	12	13
14	15	16	17	18	19	20
21	22	23	24	25	26	27
28	29	30				

MAY

S	M	T	W	T	F	S
			1	2	3	4
5	6	7	8	9	10	11
12	13	14	15	16	17	18
19	20	21	22	23	24	25
26	27	28	29	30	31	

JUNE

S	M	T	W	T	F	S
						1
2	3	4	5	6	7	8
9	10	11	12	13	14	15
16	17	18	19	20	21	22
23	24	25	26	27	28	29
30						

JULY

S	M	T	W	T	F	S
					1	2
3	4	5	6	7	8	9
10	11	12	13	14	15	16
17	18	19	20	21	22	23
24	25	26	27	28	29	30
31						

AUGUST

S	M	T	W	T	F	S
						1
2	3	4	5	6	7	8
9	10	11	12	13	14	15
16	17	18	19	20	21	22
23	24	25	26	27	28	29
30	31					

SEPTEMBER

S	M	T	W	T	F	S
					1	2
3	4	5	6	7	8	9
10	11	12	13	14	15	16
17	18	19	20	21	22	23
24	25	26	27	28	29	30

OCTOBER

S	M	T	W	T	F	S
						1
2	3	4	5	6	7	8
9	10	11	12	13	14	15
16	17	18	19	20	21	22
23	24	25	26	27	28	29
30	31					

NOVEMBER

S	M	T	W	T	F	S
		1	2	3	4	5
6	7	8	9	10	11	12
13	14	15	16	17	18	19
20	21	22	23	24	25	26
27	28	29	30			

DECEMBER

S	M	T	W	T	F	S
				1	2	3
4	5	6	7	8	9	10
11	12	13	14	15	16	17
18	19	20	21	22	23	24
25	26	27	28	29	30	31

Calendar of Meetings *(continued from back cover)*

11th Topical Conference on Radio Frequency in Plasmas
17-19 May 1995
Palm Springs, CA
Abstract Deadline: N/A
Contact: Ron Prater
General Atomics
3550 General Atomics Court
San Diego, CA 92121-1194
(619) 455-3000

Seventh Rochester Conference on Coherence and Quantum Optics
7-10 June 1995
Rochester, NY
Abstract Deadline: N/A
Contact: Emil Wolf
University of Rochester
Box 41, Administration Bldg.
Rochester, NY, 14627
(716) 275-4397
Fax: (716) 473-0687

22nd International Conference on Phenomena in Ionized Gases
31 July - 4 August 1995
Hoboken, NJ
Abstract Deadline: N/A
Contact Kurt Becker
City College
City University of New York
Convent Avenue & 138th Street
New York, NY 10031
(212) 650-5613
Fax: (212) 650-6940

12th International Symposium on Plasma Chemistry
20-25 August 1995
Minneapolis, MN
Abstract Deadline: N/A
Contact: Lori Graven
ISPC12
315 Pilsbury Drive S.E.
University of Minnesota
Minneapolis, MN 55455-0139
(612) 625-9023
Fax: 612-626-1632

Third Int'l Conference on the Applications of Diamond and Related Materials
21-24 August 1995
Gaithersburg, MD
Abstract Deadline: N/A
Contact: Albert Feldman
NIST
Gaithersburg, MD 20899
(301) 975-2000
(301) 841-4500

Ninth Int'l Conference on Liquid and Amorphous Metals
27 August - 1 September 1995
Chicago, IL
Abstract Deadline: N/A
Contact: Jlhn van Zytveld
Physics Department
Calvin College
3201 Burton SE
Grand Rapids, MI 48546
(616) 957-6340
Fax: (616) 957-6501

The Second Int'l Conference on Research and Communications in Physics (RACIP2)
18–22 September 1995
Tokyo, Japan
Contact: Secretariat of RACIP2 Organizing Committee
The Physical Society of Japan
Kikai-Shinko Bldg., Room 21
Shiba-Koen 3-5-8
Minato-ku, Tokyo 105 JAPAN
Tel: 81-3-3434-2671
Fax: 81-3-3432-0997
e-mail: racip2@atlas.phy.metro-u.ac.jp

Intersociety Polymet Conference
7-10 October 1995
Baltimore MD
Abstract Deadline: N/A
Contact: Jeffrey A. Forger
Society of Plastics Engineers
14 Fairfield Drive
Brookfield, CT 06804
(203) 775-0471
Fax: (203) 775-8940

Int'l Symposium on the Science and Technology of Atomically Engineered Materials
30 October - 4 November 1995
Richmond, VA
Abstract Deadline: N/A
Contact: P. Jena
Physics Department
Virginia Commonwealth University
Richmond, VA 23284
(804) 367-8991
Fax: (804) 367-7073

CALENDAR OF MEETINGS

APS Meetings

Laser Science (Joint with OSA)
2–7 October 1994
Dallas, TX
Abstract Deadline: Passed
Contact: OSA Meetings Department
2010 Massachusetts Avenue, NW
Washington, DC 20036
(202) 223-0920

Ohio Section
14–15 October 1994
Toledo, OH
Abstract Deadline: Passed
Contact: Scott Lee
Department of Physics and Astronomy
University of Toledo
2801 W. Bancroft Street
Toledo, OH 43606
(419) 537-4779

New York Section
14-15 October 1994
Binghamton, NY
Abstract Deadline: Passed
Contact: Fred L. Wilson
Rochester Institute of Technology
COLA-3118
1 Lomb Memorial Drive
Rochester, NY 14623
(716) 475-6204
Fax: (716) 383-8854

Texas Section
14–15 October 1994
Austin, TX
Abstract Deadline: Passed
Contact: C.A. Quarles
Department of Physics
Texas Christian University
Fort Worth, TX 76129
(817) 921-7375
Fax: (817) 921-7110

Nuclear Physics
26–29 October 1994
Williamsburg, VA
Abstract Deadline: Passed
Contact: Dr. Virginia R. Brown
Lawrence Livermore National Laboratory
L–297, E Division
P. O. 808
Livermore, CA 94550
(510) 422-4092

Southeastern Section
10–12 November 1994
Newport News, VA
Abstract Deadline: Passed
Contact: Dr. Cecil G. Shugart
Memphis State University
Department of Physics
Memphis, TN 38152
(901) 678-3121

Plasma Physics
7–11 November 1994
Minneapolis, MN
Abstract Deadline: Passed
Contact: Meetings Department
APS, One Physics Ellipse
College Park, MD 20740-3844
(301) 209-3200

Fluid Dynamics
20–22 November 1994
Atlanta, GA
Abstract Deadline: Passed
Contact: Dr. G. Paul Neitzel
Georgia Institute of Technology
School of Mechanical Engineering
Atlanta, GA 30332-0405
(404) 894-3242

Texas Section
2-4 March 1995
Huntsville, TX
Abstract Deadline: N/A
Contact: C.A. Quarles
Department of Physics
Texas Christian University
Fort Worth, TX 76129
(817) 921-7375
Fax: (817) 921-7110

March Meeting
20–24 March 1995
San Jose, CA
Abstract Deadline: 2 December 1994
Contact: Meetings Department
APS, One Physics Ellipse
College Park, MD 20740-3844
(301) 209-3200

Joint April Meeting with AAPT
18–21 April 1995
Washington, D. C.
Abstract Deadline: 6 January 1995
Contact: Meetings Department
APS, One Physics Ellipse
College Park, MD 20740-3844
(301) 209-3200

Atomic, Molecular, and Optical Physics (Joint with the Canadian Association of Physicists)
17-19 May 1995
Toronto, Canada
Abstract Deadline: N/A
Contact: Dr. A. David May
Department of Phyics
University of Toronto
60 St. George Street
Toronto, Ontario MS5 1A7
Canada
Fax: (416) 978-5848

Texas Section
27-28 October 1995
Lubbock, TX
Abstract Deadline: N/A
Contact: C.A. Quarles
Department of Physics
Texas Christian University
Fort Worth, TX 76129
(817) 921-7375
Fax: (821) 921-7110

Texas Section
15-16 March 1996
Abilene, TX
Abstract Deadline: N/A
Contact: C.A. Quarles
Department of Physics
Texas Christian University
Fort Worth, TX 76129
(817) 921-7375
Fax: (817) 921-7110

Sponsored Meetings

47th Annual Gaseous Electronics Conference
18–21 October 1994
Gaithersburg, MD
Abstract Deadline: Passed
Contact: Jean W. Gallagher
Bldg. 221, Rm. A 323
NIST
Gaithersburg, MD 20899-0001
Fax: (301) 926-0416
e-mail: jwg@enh.nist.gov

Int'l Symposium on Computational Molecular Dynamics
24-26 October 1994
Minneapolis, MN
Abstract Deadline: Passed
Contact: Michael J. Olsen
University of Minnesota
1200 Washington Avenue South
Minneapolis, MN 55415
(612) 625-1818
Fax: (612) 624-8861

4th Conference on Radiation Protection and Dosimetry
24–27 October 1994
Orlando, FL
Contact: J.S. Bogard
ORNL
P.O. Box 2008
Oak Ridge, TN 37831-6379
Tel: (615) 574-5851
Fax: (615) 574-9174

13th Int'l Conference on Applications of Accelerators in Research and Industry
7-10 November 1994
Denton, TX
Abstract Deadline: Passed
Contact: Jerome L. Duggan
University of North Texas
Department of Physics
P.O. Box 5368
Denton, TX 76203
(817) 565-3232
Fax: (817) 565-2227

North American Conference on Smart Structures and Materials
26 February - 3 March 1995
San Diego, CA
Abstract Deadline: N/A
Contact : J. Terrence Montoyne
International Society for Optical Engineering
P.O. Box 10
Bellingham, WA 98227
(206) 676-3290
Fax: (206) 647-1445

International Sherwood Fusion Theory Conference
3-5 April 1995
Incline Village, NV
Abstract Deadline: N/A
Contact: Thomas Kaiser
Lawrence Livermore National Laboratory
PO Box 808, L-630
Livermore, CA 94550
(510) 423-8371
Fax: (510) 423-3484
e-mail: kaiser@casablanca.llnl.gov

Bulletin of The American Physical Society Gaseous Electronics Vol. 39, No. 6, 1439–1500, October 1994

0003-0503(199410)39:6;1-X

Program of the 47th Annual Gaseous Electronics Conference 18-21 October 1994

47th Annual Gaseous Electronics Conference

Tuesday, October 18		Wednesday, October 19		Thursday, October 20		Friday, October 21	
AA. 8:00 - 10:00 HIGH DENSITY PLASMA PROCESSING RED AUDITORIUM	AB. 8:00 - 10:00 ELECTRON-METAL ATOM COLLISION GREEN AUDITORIUM	EA. 8:00 - 10:00 MAGNETICALLY ENHANCED PLASMAS I RED AUDITORIUM	EB. 8:00 - 10:00 TRANSPORT AND ENERGY DISTRIBUTIONS GREEN AUDITORIUM	KA. 8:00 - 10:00 FLAT PANEL DISPLAYS RED AUDITORIUM	KB. 8:00 - 10:00 ELECTRON COLLISIONS GREEN AUDITORIUM	PA. 8:00 - 10:00 INDUCTIVELY COUPLED PLASMAS III RED AUDITORIUM	PB. 8:00 - 10:00 PLASMA TECHNIQUES FOR WASTE TREATMENT II GREEN AUDITORIUM
BREAK							
BA. 10:15 - 12:00 NEGATIVE IONS IN PLASMAS RED AUDITORIUM	BB. 10:15 - 12:00 DIAGNOSTICS GREEN AUDITORIUM	F. 10:30 - 11:30 WILLIAM P. ALLIS PRIZE LECTURE G. 11:30 - 12:00 BUSINESS MEETING RED AUDITORIUM		L. 10:15 - 12:15 POSTER SESSION LA - Plasma Techniques for Waste Treatment I LB - Coronas, Arcs, and Breakdown LC - Plasma Displays LD - Electron Collisions LECTURE ROOM A, LECTURE ROOM B, EMPLOYEE LOUNGE		QA. 10:15 - 12:00 INNOVATIVE PLASMA APPLICATIONS RED AUDITORIUM	QB. 10:15 - 12:00 DUSTY PLASMAS GREEN AUDITORIUM
LUNCH							
CA. 13:30 - 15:30 PLASMA SURFACE INTERACTIONS RED AUDITORIUM	CB. 13:30 - 15:30 DIAGNOSTICS AND CONTROL GREEN AUDITORIUM	HA. 13:30 - 15:30 INDUCTIVELY COUPLED PLASMAS I RED AUDITORIUM	HB. 13:30 - 15:30 ELECTRON-MOLECULE SCATTERING GREEN AUDITORIUM	MA. 13:30 - 15:30 DIAMOND FILMS RED AUDITORIUM	MB. 13:30 - 15:30 GLOWS GREEN AUDITORIUM	13:30 - 15:30 NIST Lab Tours	
BREAK							
D. 15:45 - 17:30 POSTER SESSION DA - Electrical-Optical Diagnostics DB - Electron Collisions DC - Electron-Ion Recombinations and Photon Processes DD - Charged Particle Transport and Energy Distributions LECTURE ROOM A, LECTURE ROOM B, EMPLOYEE LOUNGE		J. 15:45 - 17:30 POSTER SESSION JA - Microwave Discharges JB - Magnetically Enhanced Plasmas II JC - Positive Columns JD - Plasma Processing-Etching and Deposition JE - Plasma Chemistry JF - Heavy Particle Interactions LECTURE ROOM A, LECTURE ROOM B, EMPLOYEE LOUNGE		N. 15:45 - 17:30 POSTER SESSION NA - RF Capacitively Coupled Glows NB - Inductively Coupled Plasmas II NC - Cathodes and Sheaths ND - Dusty Glows LECTURE ROOM A, LECTURE ROOM B, EMPLOYEE LOUNGE		15:45 - 17:30 NIST Lab Tours	
		GEC REFERENCE CELL USERS 19:30 HILTON HOTEL		SOCIAL HOUR 18:30 - 19:30 BANQUET 19:30 - 21:30 HILTON HOTEL			

BULLETIN OF THE AMERICAN PHYSICAL SOCIETY